From Institute of Vegetative Physiology
of University of Würzburg
Director: Prof. Dr. Michaela Kuhn

FoxO3-mediated, inhibitory effects of CNP on the profibrotic activation of lung fibroblasts

Inaugural Dissertation
to award the doctoral degree
of the faculty of medicine
of Julius-Maximilians-University of Würzburg

submitted by
Anna-Lena Friedrich
born in Schweinfurt

Würzburg, September 2023

Referent: Prof. Dr. Michaela Kuhn
Co-referent: Prof Dr. Srikanth Karnati

Dean: Prof. Dr. Matthias Frosch

Day of doctoral defense: 23.04.2024

The MD student is a dentist

Dedication

To Lukas and my family

Declaration

“I declare that I have completed this dissertation without the unauthorized help of a second party and only with the assistance acknowledged therein. Furthermore, I have appropriately acknowledged and referenced all text passages that are derived literally from or are based on the content of published or unpublished work of others.”

Schweinfurt, September 2023

Anna-Lena Friedrich

Table of Contents

1 Introduction

1.1 Pulmonary fibrosis

Pulmonary fibrosis (PF) is a chronic lung parenchymal disease caused by various insults to the lung such as toxins, autoimmune disorders, drugs, infections, or traumatic injuries. Factors like age, genetic susceptibility, and environmental factors play an important role, which can cause an initial inflammation and later induce fibrotic changes. If the causative agents of the condition are known, a simple therapy can be implemented by avoiding the substance or undergoing a short course of steroids, which can lead to improvement of the condition. (Markart et al., 2006; Thannickal et al., 2004). However, PF is mostly idiopathic which complicates the treatment of the disease.

1.1.1 Idiopathic pulmonary fibrosis

Idiopathic pulmonary fibrosis (IPF) is a chronic, interstitial, fibrotic pneumonia, exhibiting a progressive decrease of lung function through scarring of the lung parenchyma. The cause of this disease is unknown and it is defined as a “clinical entity associated with the histologic appearance of usual interstitial pneumonia (UIP)” (Raghu et al., 2011). A typical key feature of UIP, frequently detected by high-resolution computed tomography (HRCT), is honeycombing, where cystic airspaces are clustered which is usually accompanied by reticular pattern containing traction bronchiectasis (Lynch et al., 2005). Diagnosis of IPF can be confirmed based on verification of three conditions. Firstly, other known causes for interstitial lung disease need to be excluded, which is a major challenge for clinicians. Secondly, UIP pattern by HRCT should be verified. In case patients were subjected to lung tissue sampling, a combination of HRCT patterns and histopathological patterns are assessed (Raghu et al., 2018).

1.1.1.1 Pathogenesis and risk factors

The challenging feature of this disease is its exceptionally poor prognosis with a mean survival rate of 57.03 ± 3.90 months without treatment. Survival rates can be improved up to 73.26 ± 7.87 months by treatment with antifibrotic drugs like pirfenidone (Lee et al., 2021). The major issue of IPF is that the processes underlying pathogenesis of the disease are not completely understood. Two main hypotheses have been suggested. The first theory, called the inflammatory theory, suggests that the disease results from an unresolved chronic inflammatory process induced by an unrecognized insult. However, an insufficient response to anti-inflammatory therapies, such as steroids,

supports a second ‘aberrant wound healing’ theory. According to this theory, the normal wound healing mechanism is disturbed in IPF lungs. An initial epithelial cell injury activates proliferation and migration of fibroblasts and their conversion to myofibroblasts. The myofibroblasts destroy the basement membrane and encourage apoptosis of the alveolar epithelial cells. They initiate a perpetual cycle of injury where the tissue is replaced by restrictive scar tissue (Douglas et al., 2000; Kuhn et al., 1989; Selman & Pardo, 2002). Although IPF is defined to be without known etiology (idiopathic), several risk factors may contribute to its development. Prevalence rises dramatically with patient age, with an estimated prevalence range from 4.0 per 100,000 persons aged 18 to 34 years, to 227.2 per 100,000 among those 75 years or older (Raghu et al., 2006). Exposure to metal and wood dust or cigarette smoking are described as environmental risk factors, which can cause the microinjuries (Baumgartner et al., 1997; Iwai et al., 1994). Next to the sporadic form of IPF, a familial form is observed which fuels a discussion about a genetical disposition. Studies carried out in Finland show that the familial form constitutes 3.3 - 3.7% of all diagnosed IPF cases (Hodgson et al., 2002).

1.1.1.2 Clinical course and therapy

Progression of fibrosis leads to a decline in lung function, with a reduced forced vital capacity (Russell et al., 2016). The clinical picture typically presents increased dyspnea and cough severity with progression of disease, reducing the life quality of the patient dramatically (Jo et al., 2017). The clinical course of the disease is very heterogenous. After diagnosis, most patients follow a progressive but slow decline of lung function. On the other hand, a second variant with differences in the transcriptional profile is detected, which accelerates rapidly and is mainly observed in male smokers and exhibits a different transcription profile (Selman et al., 2007). In some patients, an acute exacerbation of IPF with severe deteriorations in respiratory status is observed. The acute exacerbation is defined as a worsening of dyspnea without any precipitating factor like infections or heart congestive failure. New diffuse pulmonary opacities are detected on chest radiographs and the arterial oxygen tension/ inspiratory oxygen fraction decreases to less than 30kPa. The outcome after an acute exacerbation is poor and associated with a high mortality (Ambrosini et al., 2003). The current therapeutic options provide symptomatic relief and improve survival, but do not cure the disease. In an official clinical practice guideline submitted together by the American Thoracic Society, the European Respiratory Society, the Japanese Respiratory Society, and the Latin American Thoracic Association (ATS/ERS/JRS/ALAT), a pharmacotherapy with Pirfenidone and the tyrosine kinase inhibitor Nintedanib, which targets different kinases

like endothelial and fibroblast growth factor and Platelet derived growth factor (PDGF) receptors, is recommended. Since gastro-esophageal reflux is shown to trigger IPF, an antacid therapy is suggested in case of this comorbidity (Lee, 2014; Raghu et al., 2015). In addition, some non-pharmacotherapies with a positive impact are also recommended. Similar to other chronic respiratory diseases, pulmonary rehabilitation can improve patients' physical conditions, and long-term supplemental oxygen therapy can facilitate breathing under exertion. Due to the incurability and continuous progression of IPF, lung transplantation is suggested as the final treatment option (Raghu et al., 2011; Spruit et al., 2013).

1.1.1.3 Change in the lung tissue properties observed in IPF

The fibrotic changes in IPF manifest as the conversion of fibroblasts to myofibroblasts, resulting in an increased deposition of extracellular matrix. This is associated with an elevated accumulation of type I and type III collagen, causing destruction of normal lung architecture (Sime et al., 1997; Worke et al., 2017). The dysregulated extracellular matrix in fibrosis is also influenced by alterations in its reorganization. Here, imbalances of matrix metalloproteinases (MMPs), a group of Zn^{2+}-dependent proteinases, play an important role and the expression of MMP9 was shown to be increased in the parenchyma in lung fibrosis (Kim et al., 2009). The IPF myofibroblasts show a higher proliferative and migratory capacity in IPF tissue compared to cells of healthy tissue (Al-Tamari et al., 2018; Tisler et al., 2020).

1.2 Fibroblasts

Fibroblasts are localized in parts of the connective tissue and are defined as cells with an elongated cell body, long offshoots, and a typical spindle-shaped nucleus. The cells contribute to the formation of connective tissue and act as regulators of extracellular matrix homeostasis, coordinating its synthesis and degradation. A variety of signals can activate the cells what leads to proliferation and cellular differentiation, resulting in formation of myofibroblasts with an up-regulated rate of matrix production. Their activation plays an essential role in wound healing. In some cases, fibroblast activation becomes uncontrolled and produces a pathological fibrotic response resulting in various fibrotic disorders (Kendall & Feghali-Bostwick, 2014; Lüllmann-Rauch, 2003; Qu et al., 2019; Sime et al., 1997).

1.2.1 Conversion of fibroblasts to myofibroblasts

Growth factors such as transforming growth factor β (TGFβ) or PDGF as well as mechanical tension, can induce the transformation of fibroblasts into myofibroblasts. (Bonner, 2004; Hinz et al., 2001; Qu et al., 2019). Initially, the cells undergo a transformation into an intermediate form known as "proto-myofibroblast," which is identified by a migratory phenotype and the development of contractile bundles called stress fibers. These stress fibers are composed of cytoplasmic actin. As the remodeling process continues, the proto-myofibroblasts differentiate into "mature myofibroblasts" through the maximal expression and integration of α-smooth muscle actin (α-SMA) into the actin stress fibers (Figure 1) (Hermanns-Le et al., 2015; Tomasek et al., 2002). The myofibroblast transdifferentiation enhances the synthesis of Collagen1 and Collagen3 (Qu et al., 2019). These differentiated cells show an increased secretion of active extracellular matrix and display features similar to smooth muscle cells, such as myofilaments, contractility, communication through gap junctions and the expression of α-SMA (Lüllmann-Rauch, 2003). The expression of α-SMA is coordinated by TGF-β, which is increased under fibrotic conditions (Desmouliere et al., 1993).

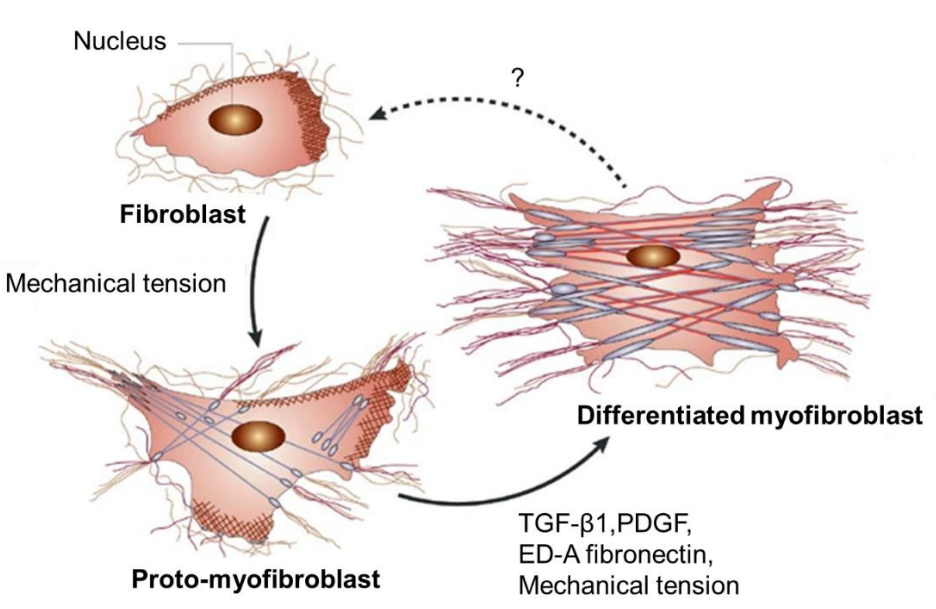

Figure 1: *Transformation of resident fibroblast into intermediate proto-myofibroblast and myofibroblast*
At first, the conversion leads to the building of stress fibers made of cytoplasmic actin and in a second step with incorporation of α-smooth muscle actin the cell develops to myofibroblast form (modified from (Tomasek et al., 2002))

1.3 Natriuretic peptides

Natriuretic peptides (NPs) are a family of three structurally related hormone/paracrine factors (Figure 2) (Sudoh et al., 1990). The first NP, atrial natriuretic peptide (ANP), was identified in rat atrial muscle in 1983 as a peptide hormone with natriuretic and diuretic activity (Flynn et al., 1983). Five years later a second peptide, with remarkably similar structure, was purified from porcine brain and is known as brain natriuretic peptide (BNP) (Sudoh et al., 1988). In 1990, the same group also sequenced the third member of the NP family in porcine brain called the C-type natriuretic peptide (CNP). All peptides possess a similar structure, especially a ring structure of 17 amino acids linked by an intramolecular disulfide linkage (Sudoh et al., 1990).

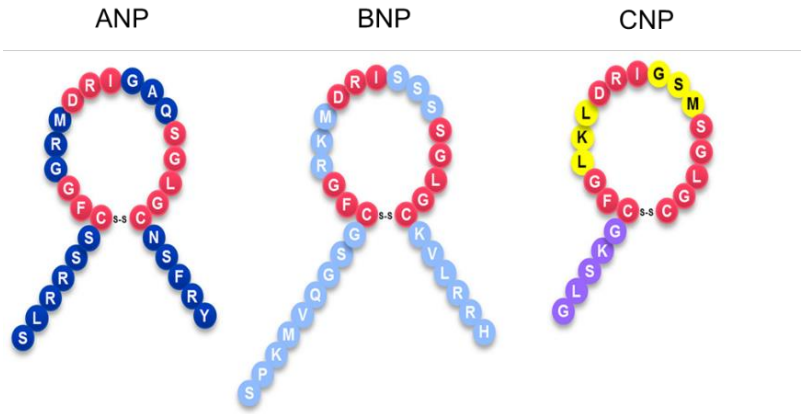

Figure 2: *Molecular structure of atrial natriuretic peptide, brain natriuretic peptide and c-type natriuretic peptide*
All three peptides possess a similar ring structure containing 17 amino acids (modified after (Ichiki et al., 2019))

1.3.1 Atrial natriuretic peptide (ANP)

In 1956, Kisch reported granules in the atrial myocytes detected by electron microscopy, but their physiological relevance in homeostasis remained unexplored (Kisch, 1956). It took around 25 years before the importance of the granules was demonstrated by intravenous injection of atrial myocardial extract in rats. Upon injection, a rapid and strong natriuretic response was detected and the existence of natriuretic hormone in the heart and a heart-renal-interaction was postulated (de Bold et al., 1981). ANP together with the later described BNP plays an important role in maintenance of intravascular volume homeostasis, which enables the peptide to protect the heart against a pathological increase of blood pressure and volume (Kuhn, 2012). Here the NPs work as a direct opponent of the Renin-Angiotensin-Aldosterone-system (RAAS) and can

reduce its diuretic effects (McMurray & Struthers, 1988). The sequencing of the hormone displays a construct of 28 amino acids with the typical ring structure anchored by a disulfide bond between Cys7 and Cys23 (Flynn et al., 1983). The ANP mRNA is translated as prepro-ANP and after removal of the signal peptide, the precursor is secreted and cleaved by the enzyme Corin to obtain mature ANP (Yan et al., 2000).

1.3.2 Brain natriuretic peptide (BNP)

Although BNP was initially purified from the brain, the hormone is predominantly secreted by the heart and works mainly as a cardiac hormone together with ANP (Mukoyama et al., 1991). BNP is secreted by the ventricular myocytes as proBNP-108 and is cleaved by enzymes to BNP-32 and N-terminal proBNP-76. Both, proBNP-108 and BNP32, circulate in human plasma (Nishikimi et al., 2010).

1.3.3 C-type natriuretic peptide (CNP)

CNP is genetically encoded by *NPPC*, that translates to a polypeptide with 126 amino acids called prepro-CNP (Savarirayan et al., 2019; Tawaragi et al., 1991). After the signal peptide is removed, the precursor is cleaved by the enzyme Furin into the pro-CNP peptide (residues 1-50) and mature CNP-53. Both peptides are secreted out of the cell and CNP-53 can be further cleaved by an unknown enzyme to generate CNP-22. Both forms, CNP53 and CNP22, elicit similar natriuretic responses and show no functional difference. However, the question why two different isoforms are expressed remains unanswered (Wu et al., 2003). CNP has several diverse functions, including the regulation of angiogenesis and vascular remodeling, activation of endochondral ossification, reproduction, and maintenance of axon-glia-interactions in central nervous system (Bubb et al., 2019; Rasband et al., 2005; Savarirayan et al., 2019; Tamura et al., 2004). As opposed to the other two peptides, very low levels of CNP are present in circulation (Igaki et al., 1996). CNP acts in a para- and autocrine manner, hence, effects are restricted to the cell itself and the neighboring cells (Prickett & Espiner, 2020). The peptide is mainly expressed by endothelial cells and chondrocytes, but is also produced in the central nervous system, the anterior pituitary gland, and renal cells (Cataliotti et al., 2002; Chusho et al., 2001; Mirczuk et al., 2019; Moyes et al., 2020; Rasband et al., 2005). Stimuli, which increase gene expression or a direct release of CNP, are shear stress and several cytokines and growth factors such as TGF β and basic fibroblast growth factor (bFGF), or lipopolysaccharides (Horio et al., 2003; Vollmar & Schulz, 1995; Zhang et al., 1999). The half-life of exogenous CNP in plasma is very short (Hunt et al.,

1994). The fast elimination is mediated by two different pathways, cleavage by the neutral endopeptidase and receptor-mediated endocytosis degradation by the Natriuretic peptide receptor C (NPR-C) (Cohen et al., 1996; Kenny et al., 1993).

1.3.3.1 Anti-inflammatory and anti-fibrotic effect of C-type natriuretic peptide

CNP exerts protective anti-inflammatory and anti-fibrotic actions in various organs. Specifically, in rodents it has been shown that infusion of exogenous, synthetic CNP inhibited pulmonary infiltration by inflammatory cells, including macrophages and monocytes, neutrophils, and lymphocytes, in monocrotaline-induced pulmonary hypertension (PH) and bleomycin-induced acute lung injury models (Itoh et al., 2004; Murakami et al., 2004). Moreover, CNP infusion into mice attenuated bleomycin-induced PF by reducing the production of inflammatory chemokines as well as collagen deposition (Kimura et al., 2016; Murakami et al., 2004). Further studies also described a protective role of exogenously administered CNP in pathological tissue remodeling observed in cardiac and hepatic fibrosis (Bae, Hino, Hosoda, Miyazato, et al., 2018; Horio et al., 2003). CNP was shown to attenuate cardiac remodeling and reduce the increase in morphometrical collagen volume fraction in mice after myocardial infarction (Soeki et al., 2005). However, the target cell populations responsible for such protective CNP actions were not explored. Most importantly, it is not known whether the endogenous endothelial hormone exerts paracrine anti-inflammatory and/or antifibrotic actions in the lung.

1.3.4 Natriuretic peptide receptors

NPs mediate their functions via binding to membrane bound receptors, namely NPR-A, NPR-B and NPR-C. The first two receptors possess guanylyl cyclase activity and are accordingly named Guanylyl cyclase-A (GC-A) and Guanylyl cyclase-B (GC-B) (Chang et al., 1989; Chinkers et al., 1989; Lowe, Camerato, et al., 1990). All three receptors differ in their ligand specificity (Figure 3). GC-A preferentially binds to ANP and BNP, GC-B to CNP while NPR-C to all three in the order ANP> CNP> BNP (Bennett et al., 1991).

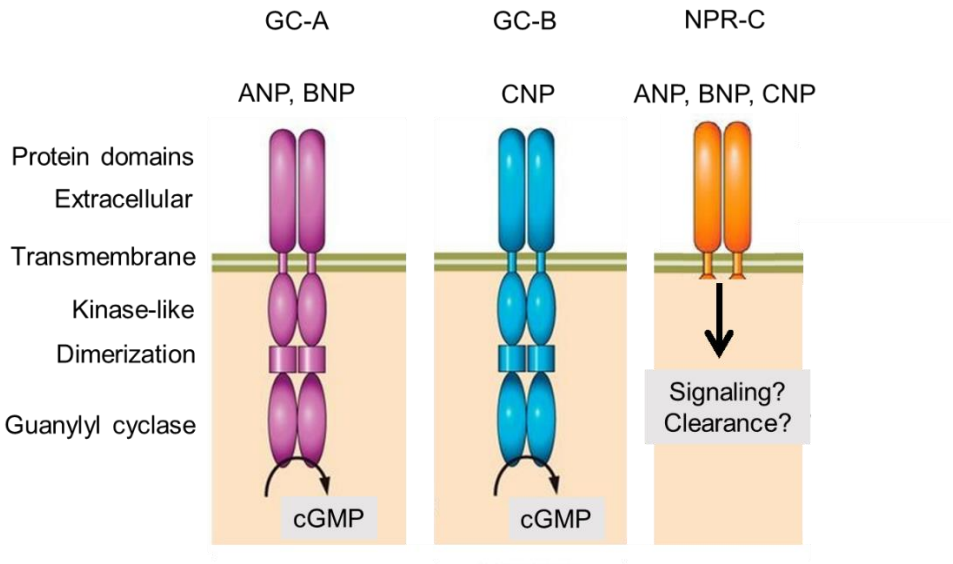

Figure 3: *Structure of the natriuretic peptide receptors activated by the natriuretic peptides GC-A and GC-B receptor possess an extracellular binding domain, a transmembrane and an intracellular domain consisting of a kinase-like, a dimerization and guanylyl cyclase domain. Receptor-binding induces cGMP formation. In opposite NPR-C receptor misses this intracellular guanylyl cyclase activity and effects a clearance and a cGMP-independent signaling function. (modified from (Kuhn, 2016))*

1.3.4.1 GC-A receptor

The GC-A receptor transcribed from NPR1 gene located in humans on chromosome 1q21-q22, consists of an extracellular domain, a membrane spanning region, and an intracellular domain. The intracellular domain can be further divided into a juxtamembrane, also referred to as kinase-like domain, a connecting dimerization domain, and a C-terminal guanylyl cyclase catalytic domain (Lowe, Klisak, et al., 1990; Wilson & Chinkers, 1995). In absence of ANP, the GC-A receptor is present as a homodimer. Ligand binding leads to an activating conformational change in the cyclase domain, resulting in conversion of cytosolic purine nucleotide Guanosine-triphosphate (GTP) to the cyclic form Guanosine 3',5'-monophosphate (cGMP) (Hardman & Sutherland, 1969; Ogawa et al., 2004). As described before, both ANP and BNP serve as ligands for GC-A receptor and are indispensable for arterial blood pressure regulation and volume homeostasis. In the heart, the receptor can also mediate an antihypertrophic effect through inhibition of cardiomyocyte growth (Kuhn, 2003).

1.3.4.2 GC-B receptor as target of C-type natriuretic peptide

The GC-B receptor transcribed from the Npr2 gene located in humans on chromosome 9p12–p21, exhibits a high degree of amino acid sequence identity with the GC-A

receptor, especially in the catalytic intracellular domain. The receptors share a similar domain organization and binding of a ligand to GC-B activates the guanylyl cyclase in a similar manner as GC-A (Chang et al., 1989; Lowe, Klisak, et al., 1990). The guanylyl cyclase leads to conversion of GTP to cyclic GMP (cGMP), which affects three groups of secondary cellular messengers: cGMP-dependent phosphodiesterases (PDEs), cGMP-dependent protein kinases (cGKs) and cGMP-gated cation channels (Figure 4) (Kuhn, 2016). cGMP leads to activation of cAMP-degrading phosphodiesterase PDE2 and inhibition of PDE3 mediating cGMP/cAMP cross-talks (Kuhn, 2016). The second group of affected enzymes are cGKs, existing in two forms: cGKI, majorly expressed in smooth muscles, platelets and cerebellum, and cGKII, expressed in brain and in intestinal cells (Pfeifer et al., 1996). cGKI is known to regulate vascular tone and platelet aggregation, whereas cGKII controls intestinal ion secretion and bone growth (Massberg et al., 1999; Pfeifer et al., 1996; Sausbier et al., 2000). Phosphorylation of the VASP protein at serine 239 serves as a reliable biochemical marker for cGK activity, as it is a well-established target of cGKI and cGKII (Smolenski et al., 1998). Other than ligand binding, the phosphorylation status of the GC-B receptor further regulates the guanylyl cyclase activity. Ligand binding immediately activates the receptor; however, continuous binding to GC-B leads to time-dependent dephosphorylation of the receptor, resulting in its desensitization (Potter, 1998).

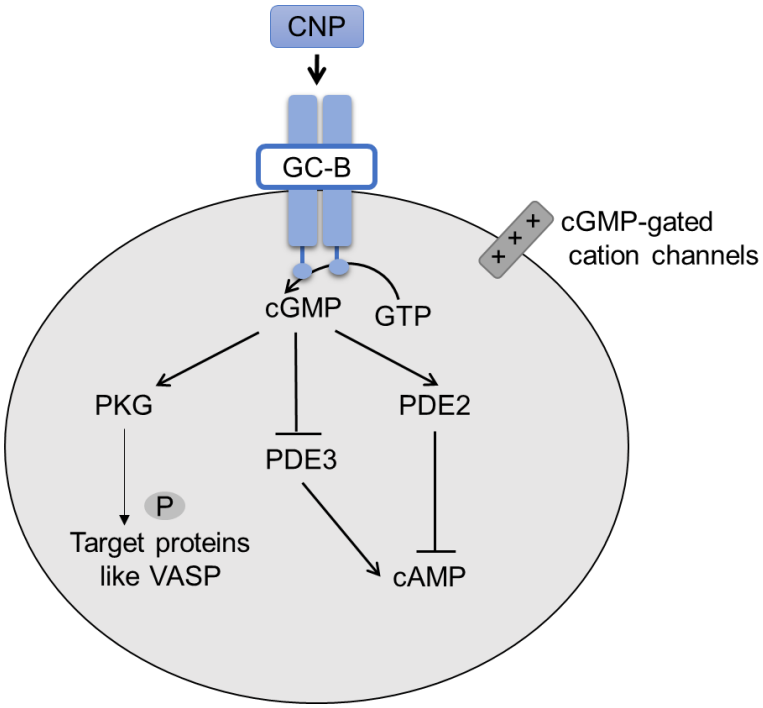

Figure 4: *GC-B receptor mediated signaling pathways activated by binding of CNP Three different pathway forms are activated by cGMP: cGMP-gated cation channels, phosphodiesterases and cGMP-dependent protein kinases (author's scheme)*

1.3.4.3 NPR-C receptor

NPR-C receptor binds to all three NPs. However, unlike GC-A and GC-B, NPR-C lacks an intracellular guanylyl cyclase domain and therefore does not lead to cGMP production on NP binding (Bennett et al., 1991; Porter et al., 1989). Instead, NPR-C was shown to have a clearance role, leading to internalization of NPs and subsequent lysosomal degradation (Almeida et al., 1989; Cohen et al., 1996). In recent years, a number of groups have reported that NPR-C exhibits signaling functions via adenylyl cyclase inhibition and activation of phospholipase 2 mediated by an inhibitory guanine nucleotide regulatory protein, Gi. (Anand-Srivastava et al., 1990; Anand-Srivastava et al., 1987; Hirata et al., 1989) The mechanisms of NPR-C underlying the switch between clearance and signaling functions are still unclear.

1.4 Platelet derived growth factor (PDGF) and receptors

1.4.1 PDGF family of growth factors

Human PDGF was purified from human platelets for the first time in 1979 by the group of Antoniades (Antoniades et al., 1979). In mammals, the PDGF family is composed of four different members, PDGF-A, PDGF-B, PDGF-C, and PDGF-D (LaRochelle et al.,

2001; Li et al., 2000). They build four disulfide linked homo-dimeric isoforms, PDGF-AA, PDGF-BB, PDGF-CC, PDGF-DD, and one hetero-dimeric form, PDGF-AB. Whereas PDGF-A is composed of 211 amino acids, the PDGF-B polypeptide contains 241 amino acids. PDGF-C and PDGF-D are even longer, consisting of 345 and 370 amino acids, respectively (Roskoski, 2018). The PDGF family of growth factors all share a common ~100 amino acids long structure with ~60% identical amino acid sequence. PDGF is synthesized by a variety of cells including, but not limited to, fibroblasts, macrophages, vascular smooth muscle cells, and neurons (Heldin & Westermark, 1999).

1.4.2 Platelet-derived growth factor Receptors (PDGFRs)

The PDGF family function by binding and activating two receptor tyrosine kinases (RTKs), PDGFR-α and PDGFR-β, which function as dimers. The receptor consists of five extracellular immunoglobulin-like domains and an intracellular tyrosine kinase domain (Figure 5). Ligand binding promotes receptor dimerization, leading to autophosphorylation and the initiation of signaling. (Claesson-Welsh et al., 1989).

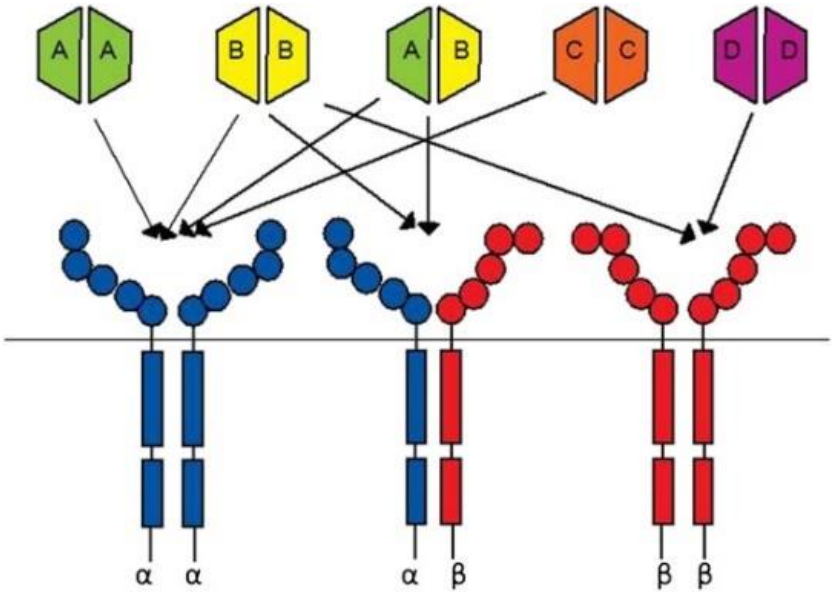

Figure 5: *PDGFα and β with their ligands*
The PDGFs bind with different affinities to their receptors: PDGF-AA, PDGF-BB, PDGF-AB and PDGF-CC to PDGFα, PDGF-BB and PDGF-AB to PDGFαβ and PDGF-BB and PDGF-DD to PDGFβ (Donovan et al., 2013)

The members of the PDGF-family interact with the RTKs at different affinities. It has been demonstrated that PDGF-A and PDGF-C predominantly bind to PDGFR-α, whereas PDGF-D binds to PDGFR-β, and PDGF-B is able to target both RTKs. This means PDGF-AA, -AB, -BB, and -CC oligomers can induce PDGFR-αα-homodimers. PDGF-AB

and -BB induce PDGFR-αβ-heterodimers. PDGF-BB and -DD induce a PDGFR-ββ dimer. Some studies have also reported that PDGF-DD stimulates both PDGFR-α and -β to the same extent (Bergsten et al., 2001; Donovan et al., 2013; Li et al., 2000).

1.4.3 Effects of PDGF in pulmonary fibrosis

The function of the PDGF family has been known for decades and established, as a serum growth factor for different cell types such as fibroblasts, smooth muscle cells, and neural glia cells (Kohler & Lipton, 1974; Ross et al., 1974; Westermark & Wasteson, 1976). Animal models of bleomycin and chronic hyperoxia induced lung injury identified a role of PDGF-B in the progression of lung fibrosis (Fabisiak et al., 1989; Walsh et al., 1993). Furthermore, alveolar macrophages in IPF patients release a significantly higher amount of PDGF compared to macrophages from healthy controls, thereby inducing profibrotic effects (Martinet et al., 1987). Yi *et al*. demonstrated that intratracheal injection of PDGF-BB causes typical fibrotic changes in lungs like increased proliferation of pulmonary cells and deposition of collagen (Yi et al., 1996).

1.5 Forkhead box transcription factor

Forkhead box transcription factors are a family of transcriptional regulators, possessing an evolutionary conserved “forkhead” or “winged-helix” DNA binding domain (Jackson et al., 2010). The first member of this family was identified in a fruit fly (*Drosophila melanogaster)* in 1989. The family was named after the head-like structure detected in embryos containing a mutation of the region-specific gene *forkhead* (*fkh*) (Weigel & Jackle, 1990; Weigel et al., 1989). Since the initial identification, at least 100 additional members of this family have been discovered, which are divided into 19 subgroups (FoxA-FoxS) (Jackson et al., 2010; Kaestner et al., 2000). FOX proteins are key regulators of gene networks involved in important processes such as proliferation, differentiation, metabolism, senescence, survival, and apoptosis (Lam et al., 2013). In recent years, several diseases could be attributed to dysfunction of Fox factors like osteoporosis, cancer and many more (Iyer et al., 2013; Lin et al., 2002).

1.5.1 Transcription family subunit FoxO

The subgroup FoxO was first identified based on chromosomal translocation in rhabdomyosarcomas (Anderson et al., 1998). In mammals, it consists of four members, FoxO1, FoxO3, FoxO4, and FoxO6. All four isoforms are able to bind DNA with their helix-turn-helix structure to the same conserved consensus core recognition sequence

5´-TTGTTTAC-3´ (Xie et al., 2012). FoxO1, FoxO3, and FoxO4, are ubiquitously expressed in a variety of tissues, whereas FoxO6 expression is restricted to the brain (Jacobs et al., 2003; Ting & Zelinski, 2017). Members of this class regulate metabolism, cell-cycle progression, oxidative stress resistance, and apoptosis, by controlling target gene expression. For example, FoxO can regulate apoptosis by activating the transcription factor of FasL, or by activating the pro-apoptotic Bcl-2 family member Bim (Carter & Brunet, 2007).

1.5.2 Regulation of FoxO activity by phosphorylation

When active, FoxO is localized in the nucleus and interacts with the target DNA sequence. In presence of growth factors like PDGF-BB and Insulin-like growth factor 1 (IGF-1), FoxO is phosphorylated at specific serine and threonine residues. This phosphorylation mediates binding to a 14-3-3 scaffold protein, followed by nuclear exclusion and proteasomal degradation (Aoki et al., 2004; Takaishi et al., 1999). FoxO phosphorylation is mainly carried out by protein kinase B (AKT) from the Phosphoinositide-3-kinase (PI3K)/ 3-phosphoinositide-dependent protein kinase (PDK1)/ AKT cascade. This cascade can be activated by insulin or growth factors like IGF-1 or PDGF-BB. AKT phosphorylates FoxO1 and FoxO3 at threonine 24 and threonine 32, respectively, resulting in cytoplasmic translocation and degradation. (Brunet et al., 1999; Medema et al., 2000; Scodelaro Bilbao & Boland, 2013). Other than AKT, the mitogen activated protein-kinase (MEK)/ extracellular signal-regulated kinase (ERK) cascade is shown to phosphorylate FoxO. It can also be activated by PDGF-BB, where via RAS/RAF/MEK signaling pathway, MEK is phosphorylated. The kinase MEK phosphorylates and activates ERK, which in turn finally phosphorylates FoxO, leading to its degradation (Lubinus et al., 1994; Roy et al., 2010).

1.5.3 Downregulation und degradation of FoxO3 in IPF

In IPF fibroblasts, the mRNA expression of FoxO3 is significantly downregulated compared to healthy fibroblasts. Furthermore, the phosphorylated, inactive form of FoxO3 was upregulated at protein level, confirming the increased degradation of FoxO3 (Al-Tamari et al., 2018). Further, microRNA-96, found to be upregulated in IPF fibroblasts, was shown to downregulate FoxO3 mRNA expression by binding to its 3`-untranslated region (Nho et al., 2014).

Functionally, siRNA mediated FoxO3 knockdown in healthy fibroblasts led to increased proliferation confirming an antiproliferative effect of the factor (Al-Tamari et al., 2018).

The antiproliferative effect was an outcome of cell cycle arrest mediated by increased expression of cyclin-dependent kinase inhibitor p27(kip1) (Schmidt et al., 2002). Also, fibroblast-myofibroblast differentiation markers, collagen1 and collagen3 exhibited elevated expression upon FoxO3 knockdown, demonstrating the antifibrotic effect of FoxO3 (Al-Tamari et al., 2018). Studies with cardiac fibroblasts have also shown that FoxO3 silencing reinforces TGFβ induced transformation of myofibroblasts, while inhibition of FoxO3 degradation had the opposite effect (Vivar et al., 2020). These data established FoxO3 as a negative regulator of myofibroblast conversion.

1.6 Aims of the study

Pathologically altered lung (myo-) fibroblasts exhibiting increased proliferation, migration, and collagen production, drive IPF development and progression (Al-Tamari et al., 2018; Sime et al., 1997; Tisler et al., 2020; Worke et al., 2017). Fibrogenic factors such as PDGF-BB contribute to these pathological alterations (Yi et al., 1996) and endogenous counter-regulating factors are barely known. Published studies have described a protective role of exogenously administered CNP in pathological tissue remodeling, for example in cardiac and hepatic fibrosis (Bae, Hino, Hosoda, Miyazato, et al., 2018; Horio et al., 2003). CNP and its cGMP producing GC-B receptor are expressed in the lung, but it is not known whether the endogenous hormone exerts paracrine anti-inflammatory and antifibrotic actions on lung fibroblasts (Hirsch et al., 2003; Nakanishi et al., 1999). Previous data from AG Kuhn indicate that CNP prevents PDGF-BB induced collagen1 and 3 expression in isolated murine lung fibroblasts, however, the receptor responsible for this effect has not yet been investigated. Furthermore, the effect of CNP on PDGF-BB induced migration and proliferation was not explored.

Therefore, based on these previous findings, this thesis aimed to specifically address the following:

1. Investigate whether GC-B mediates effects of CNP on PDGF-BB induced collagen expression in murine lung fibroblasts

2. Determine if CNP exerts an effect on PDGF-BB induced murine fibroblast proliferation and migration

3. Examine the human physiological and pathophysiological relevance of the murine findings by employing human lung fibroblasts isolated from patients with IPF and controls

2 Materials and Methods

2.1 Materials

2.1.1 Cell culture medium and reagents

Table 1: Human fibroblast growth medium

Ingredients:	Concentration:	Company:
MCDB 131 medium (-) L-Glutamine	93%	*Gibco Cell Culture, New York (10372-019)*
Fetal Calf Serum (FCS)	5%	*Gibco Cell Culture, New York (10270-106)*
Penicillin/Streptomycin (100U/ml)	100U/ml	*Gibco Cell Culture, New York (15140122)*
L-Glutamine 2mM	2mM	*Gibco Cell Culture, New York (A29168-01)*
Human FGF-basic	2ng/ml	*Peprotech, Hamburg (#100-18B-10KG)*
Recombinant Human EGF	0.5ng/ml	*Gibco Cell Culture, New York (PHG0314)*
Insulin solution human	5µg/ml	*Sigma-Aldrich GmbH, Steinheim (19278)*

Table 2: Murine fibroblast growth medium

Ingredients:	Concentration	Company
Dulbecco`s Modified Eagle Medium (DMEM) F-12 Nutrient Mixture (Ham)	89%	*Gibco Cell Culture, New York (11320-074)*
Fetal Calf Serum	10%	*Gibco Cell Culture, New York (10270-106)*
Penicillin/Streptomycin (100U/ml)	1%	*Gibco Cell Culture, New York (15140122)*

Table 3: Cell culture reagents

Name:	Company:
Complete Mini Protease inhibitor cocktail tablets	*Roche Diagnostics GmbH, Mannheim (11836153001)*
C-type natriuretic Peptide (CNP)	*Bachem, Bubendorf (4019911.1000)*
Dimethyl sulfoxide (DMSO)	*Sigma-Aldrich GmbH, Steinheim (D5879)*
4-Hydroxy-Tamoxifen Ready Made Solution	*Sigma-Aldrich GmbH, Steinheim (SML1666)*
PhosSTOP EASYpack	*Roche Diagnostics GmbH, Mannheim (04906837001)*
Pierce ™ RIPA Buffer	*Thermo Fisher Scientific GmbH, Dreieich (89900)*
Recombinant Human PDGF-BB	*Peprotech, Hamburg (100-14B)*
Recombinant Murine PDGF-BB	*Peprotech, Hamburg (315-18)*
Trypsin-EDTA 0.25% (1x)	*Gibco Cell Culture; New York (25200-056)*

2.1.2 Other chemicals and reagents:

Table 4: Other chemicals and reagents

Name:	Company:
Agarose	*Bio&Sell GmbH, Feucht (B20.46.500)*
Ammoniumpersulfate (APS, 10 %)	*Sigma-Aldrich GmbH, Steinheim (A3678)*
Bromophenolblue, pH 6,7	*Sigma-Aldrich GmbH, Steinheim (B5525)*
BSA-Endotoxin low Bovine serum Albumin	*Gerbu Biotechnik GmbH, Heidelberg (1063.0500)*
Chromatography paper	*Hartenstein, Würzburg (GB46)*
Dispase® II (neutral protease, grade II)	*Roche Diagnostics GmbH, Mannheim (04942078001)*
EDTA	*MERCK KGaA, Darmstadt (108418.1000)*
Ethanol denatured ≥99.8%	*Carl Roth GmbH + CO. KG, Karlsruhe (K928.3)*
GenLadder (100bp+1.5kb)	*Genaxxon bioscience GmbH, Ulm (M3094.5050)*
Glycine	*Sigma-Aldrich GmbH, Steinheim (1.04169.1000)*
Hank´s Balanced Salt Solution	*Sigma-Aldrich GmbH, Steinheim (H9394)*
3-Isobutyl-1-Methylxanthine	*Sigma-Aldrich GmbH, Steinheim (17018)*
Isopropanol	*Carl Roth GmbH + CO. KG, Karlsruhe (CP41.3)*
ß-Mercaptoethanol	*Sigma-Aldrich GmbH, Steinheim (M7522)*
Milk powder blotting grade	*Carl Roth GmbH + CO. KG, Karlsruhe (T145.2)*
Nitrocellulose Blotting membrane Nucleic acid and Protein application	*GE Healthcare, Freiburg (10600001)*
N,N,N´,N´-tetramethylethylendiamine	*Sigma-Aldrich GmbH, Steinheim (T9281)*
PageRuler Prestained Protein Ladder, 10 - 170 kDa,	*Thermo Fisher Scientific GmbH, Dreieich (26616)*
Paraformaldehyde (4%)	*PanReac AppliChem, Darmstadt (252931.1214)*
PCR Red Master Mix	*Genaxxon bioscience GmbH, Ulm (M3029)*
Pierce™ ECL Western Blotting Substrate	*Thermo Fisher Scientific GmbH, Dreieich (32106)*
PCR Primer Antisense	*Eurofins Scientific, Germany*
PCR Primer Sense	*Eurofins Scientific, Germany*
Proteinase K Gennox	*Genaxxon bioscience GmbH, Ulm (M3036)*
Rotiphorese®Gel 30	*Carl Roth GmbH + CO. KG, Karlsruhe (3029.1)*
Sodium acetate	*MERCK KGaA, Darmstadt (1.06268.0250)*
Sodium-Dodecyl sulfate (SDS)	*Serva Electrophoresis GmbH, Heidelberg (20765)*
Triton™ X-100	*Sigma-Aldrich GmbH, Steinheim (T9284)*
Trizma® base	*Sigma-Aldrich GmbH, Steinheim (T6066)*
Tween®	*Sigma-Aldrich GmbH, Steinheim (P1379)*

2.1.3 Equipment

Table 5: Equipment

Name:	*Company:*
Balance	*Sartorius,Göttingen (1204)*
Biometra Fastblot™	*Analytik Jena, Jena*
Electrophoresis chamber	*Institute of Physiology*
FluorChem SP Chemiluminescence Detection-system	*Alpha Innotech GmbH, Germany*
Fine balance	*Sartorius, Göttingen (TE214S)*
Fluorescent Microscope BX41	*Olympus, Shinjuku*
Heraeus FRESCO 21 Centrifuge	*Thermo Fisher Scientific GmbH, Dreieich*
Heraeus Megafuge 16R Centrifuge	*Thermo Fisher Scientific GmbH, Dreieich*
Heraeus Multifuge 1 S-R	*Thermo Fisher Scientific GmbH, Dreieich*
Infinite® M Plex	*Tecan Group, Männedorf*
Microscope CKX41	*Olympus, Shinjuku*
Polyacrylamide gel electrophoresis-system	*PEQlab a VWR company, Erlangen*
Power Supply 250V	*VWR International, Radnor*
Simpli Nano spectrophotometer	*GE Healthcare Life Sciences*
Thermomixer compact	*Eppendorf AG, Hamburg*
T1 Thermocycler	*Biometra, Göttingen*

2.1.4 Kits

Table 6: Kits

Name:	Company:
BCA Assay: Protein Assay Kit	*interchim® uptima, Germany*
Cell Fractionation Kit	*NanoTools Antikörpertechnik GmbH und Co. KG, Teningen(3004)* (3002-0150/CF)
BrdU Cell Proliferation ELISA Kit (colorimetric)	*Roche Diagnostics GmbH, Mannheim (11647229001)*

2.2 Methods:

2.2.1 Cell culture

2.2.1.1 Human lung fibroblasts

Human lung fibroblasts from lung specimens of control and IPF patients were provided by University of Giessen and Marburg Lung Center Biobank. The cells were used for experiments after thawing from passage 3-7.

The cells were cultured in the incubator at 37°C and 5% CO_2 in 10 cm dishes with growth medium (Table 1). At a confluency of around 95% percent, the fibroblasts were subcultured by trypsinization. Shortly, medium was aspirated and cells were washed with

phosphate-buffered saline (PBS) (Table 13). 1ml Trypsin was added and incubated for 3-5 minutes at 37°C until the cells detached. DMEM medium containing 10% FCS and 1% Penicillin/Streptomycin was added to neutralize the trypsin. The cell suspension was collected in a falcon for the following centrifugation at 300g for 5min. It was resuspended in fresh human fibroblast medium and seeded into new culture plates.

Human fibroblasts were stimulated and treated under serum starvation conditions. (MCDB-131 basal medium + 1% L-glutamine + 1% Penicillin/Streptomycin).

Surplus cells were frozen in liquid nitrogen for later use. After trypsinization, one million cells were resuspended in 1ml medium containing 5% dimethyl sulfoxide (DMSO). After this, the cells were aliquoted in cryovials and stored overnight in a box filled with isopropanol in -80°C freezer. The following day the aliquots were transferred into liquid nitrogen for longer storage.

2.2.1.2 Primary mouse lung fibroblasts

2.2.1.2.1 Isolation of Primary mouse lung fibroblasts

Primary mouse lung fibroblasts were isolated from three to six months old mice. The mice were killed with cervical dislocation and intact lungs were perfused with ice cold PBS via the right ventricle. After that, lungs were isolated, minced into small pieces, washed with Hank's Balanced Salt Solution and digested with 5U/ml Dispase solution for 60min at 37°C by gentle shaking. The cell suspension obtained after the digestion was filtered through a 70µm strainer. The filtrate was centrifuged twice for 5 minutes each at 300g and the cells were resuspended in fresh fibroblast medium (Table 2) and seeded into 25cm^2 flasks. The flasks were washed after three hours with PBS and medium was replaced. As fibroblasts exhibit strong adherence compared to other cell types, washing and changing of medium after a short time of isolation helps to remove other contaminating cell types. The purity of the isolation method has been previously verified by immunocytochemistry for fibroblast markers Vimentin, α Smooth Muscle Actin and PDGFRα by Eva Lessmann (Institute of Physiology, Würzburg). At a confluency of around 95% cells were split and used for the experiments in passage 1-2.

2.2.1.2.2 Generation of GC-B-Knock out (KO) fibroblasts

To generate knock out of the GC-B receptor *in vitro*, fibroblasts from Col1a2Cre^{ERT2}; GC-B$^{flox/flox}$ mice were isolated and treated with 100nM and 200nM 4-Hydroxy-Tamoxifen (4-OH Tamox) in passage 1 for 72 hours. The added 4-OH Tamox is able to bind in the

cytoplasm at mutated hormone-binding domains of the estrogen receptor, which are fused to the Cre recombinase. This ligand-binding activates and leads to the translocation of the Cre-recombinase from the cytoplasm to the nucleus, where the cre/loxP-recombination system takes effect. The recombinase is able to delete a DNA-sequence, which is framed by two loxP-acid sequences, prohibiting the gene expression in this case the GC-B receptor. After 72 hours, medium containing 4-OH Tamox was removed and the cells were split and seeded for experiments. For confirmation of KO, both concentrations of 4-OH Tamox were used. For all later experiments, only 200nM 4-OH Tamox was used.

Fibroblasts were cultured in murine fibroblast growth medium (Table 2) and for serum starvation DMEM/F12 containing 1% Penicillin/Streptomycin was added and fibroblasts were stimulated under these conditions.

2.2.2 Western blot analysis

2.2.2.1 Stimulation for Western Blot

Fibroblasts (both human and murine) were serum starved for 24 hours in appropriate medium, followed by pretreatment with CNP 10nM and 100nM for 30 minutes. After this 50ng/ml PDGF-BB was added for 30 more minutes to check for the phosphorylation of VASP, FoxO3, ERK and AKT. To investigate the changes in Collagen1 and MMP9 expression, PDGF-BB stimulation was carried out for 24 hours.

2.2.2.2 Protein isolation from cells

Proteins were isolated from cultured and stimulated cells after washing them with PBS followed by adding of 120µl or 90µl RIPA lysis buffer containing protease and phosphatase inhibitor for 6cm or 3cm dishes respectively. Cells were incubated for 10 minutes on ice and then scratched with a cell scraper. After collecting them in 1,5ml Eppendorf tubes, the samples were centrifuged at 14000RPM and supernatants were transferred to new labelled tubes. The lysates were directly frozen in liquid nitrogen and stored in -80°C.

2.2.2.3 Cell fractionation

To check for the expression of proteins in the different compartments of the cell, in our case from the membrane, subcellular fractionation of cell lysates was carried out.

After appropriate stimulation, the fibroblasts were washed with PBS and scraped off with cell scraper from the dishes. Cells with PBS were collected in a falcon and centrifuged for 5 minutes at 300g. After removing of the supernatant, the pellet was resuspended in 1ml PBS and was transferred to a 1,5ml Eppendorf tube. The tubes were centrifuged at 1000g for 10 minutes and the supernatant was removed. Pellets were directly frozen in liquid nitrogen and stored at -80°C.

For fractionation the Cell Fractionation kit (NanoTools) was used. Before beginning, the lysis buffers containing Protease and Phosphatase inhibitor were incubated at 37°C. To the thawed pellet 150µl Cell fractioning buffer Cytoplasm (CF-CYT) was added and carefully resuspended under optical control until the pellet was completely dissolved. The buffer was centrifuged for 8 minutes at 1000g at 4°C and the supernatant (cytoplasmic fraction) was collected. The pellet was resuspended in 150µl Cell fractioning buffer Membrane (CF-MEM) and incubated for 5 minutes at room temperature (RT). The samples were centrifuged again for 8 minutes at 2000g and the supernatant (membrane fraction) was separated. The fractions were quantified and used for western blotting.

2.2.2.4 Protein quantification

For protein quantification the Biuret reaction in combination with the Bicinchoninic acid Assay (BCA) was used (Smith et al., 1985). This assay is based on binding of Cu^{2+} to peptide-connections resulting in the reduction of Cu^{2+} to Cu^{+}. This leads to the building of a colored complex of the copper ion with the Nitrogen of the BCA in alkaline milieu and the increase in color intensity (measured by photometer at 560nm wavelength) is directly proportional to the protein concentration. Different concentrations of bovine serum albumin (BSA) in range of 0.05 - 1mg/ml were used as standard and pipetted as duplicates. RIPA buffer was used for background control and samples were also pipetted in minimum duplicates to exclude pipetting failures. For reaction 300µl of BCA-Cu_2SO_4 solution at ratio of 50:1 was added. After incubating 30 minutes at 37°C the color intensity was recorded in the ELISA microplate reader. Protein concentrations were directly calculated according to the standard curve of the BSA standards. Then the volumes of the supernatants were measured and transferred in new Eppendorf tubes.

In the last step the proteins were prepared for western blotting by adding of 3x Laemmli buffer (Table 12) in ratio 1:3. The Sodium Dodecyl Sulfate (SDS) in this buffer together with the SDS in the running buffer (Table 15) had the effect to overlay negative charge on the single proteins resulting in an equal electrical charge of all proteins. This allows

the proteins to be separated later in the gel according to their molecular weight. β-mercaptoethanol breaks the disulphide bridges and along with SDS and heating the samples at 95°C for 10min, helped in denaturing and linearizing of the proteins.

The samples were cooled down at RT and directly used for western blot or frozen at -20°C for later use.

2.2.2.5 SDS Polyacrylamide gelelectrophoresis (SDS-PAGE)

For separation of the proteins a Polyacrylamide gel consisting of a stacking and resolving gel was used. The proteins migrate under electric field towards cathode (+) and are separated according to their chain length that is proportional to their molecular weight. The gel was prepared between two glass plates of a PAGE system. Depending on the molecular weight of the proteins to be resolved, an 8 or 10% resolving gel (Table 14) was pipetted into the glass plate cassette. To prevent contact with air, Isopropanol was added on top until the gel was polymerized for around 30 minutes. After removing the Isopropanol and washing with ddH_2O, the stacking gel solution (Table 16) was put in the cassette and a comb was inserted. After polymerization the comb was carefully removed, the wells were cleaned to remove any gel pieces and the chamber was filled with running buffer (Table 15). Along with molecular weight marker, 10 or 30µg of samples were loaded, depending on the proteins, that need to be checked. To allow stacking of samples, the gel was run for 1 hour at 75V. As soon as the protein samples reached the resolving gel, the voltage was set to 130V und run for 1-2 hours.

2.2.2.6 Semi-dry-transfer

In this step the proteins separated on the gel were transferred to a Nitrocellulose membrane in a semi dry transfer chamber. Therefore, four chromatography paper, the membrane and the gel were incubated for 15 minutes in transfer buffer (Table 20) and then arranged in the blotting chamber in the following order: two Chromatography paper, membrane, gel and two paper again on top. For transfer the voltage was set to 17V for 1hr.

2.2.2.7 Blocking and developing of membranes

Once the proteins were transferred, the membranes were cut according to the size of proteins. To minimize non-specific binding, the membranes were blocked for 1 hour on shaker at RT with 5% bovine serum albumin (BSA) in Tris-buffered saline with Tween20 (TBS-T) (Table 19) or 5% milk in TBS-T. Overnight the membranes were incubated in primary antibodies, which were diluted in blocking buffer. Next day, 1xTBS-T buffer was

used to wash the membranes thrice for 10min and they were incubated with a dilution of secondary Horseradish peroxidase-conjugated antibodies in blocking buffer. After incubation of the membranes for 1hr at RT with gentle shaking, 1x TBS-T was used to wash them 3 times for 10min. For detection of the signal, membranes were incubated with ECL substrate in the Image reader (FluorChem SP Chemilumineszenz detection system). The exposure time was adapted to the base of signal intensity.

2.2.2.8 Densitometric analysis of the immunoblots

Western blots were quantified using the FluorChem Sp software. Expression was quantified using bands intensity values (in arbitrary units), which were normalized to the housekeeping genes (GAPDH or Na^+-K^+ ATPase).

2.2.3 Radioimmunoassay (RIA)

To investigate the cGMP response to CNP in the lung fibroblasts, RIA was performed. In short, fibroblasts (murine and human) were washed 3 times with PBS and serum starved for 3 hours, followed by 15min incubation with unspecific phosphodiesterase inhibitor 3-Isobutyl-1-Methylxanthin (IBMX) to prevent the reconversion of cGMP in GMP. Then cells were stimulated with different concentrations of CNP (0, 0.1, 1, 10, 100nM) for 15 minutes. After stimulation, medium was removed and 70% ice cold Ethanol was immediately added to stop the reaction. The plate was stored in -80 for overnight. Next day, liquid was evaporated in water bath and the pellet was dissolved with Sodium acetate (50mM, pH 6,0). The further steps to measure the cGMP amount by RIA was kindly accomplished by Lisa Krebes (Institute of Physiology, Würzburg).

RIA allows to measure the small amount of cGMP with a very high sensitivity and is based on an antigen-antibody-reaction. cGMP in the samples is acetylated and this acetylated cGMP competes with radioactive marked cGMP (^{125}Iodine-cGMP; Tracer) for binding to a cGMP-antibody. The unbound radioactive tracer is measured. The difference between the radioactive amount added in the beginning and the unbound radioactive tracer allows to calculate the cGMP amount based on standard curves. This means higher cGMP concentration in samples corresponds to a lower measured radioactive intensity.

2.2.4 Genotyping

To check for the expression of Cre recombinase and the knockout of the GC-B-receptor in GC-B$^{flox/flox}$ and Col1a2Cre^{ERT2}; GC-B$^{flox/flox}$ mice and also fibroblasts, DNA from tails

and cells were isolated and Polymerase Chain Reactions (PCRs) for Col1a2Cre^{ERT2} and GC-B^{flox} were carried out.

2.2.4.1 Isolation of genomic DNA from tissue

To isolate the Deoxyribonucleic acids (DNA) from the tails, 200µl lysis buffer with 10µl Proteinase K Gennox was added and incubated for 30 minutes at 55°C with 1100RPM shaking in the thermomixer. Proteinase K degraded the proteins and released nucleic acids. To stop the reaction, the samples were heated at 95°C for 25 minutes. After centrifugation at 20 000g for 10 minutes, the supernatant containing the DNA was transferred to 1,5ml Eppendorf tubes. DNA was precipitated by adding of 50µl 3M sodium acetate and 450µl Isopropanol followed by inverting for 10 times. The samples were centrifuged again at 20 000g for 30 minutes and supernatant was removed. The pellet with the DNA was washed with 50µl of 70% Ethanol and again spun at 20 000g for 20 minutes. After removing the supernatant, the pellet was centrifuged once more at 20 000g for 5 minutes to remove the residual liquid and dried. As a last step the DNA pellet was resuspended in 20µl TE-Buffer. The DNA concentration and purity was measured spectrophotometrically with SimpliNano spectrophotometer. Here the absorption of 2µl sample was checked at a wavelength of 260nm and the dilution factor could be corrected where necessary. With a second measurement at wavelength 280nm it was possible to exclude contamination with proteins. This is given when the quotient of the optical density OD260/OD280 is between 1.6 and 2.2. For blank reduction the absorption was also measured with 2µl RNAase free water.

2.2.4.2 Isolation of genomic DNA from fibroblasts

The cell pellets were collected after trypsinization as described under cell fractionation (2.2.2.3). Samples were digested in 495µl digestion buffer + 5µl Proteinase K and incubated for 5 minutes at 55°C with gentle shaking. The reaction was stopped by heating at 95°C for 20 minutes without shaking. From this point the DNA extraction was performed in the similar manner as DNA extraction from tails (2.2.4.1). The only difference was that the pellet was washed this time with 1000µl 70% Ethanol instead of 50µl.

2.2.4.3 PCR and DNA Gel electrophoresis

Polymerase chain reaction (PCR) is a technique that allows amplification of target DNA sequences by employing target specific primers. In order to confirm the differences in

the genotype, PCR was performed from the isolated DNA (200ng) by preparing a 25µl PCR reaction mixture as mentioned below in Table 7.

Table 7: PCR reaction mixture

Ingredients:	Volume:
PCR-H_2O	8.5µl
PCR Red MasterMix	12.5µl
Primer Sense	1µl
Primer Antisense	1µl
DNA	2µl
Complete volume:	25µl

Genotyping PCRs for Cre (Table 8), GC-B$^{flox/flox}$ and GC-B KO allele (Table 9) were performed using sequence specific primers (Table 10).

Table 8: Program PCR for Col1a2Cre^{ERT2} allele

No. of cycles:	Temperature:	Time:	Step:
1	94°C	3 minutes	Initial denaturation
35	94°C	30 sec	Denaturation
	62°C	30 sec	Annealing
	72 °C	30 sec	Elongation
1	72 °C	2 minutes	Final Elongation
1	4 °C		Hold

Table 9. Program PCR for GC-B$^{flox/flox}$ and GC-B-KO allele

No. of cycles:	Temperature:	Time:	Step:
1	99°C	3 minutes	Initial denaturation
34	94°C	30 sec	Denaturation
	58°C	30 sec	Annealing
	72 °C	30 sec	Elongation
1	72 °C	2 minutes	Final Elongation
1	4 °C		Hold

After PCR 1x TAE (Table 18) was prepared. The products of the PCR were separated on a 2% agarose gel by running for 40 minutes at 80V. To confirm the size of the DNA bands and ensure the validity of the experiment, 7µl of GenLadder (100bp DNA ladder) was used.

Table 10: List of Primers

Name:	Primer:	Sequenz (5`- 3`):	Length:
Col1a2Cre^{ERT2}	iFibrofwd	TCCAATTTACTGACCGTACACCAA	500bp (Cre)
	iFibrorew	CCTGATCCTGGCAATTTCGGCTA	
GC-B$^{flox/flox}$; GC-B-KO	D1	GGACGACCCATCCTGTGATA	150bp (KO), 600bp ($^{flox/flox}$)
	R3	GTTACAAACAAAAGCAAGATAAATACC	

2.2.5 Immunocytochemistry

The confluent fibroblasts were split into a 24 well plate containing 12mm coverslips with around 40 000 cells per well. After defined stimulation, cells were washed once with PBS and fixed by adding 250µl of 4% paraformaldehyde (PFA) to each well for 10 minutes at RT. The plate was washed three times with PBS, permeabilized with 0,1% Triton X-100 in PBS for 2 minutes to enable staining of the intracellular collagen and blocked with 250µl blocking buffer (2% BSA in PBS) for 1 hour at RT with shaking. The primary antibody diluted in PBS with 2% BSA was incubated overnight. Next day, coverslips were washed and fluorescent labelled secondary antibodies diluted in PBS with 2% BSA was added for one hour. From this step forward the experiment was performed in dark to prevent a bleaching of the fluorescent labelling. After last wash, the coverslips were removed from the wells, dried and mounted on glass slide with DAPI containing mounting medium. The slides were dried overnight in dark at +4°C and then sealed with nail polish. Pictures were taken using the BX41 fluorescence microscope (Olympus) and evaluated with ImageJ.

2.2.6 Gap closure migration assay

In the gap closure migration assay, we examined the time needed by the migrating fibroblasts to close a mechanical scratch in a confluent fibroblast layer.

The confluent fibroblasts in 24 well plate were starved for 24 hours. Then a scratch was made with a 100µl pipette tip manually and checked under the microscope. To remove the detached cells, the plate was washed with PBS. Medium without CNP and with CNP 10nM and 100nM was added to the cells. After incubation for 30 minutes, fibroblasts were stimulated with 50ng/ml PDGF-BB. Unstimulated cells were kept as controls. Immediately after addition of PDGF-BB, first pictures of the gaps were recorded and labeled as time point zero. The location was marked to relocate it for the following time points. From now pictures at 4 hours, 8 hours and 24 hours were taken at the same point in each well.

The quantification of the gap was done according to the gap size measured at time point zero. Every following time point was calculated as percentage of the scratch at the beginning and measured with ImageJ.

2.2.7 BrdU Proliferation assay

The proliferation of the cells was reviewed using colorimetric BrdU incorporation assay kit. This kit works by measuring Bromodeoxyuridine (BrdU), an analog of Thymidine or Deoxyuridine, which is incorporated into newly synthesized DNA.

10 000 fibroblasts per well were seeded in 96 well plate and serum starved for 24 hours. Next day, the cells were pretreated with CNP 10nM and 100nM for 30 minutes, followed by 50ng/ml PDGF-BB stimulation. 22 hours after stimulation, BrdU labeling solution was used for incubation of the cells for 2 hours. After this, wells were washed with PBS and FixDenat solution was added for 30 minutes to fix the cells. After fixation, cells were incubated for 90 minutes with anti BrdU Peroxidase antibody. Again, the wells were washed thrice with PBS and substrate solution was added until color developed. In ELISA microplate reader the absorbance was measured at 370nm with reference at 492nm. Blank (medium without cells) and background (cells without BrdU) controls were kept to ensure validity of the experiment.

2.2.8 Statistical analysis

For the statistical evaluation Graph Pad Prism 8.0.1 was used. All data are expressed as Mean ± standard error of the mean (S.E.M.) Statistical comparisons of samples were performed by Student's unpaired t test for comparing two groups or ordinary one-way ANOVA for multiple comparisons with post hoc test. Difference with $p<0.05$ between the groups was considered significant.

3 Results

3.1 Antifibrotic CNP effect on murine lung fibroblasts- Role of the GC-B-receptor

3.1.1 Confirmation of the GC-B-receptor knock out (KO)

3.1.1.1 Confirmation with PCR and DNA gel electrophoresis

To investigate the role of the GC-B receptor in mediating the CNP driven protective effects, GC-B knock-out (KO) murine lung fibroblasts were generated *in vitro*. Fibroblasts were isolated from mice with the following genotypes: Col1a2Cre^{ERT2}; GC-B$^{flox/flox}$ and GC-B$^{flox/flox}$. Fibroblasts were treated with DMSO as vehicle or 4-Hydroxy Tamoxifen (4-OH Tamox) for 72 hours. In Col1a2Cre^{ERT2}; GC-B$^{flox/flox}$ mice, Cre recombinase is expressed in fibroblasts under the collagen 1a2 promoter. This Cre recombinase is activated by 4-OH Tamox binding, leading to its nuclear translocation and removal of the loxP-framed GC-B receptor DNA.

First, the genotypes were validated and 4-OH Tamox induced Cre KO was demonstrated. PCR reactions with sequence specific primers followed by DNA gel electrophoresis was performed with DNA isolated from mice tails and fibroblasts treated with 4-OH Tamox. Cre recombinase was exclusively present in tails (Figure 6, A) and fibroblasts (Figure 6, B, upper gel) isolated from Col1a2Cre^{ERT2}; GC-B$^{flox/flox}$ mice but not in the GC-B$^{flox/flox}$ samples, confirming the genotypes were correct.

Lastly, the GC-B-receptor KO after 4-OH Tamox treatment was verified. DNA isolated from untreated and treated fibroblasts both showed a band of 600 bp, corresponding to GC-B *flox* allele. However, only the 4-OH Tamox treated fibroblasts isolated from Col1a2Cre^{ERT2}; GC-B$^{flox/flox}$ mice displayed the 150 bp GC-B KO band (Figure 6, B, lower gel), indicating a GC-B KO on a genetic level exclusively in the Col1a2Cre^{ERT2}; GC-B$^{flox/flox}$ fibroblasts.

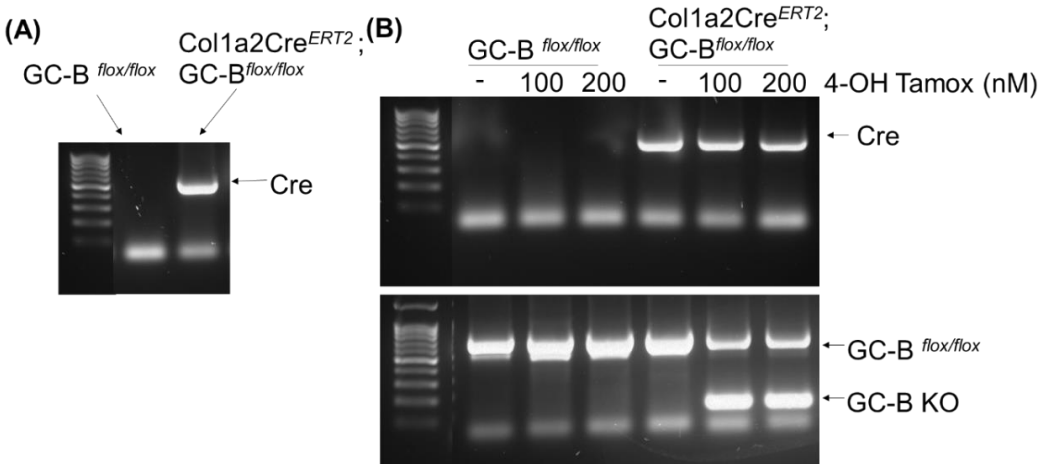

Figure 6: *Verification of mice genotypes and in vitro GC-B knock out by DNA gel electrophoresis*
Lung fibroblasts were isolated from mice with genotypes GC-B$^{flox/flox}$ and Col1a2Cre^{ERT2}; GC-B$^{flox/flox}$ and treated with 4-OH Tamox for 72 hours in passage 1. DNA from the tails of the mice (A) and 4-OH Tamox treated fibroblasts (B) was isolated. DNA was amplified by sequence specific primers using PCR, separated by gel electrophoresis and confirmed for Cre sequence and induction of GC-B KO by 4-OH Tamox treatment.

3.1.1.2 Confirmation of GC-B KO at protein level

Once the KO was confirmed at the genetic level, it was further validated at level of protein expression by carrying out a western blot for GC-B receptor (Figure 7). Treatment with 4-OH Tamox led to a significant decrease in membrane GC-B expression in fibroblasts isolated from Col1a2Cre^{ERT2}; GC-B$^{flox/flox}$ mice compared to the GC-B$^{flox/flox}$ group. These results confirm the elimination of GC-B protein by 4-OH Tamox treatment.

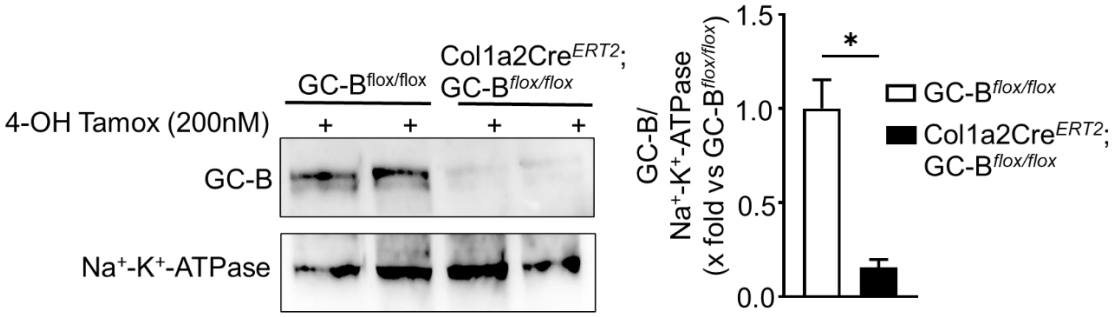

Figure 7: *Confirmation of GC-B KO by western blotting for membrane GC-B receptor*
*Lung fibroblasts isolated from the mice with GC-B$^{flox/flox}$ and Col1a2Cre^{ERT2}; GC-B$^{flox/flox}$ genotypes were treated for 72 hours with 4-OH Tamox, followed by sub-cellular fractionation. Membrane fractions were checked for GC-B receptor expression by western blotting. Na$^+$-K$^+$ ATPase was used as a loading control. (n=3 mice per genotype, *p<0.05)*

3.1.1.3 Investigation of cGMP response to CNP after 4-OH Tamox treatment

Binding of CNP to the GC-B receptor leads to activation of intracellular guanylyl cyclase, resulting in the conversion of Guanosine triphosphate (GTP) to the second messenger cGMP, which in turn leads to activation of downstream signaling pathways (Kuhn, 2016). Fibroblasts from both groups (GC-B$^{flox/flox}$ and Col1a2Cre^{ERT2}; GC-B$^{flox/flox}$) were pretreated with 4-OH Tamox and stimulated with different CNP concentrations (10nM and 100nM) and resulting cGMP levels were measured by radio immunoassay (RIA) (Figure 8).

CNP stimulation resulted in an upregulation of cGMP production in both DMSO treated groups (Vehicle). This indicated that CNP was able to bind to the GC-B receptor in both groups, resulting in cGMP production. In the GC-B$^{flox/flox}$ group, pretreatment with 4-OH Tamox did not have an effect on CNP induced cGMP responses compared to the DMSO treated controls. However, in the Col1a2Cre^{ERT2}; GC-B$^{flox/flox}$ group CNP stimulation did not lead to a cGMP increase, due to the KO of the GC-B receptor.

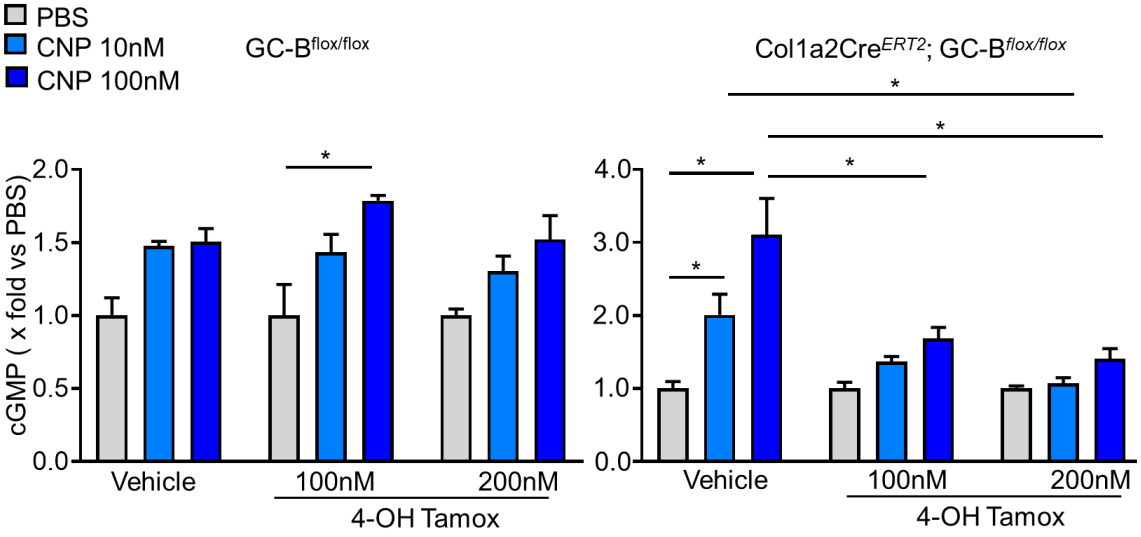

Figure 8: *cGMP response to CNP after 4-OH Tamox treatment*
*cGMP response in vehicle and 4-OH Tamox (100nM and 200nM) treated GC-B$^{flox/flox}$ and Col1a2Cre^{ERT2}; GC-B$^{flox/flox}$ lung fibroblasts after 15 minutes stimulation with 10nM and 100nM. CNP was measured by RIA. (GC-B$^{flox/flox}$: n=4 replicates from 1 mouse, Col1a2Cre^{ERT2}; GC-B$^{flox/flox}$: n=8 replicates from 2 mice, * p<0.05)*

3.1.1.4 Effect of 4-OH Tamox treatment on CNP induced VASP phosphorylation

One of the downstream signaling pathways activated by cGMP is cGMP dependent kinase 1 (cGKI), which phosphorylates the VASP protein at Serine 239 (Bae, Hino,

Hosoda, Son, et al., 2018). Therefore, VASP phosphorylation can indicate CNP mediated activation of the GC-B receptor.

CNP stimulation (100nM) led to a marked increase in $VASP_{Ser239}$ phosphorylation in the vehicle treated Col1a2Cre^{ERT2}; GC-B$^{flox/flox}$ fibroblasts as observed by western blotting (Figure 9). Notably, 4-OH Tamox treatment resulted in loss of this effect. This further substantiates the functional deletion of GC-B receptor by 4-OH Tamox, thereby preventing the initiation of this downstream signaling cascade.

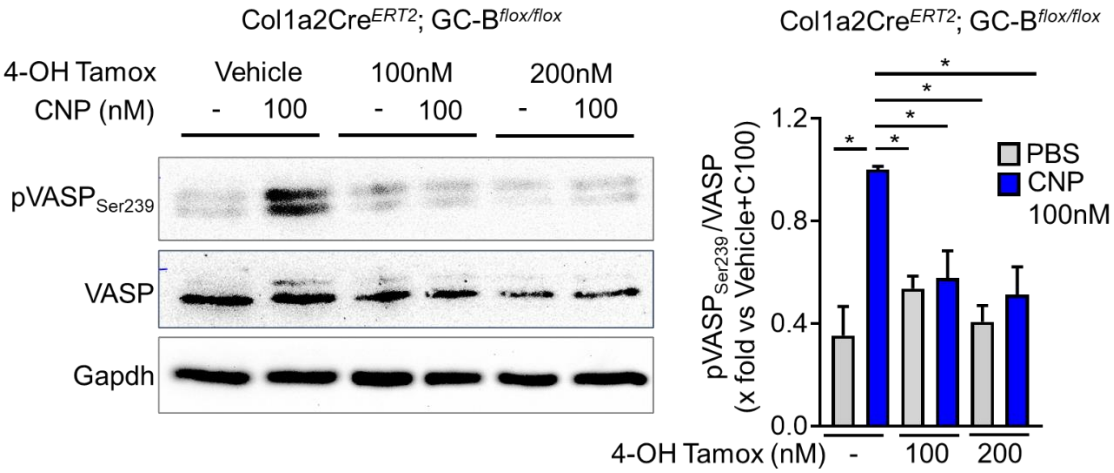

Figure 9: *Western blot for phosphorylation of VASP (Serine239) as a downstream target of the CNP/GC-B/cGMP signaling pathway*
*Vehicle and 4-OH Tamox (100nM and 200nM) treated Col1a2Cre^{ERT2}; GC-B$^{flox/flox}$ cells were stimulated with 100nM CNP for 15 minutes, after 24 hours serum starvation. Proteins were isolated and checked for phosphorylation of $VASP_{Ser239}$ by western blotting. Gapdh was used as a loading control. (n=4, *p<0.05)*

As the KO was successfully induced by 4-OH Tamox, the lung fibroblasts isolated from Col1a2Cre^{ERT2}; GC-B$^{flox/flox}$ *mice* treated with 4-OH Tamox (for 72 hours in passage 1) are from now referred to as the knock out (KO) group. They are compared to cells from wildtype mice treated with 4 -OH Tamox, now referred to as controls.

3.1.2 Antifibrotic effects of CNP are prevented in GC-B knock out fibroblasts

To determine if the preventive effect of CNP on PDGF-BB mediated collagen and MMP9 expression, (previously described by Eva Lessmann) are via the GC-B receptor, experiments comparing the control and GC-B KO fibroblasts were performed. The standard experimental plan included treatment of fibroblasts with 4-OH Tamox in passage 1 for 72 hours, followed by splitting for experiments. Both control and KO group

were divided into four conditions and one of these conditions was left unstimulated to serve as a control group. Next, two groups were pretreated with CNP at either 10nM or 100nM, for 30 minutes. All three groups were then stimulated with 50 ng/ml PDGF-BB for 30 minutes and phosphorylation of VASP, FoxO3, AKT, and ERK was assessed. Additionally, the groups were also stimulated for 24 hours followed by assessment of collagen 1/3 and MMP9 expression.

3.1.2.1 Knock out of GC-B receptor abolishes CNP induced phosphorylation of VASP

To demonstrate that in this experimental set up the GC-B/cGMP cascade is exclusively activated by CNP, VASP phosphorylation at serine 239 was checked (Figure 10). PDGF-BB stimulation alone did not show any effect on VASP phosphorylation in both the control and KO fibroblasts as observed by western blotting. These data indicate that treatment with the growth factor alone did not stimulate the cGMP dependent signaling pathway. Similar to previous observations (Figure 9), CNP led to a significant increase in VASP phosphorylation in the control fibroblasts, while this effect was abrogated in the KO fibroblasts, confirming the activation of cGMP signaling pathway by CNP/GC-B alone.

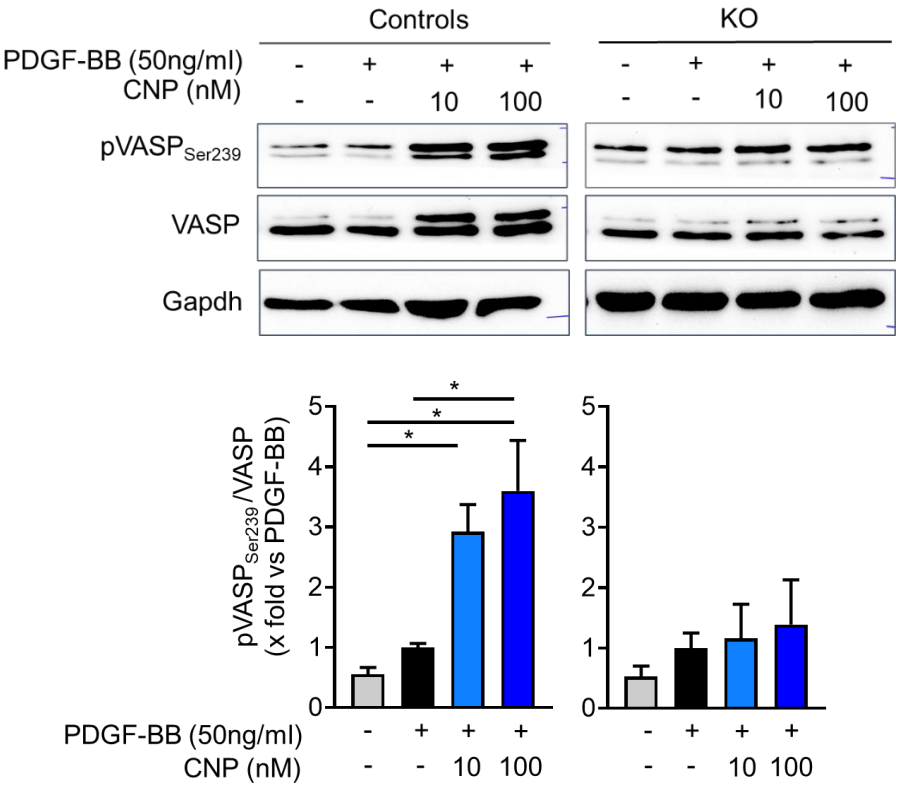

Figure 10: *Western blot for VASP (Ser239) phosphorylation to check the activation of intracellular signaling by CNP/GC-B pathway*
*Control and KO fibroblasts were treated with CNP (10nM and 100nM) for 30 minutes, followed by PDGF-BB (50ng/ml) stimulation. Proteins were isolated and phosphorylation of VASP and total VASP was analyzed by western blotting. Gapdh was used as a loading control. (n=3 mice per genotype, *p<0.05)*

3.1.2.2 Knock out of GC-B prevents the effect of CNP on PDGF-BB induced collagen 3 expression

In IPF, profibrotic mediators such as TGFß and PDGF-BB lead to an increased accumulation of extracellular and collagenous matrix (Worke et al., 2017; Yi et al., 1996). Specifically, collagen 1 and collagen 3 isoforms are shown to be altered (Gingery et al., 2014). Indeed, previous data from our lab showed that PDGF-BB stimulation led to a marked increase in collagen 1, collagen 3, and MMP9 expression in murine lung fibroblasts and this effect was attenuated by CNP pretreatment. In this thesis, the role of GC-B in mediating the CNP-driven reduction was explored (Figure 11). In the control fibroblasts, PDGF-BB led to a significant increase in collagen 3 expression, as assessed by immunocytochemistry and fluorescence quantification. Pretreatment with CNP at both concentrations prevented PDGF-BB induced collagen 3 expression significantly. Interestingly, in the GC-B receptor KO fibroblasts the effect of PDGF-BB on collagen 3 expression was present but the preventive effect of CNP was not observed. These

results suggest that the peptide did not affect the collagen 3 expression levels, likely due to the absence of GC-B receptor.

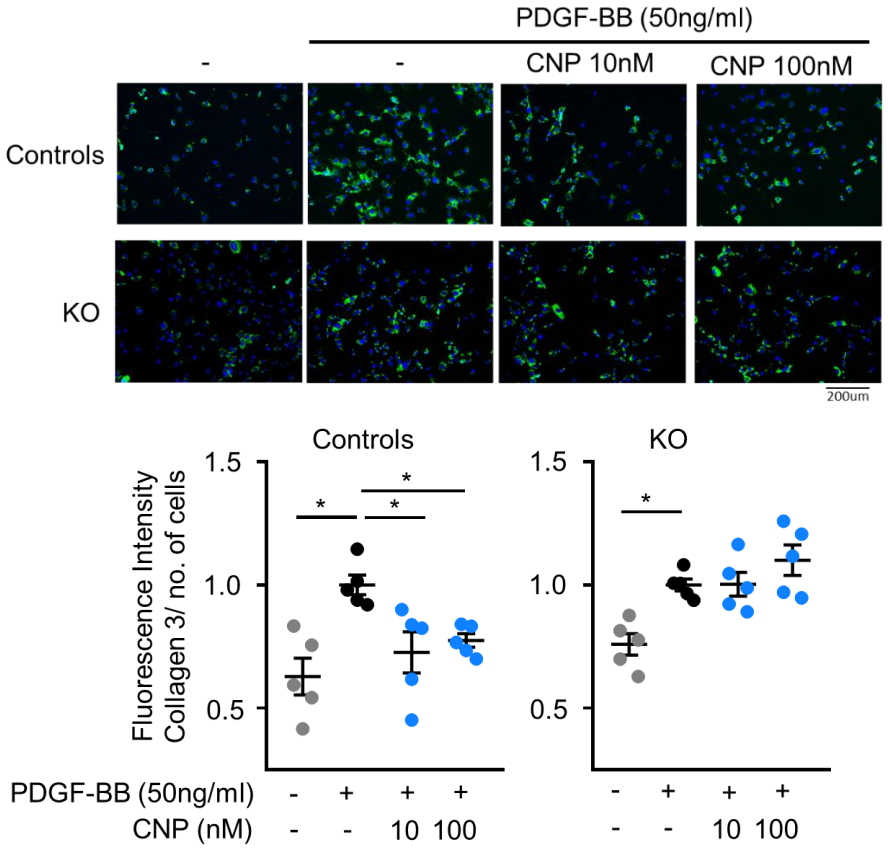

Figure 11: *Effect of CNP on PDGF-BB mediated collagen 3 expression*
*Control and KO fibroblasts were serum starved (24 hours), treated with CNP (10nM and 100nM) for 30 minutes followed by PDGF-BB (50ng/ml) stimulation for 24 hours. Collagen 3 expression was checked by Immunocytochemistry and fluorescence intensity was analyzed by ImageJ. (n=5 mice, *p<0.05)*

3.1.2.3 Knock out of GC-B prevents the effect of CNP on PDGF-BB induced collagen 1 expression

The effect of CNP on PDGF-BB induction of collagen 1 in GC-B KO fibroblasts was examined by western blotting (Figure 12). Both the control and KO fibroblasts were stimulated with CNP, followed by PDGF-BB. After 24 hours of stimulation, the proteins were isolated and collagen 1 expression was detected by western blotting. In both genotypes, PDGF-BB led to a clear and significant gain in collagen 1 expression. However, the response to the pretreatment with CNP was different between the two groups. In the control fibroblasts a decrease in collagen 1 levels compared to PDGF-BB was observed, while in the KO cells the expression remained unchanged. This observation again verified that the GC-B receptor is responsible for the preventive effect of CNP on PDGF-BB induced collagen expression.

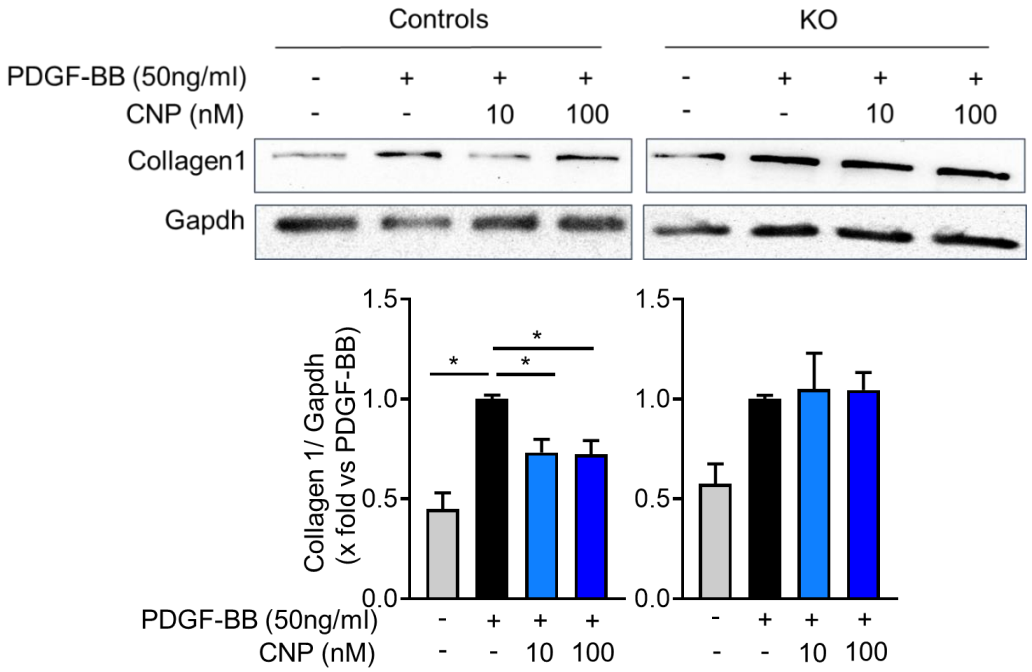

Figure 12: *Effect of CNP on PDGF-BB mediated collagen 1 expression*
*Control and KO fibroblasts were serum starved (24 hours), pre-treated with CNP (10nM and 100nM) for 30 minutes followed by PDGF-BB (50ng/ml) stimulation for 24 hours. Proteins were isolated and collagen 1 expression was analyzed by western blotting followed by densitometric analysis. Gapdh was used as a loading control. (n=3 mice per genotype, *p<0.05)*

3.1.2.4 GC-B KO abolishes CNP mediated decrease of PDGF-BB induced migration

Changes in fibroblast proliferation, migration, and differentiation govern the controlled remodeling of the extracellular matrix in its physiological state. However, in lung fibrosis, these processes are exaggerated (Bonnans et al., 2014). Several reports have shown that activated fibroblasts in IPF exhibit a highly proliferative and invasive phenotype induced by PDGF-BB (Al-Tamari et al., 2018; Li et al., 2011). Hence, we aimed to study whether CNP can moderate PDGF-BB induced proliferative and migratory phenotype *in vitro*. Indeed, PDGF-BB stimulation led to a marked increase in migration of both control and KO fibroblasts measured by scratch/gap closure assay (Figure 13). The closing of gap was checked 4, 8, and 24 hours after stimulation, and a migration rate was calculated as percentage of the gap size at the start of the experiment (time point 0 hours). CNP pretreatment (10nM) of the control group resulted in a marked decrease in the migration, however this reduction was not observed in the GC-B KO group after CNP addition. Taken together, these results show that CNP prevents PDGF-BB induced migration via the GC-B receptor.

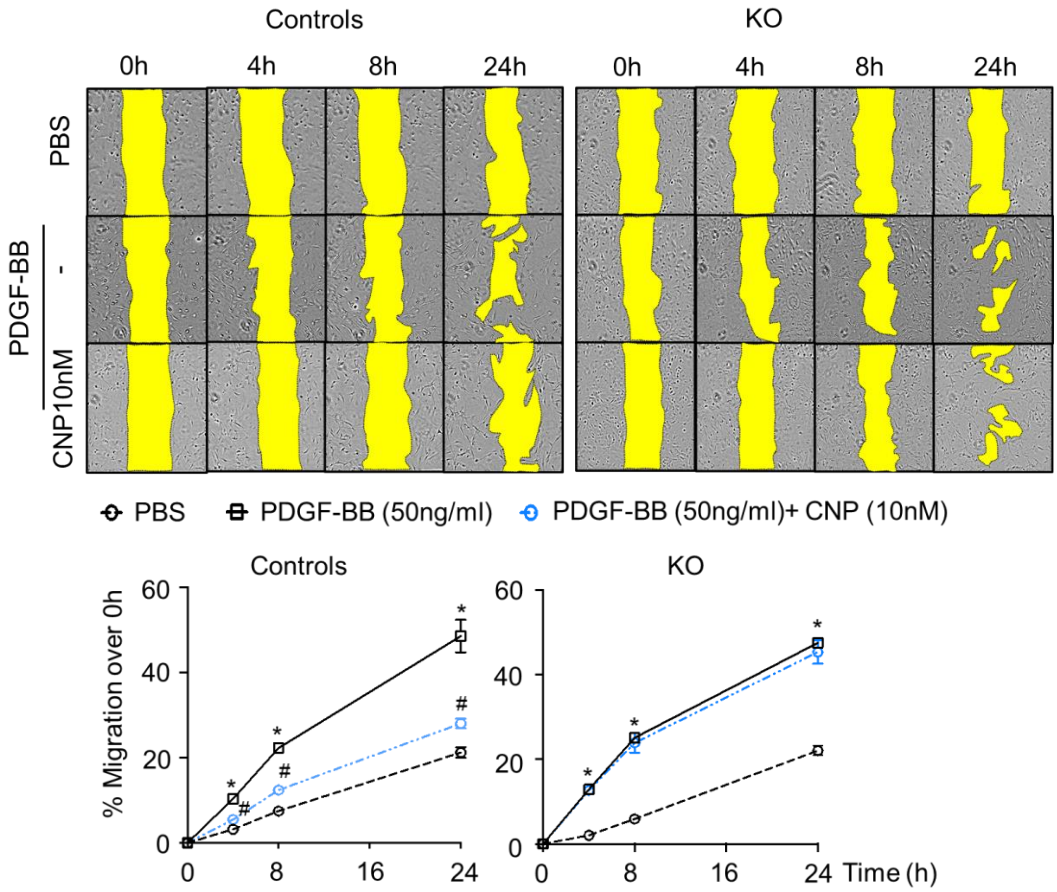

Figure 13: *Migration analysis of Control and KO fibroblasts by gap closure assay Confluent control and KO fibroblasts were serum starved (24 hours), scratched with a 100µl pipette tip and pre-treated with CNP (10nM) for 30 minutes, followed by PDGF-BB (50ng/ml). Migration was assessed after 0, 4, 8 and 24 hours under the microscope. The size of the scratch was measured using ImageJ and calculated as percentage of the gap size at time point 0. (n= 6 wells from 2 mice per genotype, *p<0.05 vs PBS, #p<0.05 vs PDGF-BB)*

3.1.2.5 Knock out of GC-B inhibits the effect of CNP on PDGF-BB induced MMP9 expression

Cell migration is an important mechanism involved in the repair of the respiratory epithelium and MMP9 controls this migration of repairing cells by remodeling the provisional extra cellular matrix (Legrand et al., 1999). An increased MMP9 expression is also described in pulmonary lung fibrosis and seems to promote the migration of bronchiolar cells into the diseased regions (Betsuyaku et al., 2000; Kim et al., 2009). Interestingly, previous studies from our group have shown that PDGF-BB leads to a marked increase in MMP9 expression, which was attenuated by CNP pretreatment. In this thesis a similar effect on MMP9 expression was observed in control fibroblasts upon treatment with CNP. In contrast, the KO fibroblasts treated with CNP showed no significant attenuation on PDGF-BB induced MMP9 expression (Figure 14).

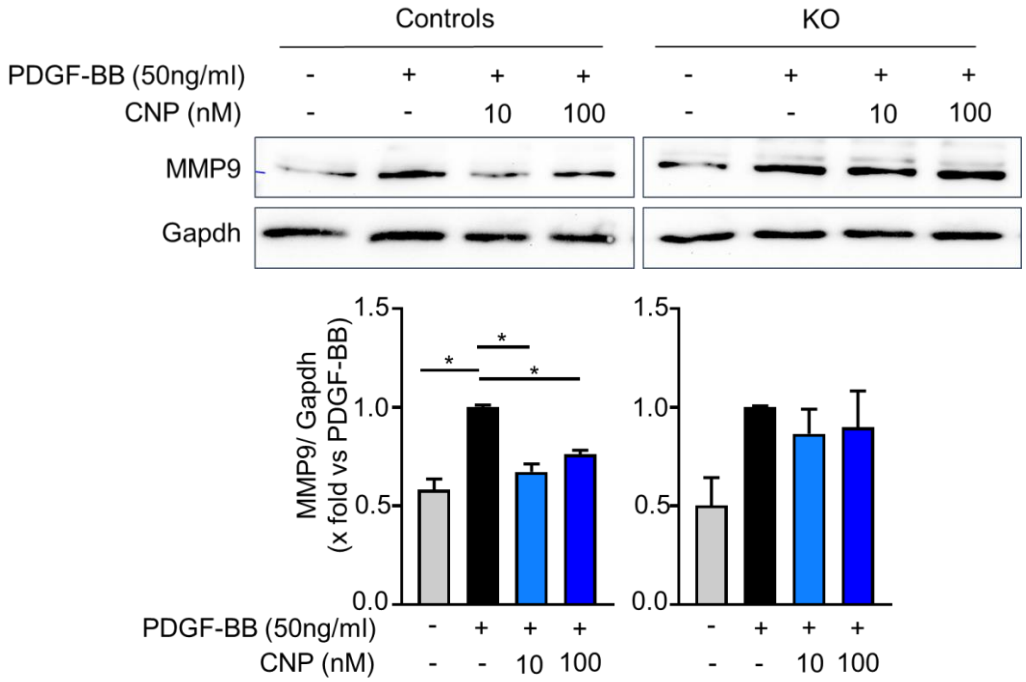

Figure 14: *Effect of CNP on PDGF-BB mediated MMP9 expression*
*Control and KO fibroblasts were serum starved (24 hours), pre-treated with CNP (10nM and 100nM) for 30 minutes followed by PDGF-BB (50ng/ml) stimulation for 24 hours. Proteins were isolated and MMP9 expression was analyzed by western blotting followed by densitometric analysis. Gapdh was used as a loading control. (n= 3 mice per genotype, *p<0.05)*

3.1.2.6 GC-B receptor knock out impedes CNP mediated antiproliferative effect

Next, the effect of PDGF-BB on fibroblast proliferation was assessed. PDGF-BB stimulation significantly increased proliferation of lung fibroblasts compared to non-stimulated cells in both control and KO groups as assessed by a BrdU incorporation assay (Figure 15). Interestingly, PDGF-BB boosted the proliferation of KO fibroblasts to a greater extent than the control cells. To verify the anti-proliferative and preventive effect of CNP, cells were pretreated with the peptide before PDGF-BB stimulation. CNP reduced the proliferative effect of PDGF-BB in control cells, however, this effect was removed in the KO group with the PDGF-BB induced proliferation remaining unchanged.

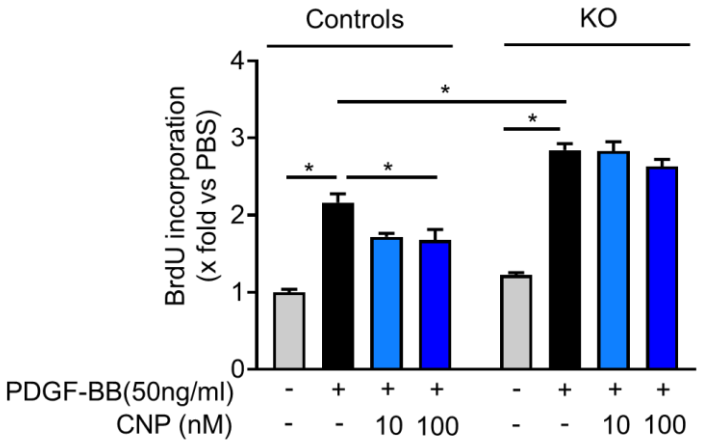

Figure 15: *BrdU incorporation assay to investigate the effect of CNP on PDGF-BB induced proliferation*
*Control and KO fibroblasts were pre-treated with CNP (10nM and 100nM) for 30 minutes followed by PDGF-BB (50ng/ml) stimulation for 24 hours. Proliferation was analyzed by BrdU incorporation assay. (n= 10 wells from 2 mice per genotype, *p<0.05)*

3.1.2.7 Effect of CNP on PDGF-BB induced FoxO3 phosphorylation was abolished after GC-B knock out

To explore the mechanism underlying the effects of CNP-GC-B signaling on PDGF-BB induced fibrotic changes, the regulation of transcription factor FoxO3 upon CNP stimulation was assessed. FoxO3 is known to be hyperphosphorylated, resulting in its downregulation, in IPF (Al-Tamari et al., 2018).

To study the FoxO3 phosphorylation state, fibroblasts were pretreated for 30 minutes with CNP and then stimulated for 30 minutes with PDGF-BB. The phosphorylation of FoxO3 in these fibroblasts was then analyzed by western blot, followed by densitometric quantification (Figure 16). Consistent with previous experiments, the control and the KO group were compared. In both groups, an increase in FoxO3 phosphorylation at threonine 32 was evident in PDGF-BB stimulated cells, with the control group exhibiting a statistically significant increase. Furthermore, this gain was significantly reversed in the control group on CNP pretreatment. In contrast, this phosphorylation was not prevented in the KO cells pretreated with CNP. This result shows that PDGF-BB leads to an increased phosphorylation and degradation of FoxO3, consistent with previously published data (Al-Tamari et al., 2018) and, interestingly, it also demonstrates that CNP prevented FoxO3 phosphorylation via the GC-B receptor.

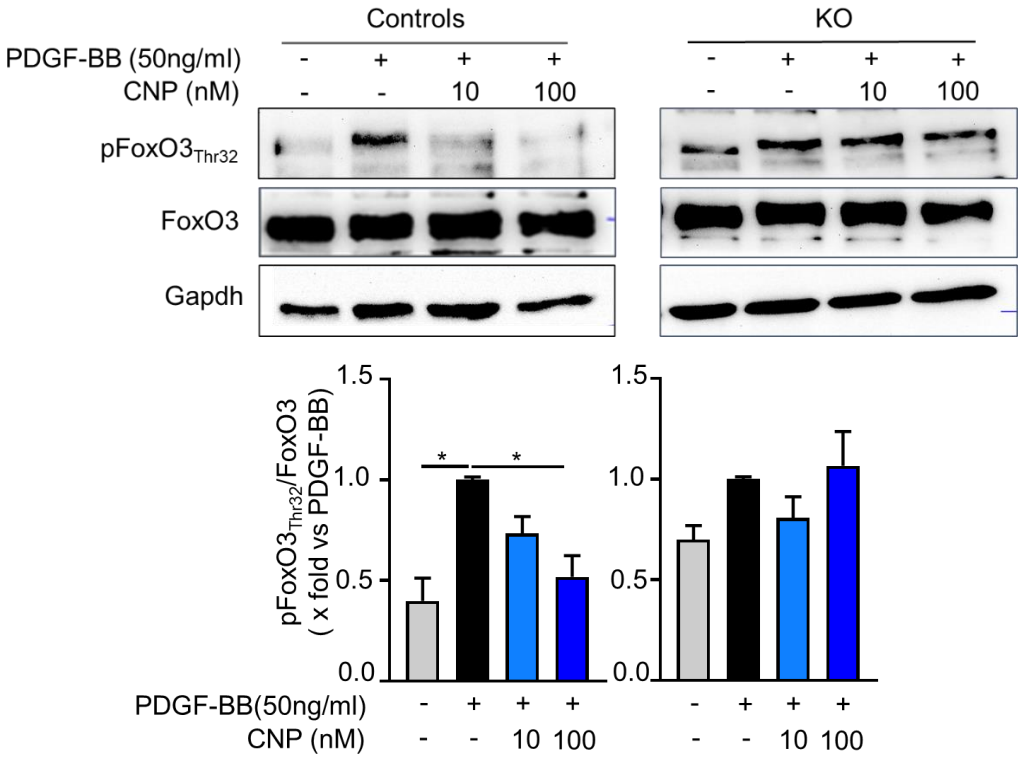

Figure 16: *Effect of CNP on PDGF-BB mediated FoxO3 phosphorylation (threonine 32) Control and KO fibroblasts were pre-treated with CNP (10nM and 100nM) for 30 minutes, followed by PDGF-BB (50ng/ml) for further 30 minutes. Proteins were isolated and FoxO3 phosphorylation and total FoxO3 was analyzed by western blotting followed by densitometric analysis. Gapdh was used as a loading control. (n= 2-3 mice per genotype, *p<0.05)*

3.1.2.8 CNP has no effect on PDGF-BB induced AKT (Ser473) phosphorylation

Having validated the association of PDGF-BB, CNP, and pFoxO3, the signaling mechanism involved in regulation of the transcription factor FoxO3 by CNP was investigated. PDGF-BB is able to activate different signal cascades, in many cases through kinases, which results in downstream phosphorylation of the AKT kinase. This kinase ultimately phosphorylates, and thereby inactivates, FoxO3 (Ghosh Choudhury et al., 2003). To investigate how CNP reduces the PDGF-BB induced phosphorylation of FoxO3 through AKT, the activatory phosphorylation of AKT was investigated (Figure 17).

In both groups, significant phosphorylation of AKT was visible after stimulation with PDGF-BB, confirming existence of functional PDGF-BB/AKT cascade in the cells. However, in both the KO and control group, pretreatment of the cells with CNP did not have any effect on PDGF-BB induced AKT phosphorylation. This result indicates that CNP does not regulate FoxO3 phosphorylation via interfering with AKT activation.

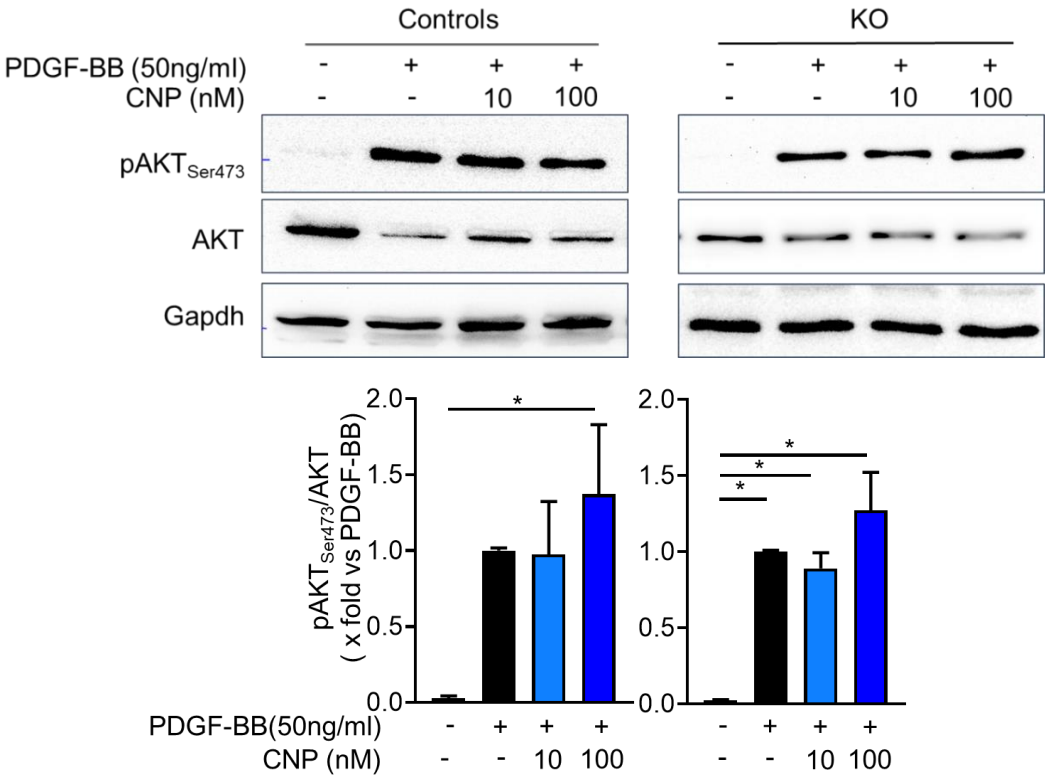

Figure 17: *Effect of CNP on PDGF-BB induced phosphorylation of AKT (serine 473) Control and KO fibroblasts were pre-treated with CNP (10nM and 100nM) for 30 minutes, followed by PDGF-BB (50ng/ml) for further 30 minutes. Proteins were isolated and AKT phosphorylation and total AKT was analyzed by western blotting followed by densitometric analysis. Gapdh was used as a loading control. (n=3 mice per genotype, *p<0.05)*

3.1.2.9 CNP shows marginal effect on PDGF-BB induced ERK1/2 phosphorylation

PDGF-BB can also induce phosphorylation of FoxO3 via the RAS/RAF/MEK pathway, resulting in phosphorylation of ERK. PDGF-BB activates the ERK kinase indirectly via phosphorylation, with activated, phosphorylated, ERK able to inactivate FoxO3 (Lubinus et al., 1994; Roy et al., 2010). To demonstrate whether CNP can interrupt this cascade, the phosphorylation of ERK was detected by western blotting (Figure 18). Firstly, in both groups of fibroblasts PDGF-BB induced a significant increase in ERK phosphorylation, confirming that the growth factor activates this cascade. CNP pretreatment in the control group led to a consistent but not significant reduction in PDGF-BB induced ERK phosphorylation however in the KO group, this effect of CNP was lost. Taken together, these results hint towards a role of ERK as a mediator in regulating CNP mediated effects on FoxO3. To conclude whether these minor changes in ERK phosphorylation are relevant, further experiments with increase in biological replicates are warranted.

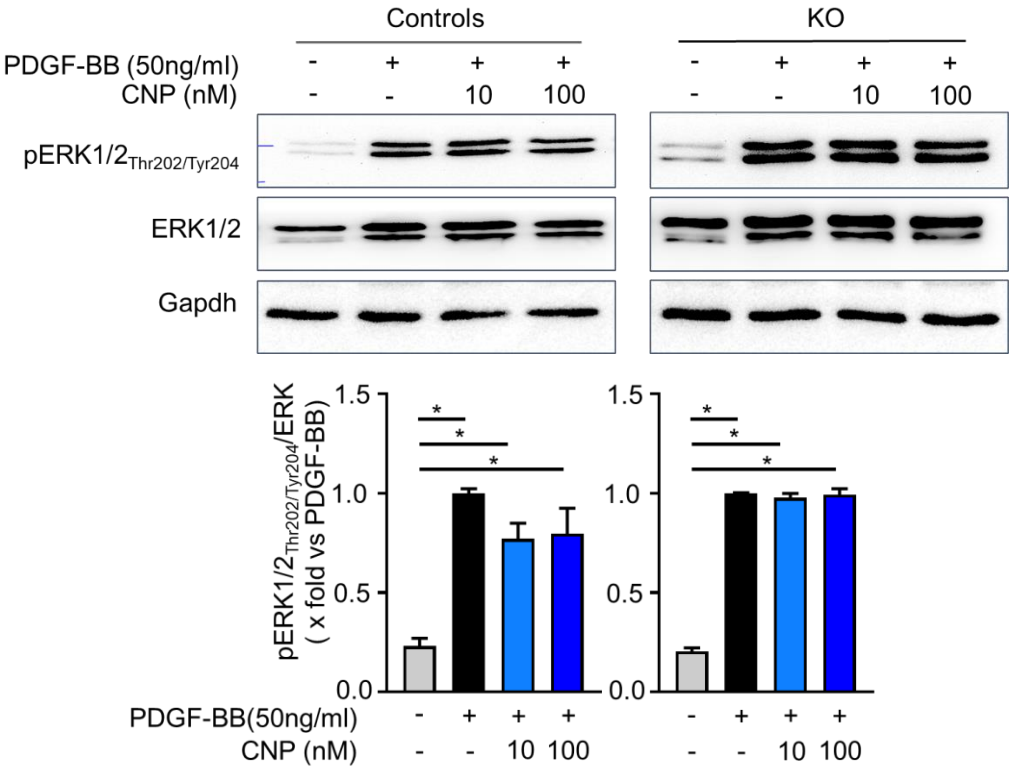

Figure 18: *Effect of CNP on PDGF-BB mediated phosphorylation of ERK (threonine 202/ tyrosine 204)*
*Control and KO fibroblasts were pre-treated with CNP (10nM and 100nM) for 30 minutes, followed by PDGF-BB (50ng/ml) for further 30 minutes. Proteins were isolated and ERK phosphorylation and total ERK were analyzed by western blotting followed by densitometric analysis. Gapdh was used as a loading control. (n=3 mice per genotype, *p<0.05)*

3.2 Antifibrotic effect of CNP on cultured human lung fibroblasts

In order to assess the physiological and pathophysiological importance of the studies conducted in murine fibroblasts, it is essential to also examine the effect of CNP in human lung fibroblasts. Therefore, we utilized lung fibroblasts isolated from lungs of IPF patients and healthy controls to study effects of CNP on PDGF-BB induced collagen expression, proliferation, and migration.

3.2.1 Control and IPF fibroblasts show increased cGMP levels in response to CNP

Firstly, the cGMP responsiveness of healthy ‘control’ and IPF fibroblasts to CNP was assessed by cGMP RIA. CNP stimulation led to an increased cGMP production in a concentration dependent manner. The increase was similar in both control and IPF fibroblasts (Figure 19,A).

This confirmed that the GC-B receptor can be activated by the peptide in both groups, leading to generation of cGMP. CNP is able to act on IPF fibroblasts, hinting that a treatment of patients could be successful under diseased conditions.

However, the absolute cGMP amount at basal level (without CNP stimulation) was significantly lower in IPF fibroblasts (Figure 19,B). Both control and IPF fibroblasts displayed an increase in absolute amounts of cGMP in response to CNP, though the increase was smaller in IPF group (Figure 19,C).

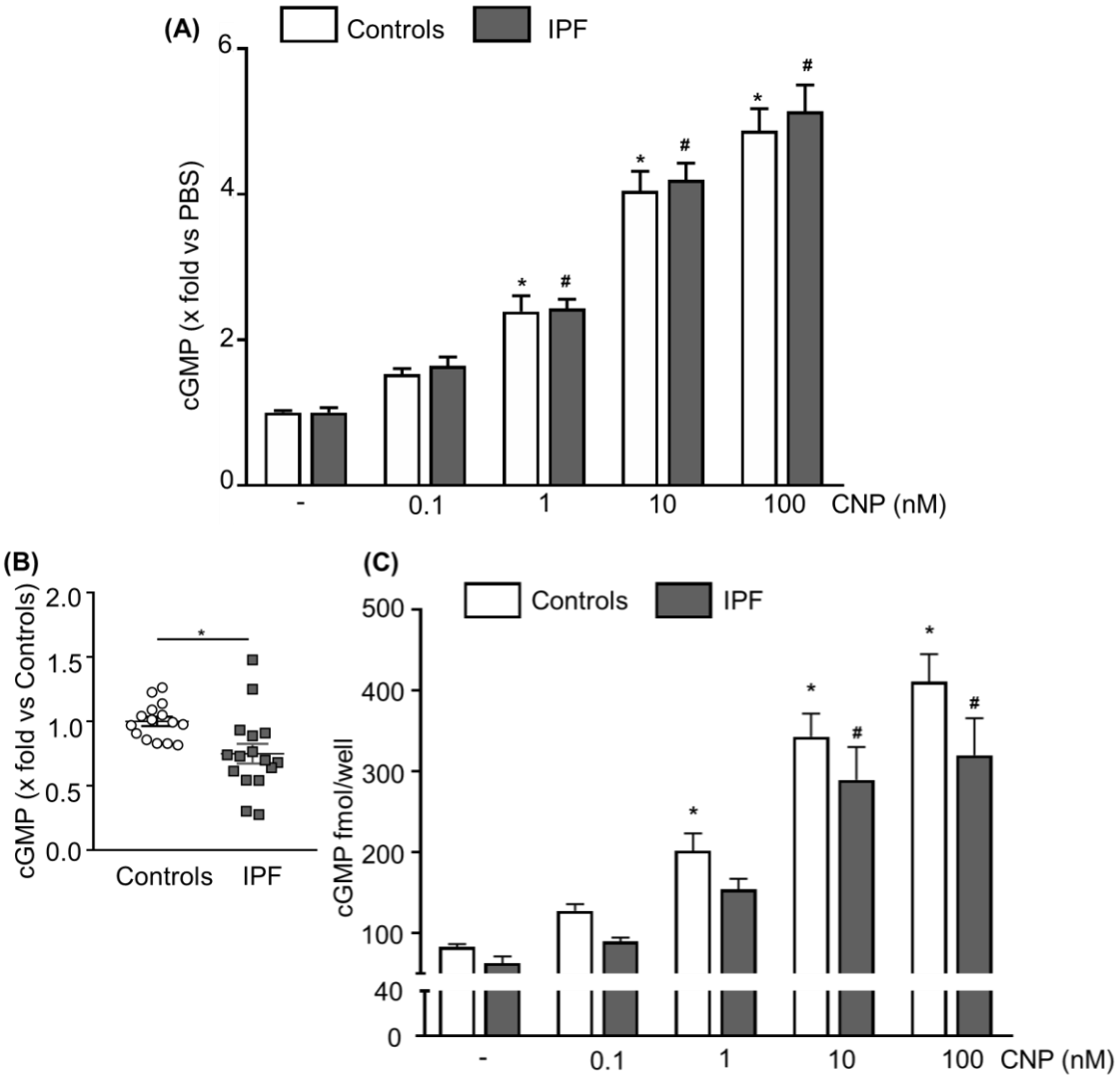

Figure 19: *cGMP response of IPF and control fibroblasts to CNP stimulation*
*Control and IPF fibroblasts were treated with increasing concentrations of CNP for 15 minutes in presence of PDE inhibitor and the cGMP levels were measured by Radioimmunoassay. Relative (A) and absolute (B, C) cGMP levels were plotted. (n=15-16 replicates from 4 biological replicates per group, *p<0.05 vs PBS Controls, #p<0.05 vs PBS IPF)*

3.2.2 Membrane GC-B expression is increased in IPF fibroblasts compared to control fibroblasts

Next, the membrane GC-B receptor and NPR-C expression was compared between IPF and control fibroblasts by western blot. Interestingly, the expression of the GC-B receptor was significant upregulated in the IPF samples in comparison to the control group (Figure 20, A-B). There was no significant difference observed in NPRC expression between the groups (Figure 20, A-C).

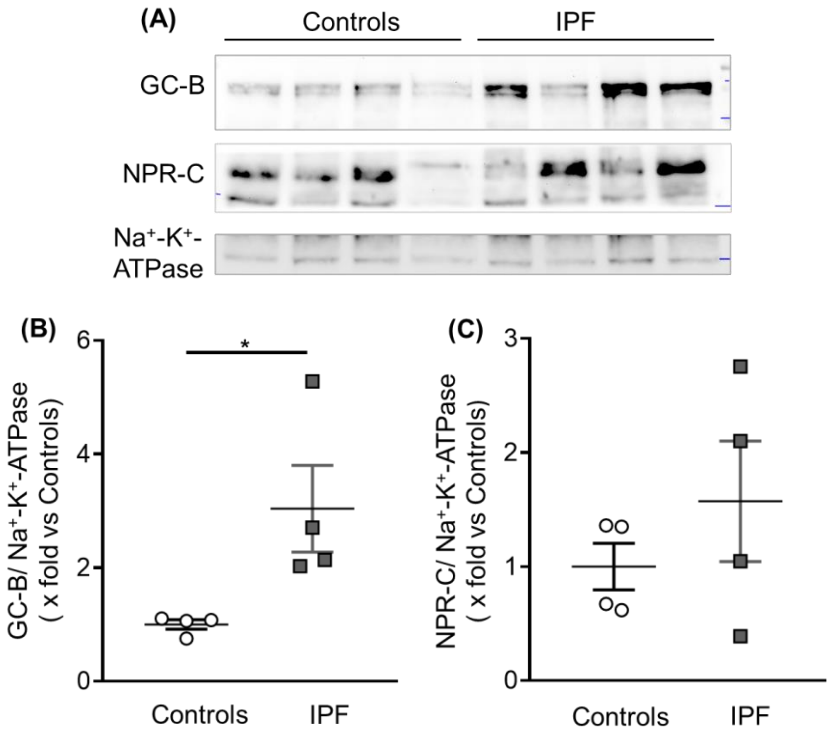

*Figure 20: Membrane GC-B and NPR-C expression in control and IPF fibroblasts Subcellular fractionation was carried out from IPF and control fibroblasts and membrane expression of the GC-B and NPR-C receptors was analyzed by western blotting. (n= 4 per group, *p<0.05)*

3.2.3 VASP phosphorylation in control and IPF fibroblasts

To assess the activation of cGMP mediated downstream signaling by CNP stimulation, phosphorylation of VASP protein was analyzed. Cells were pretreated for 30 minutes with 10nM and 100nM CNP and then stimulated with 50ng/ml PDGF-BB and VASP phosphorylation was analyzed by western blot. PDGF-BB stimulation alone did not increase VASP phosphorylation. On the other hand, CNP pretreatment led to a robust elevation in the VASP phosphorylation in both control and IPF fibroblasts, indicative of active CNP mediated cGMP-cGKI signaling (Figure 21).

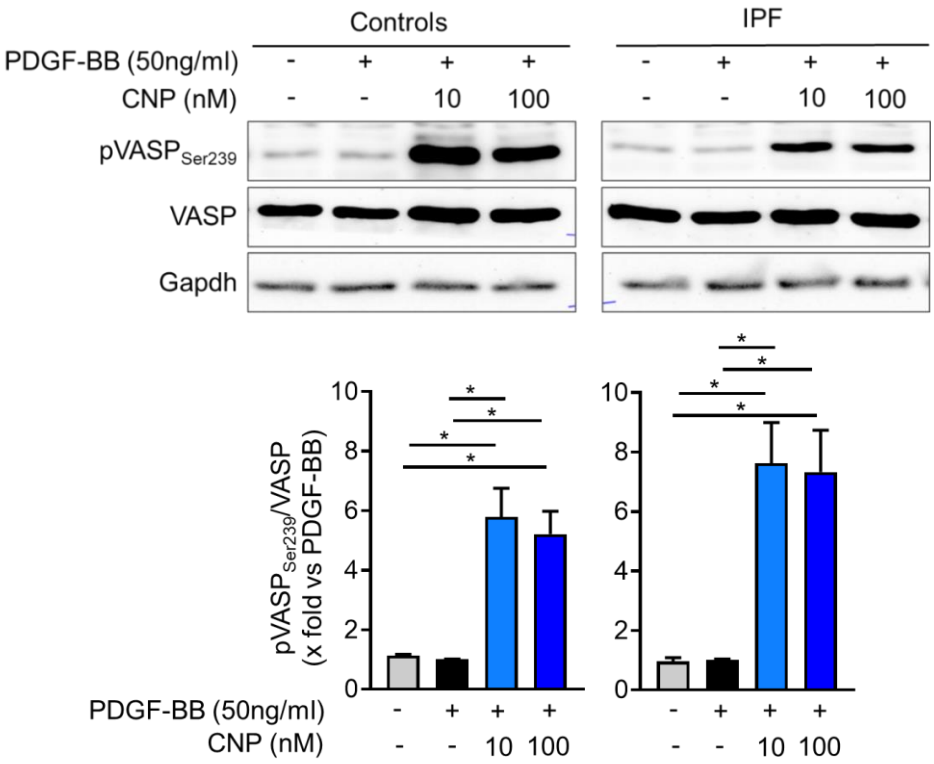

Figure 21: *Western blot for VASP phosphorylation at Serine 239 in response to CNP stimulation*
*Control and IPF fibroblasts were treated with CNP (10nM and 100nM) for 30 minutes, followed by PDGF-BB (50ng/ml) for another 30 minutes. Proteins were isolated and VASP phosphorylation and total VASP were analyzed by western blotting followed by densitometric analysis. Gapdh was used as a loading control. (n=3 per group, *p<0.05)*

3.2.4 CNP prevents PDGF-BB induced increase of collagen 1 in IPF and control fibroblasts

After confirmation of active CNP-GC-B signaling, the effect of CNP on PDGF-BB induced collagen 1 expression was studied (Figure 22). In both the control and IPF fibroblasts, PDGF-BB treatment resulted in a significant upregulation of collagen 1 expression as observed by western blot. Pretreatment with CNP (10nM and 100nM) abrogated this effect in both groups. These findings are in agreement with the results of the murine fibroblasts that show CNP is able to reduce PDGF-BB induced collagen 1 expression.

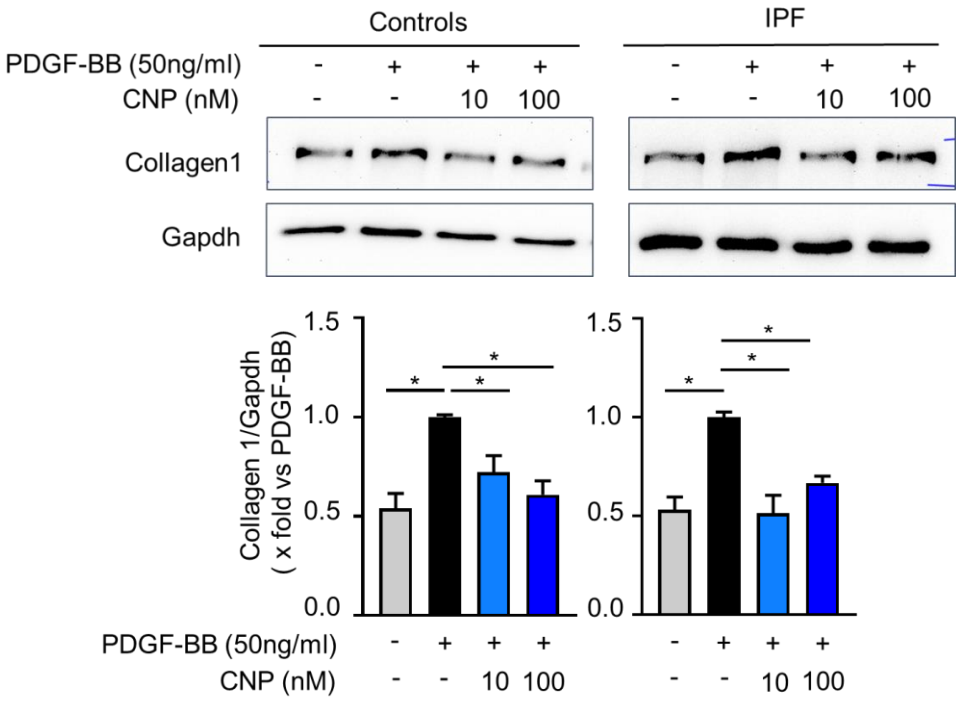

Figure 22: *Effect of CNP on PDGF-BB induced collagen 1 expression*
*Control and IPF fibroblasts were serum starved (24 hours), pre-treated with CNP (10nM and 100nM) for 30 minutes, followed by PDGF-BB (50ng/ml) stimulation for 24 hours. Proteins were isolated and Collagen 1 expression was analyzed by western blotting followed by densitometric analysis. Gapdh was used as a loading control. (n=3 per group, *p<0.05)*

3.2.5 CNP reduces PDGF-BB mediated MMP9 expression in control and IPF fibroblasts

To study the effect of CNP on MMP9, which influences the organization of the extracellular matrix, expression of MMP9 was analyzed by western blot (Figure 23). PDGF-BB significantly increased MMP9 expression, consistent with the previously observed results in murine fibroblasts. Similar to the collagen 1 expression, MMP9 was significantly reduced after pretreating the cells with CNP in both groups.

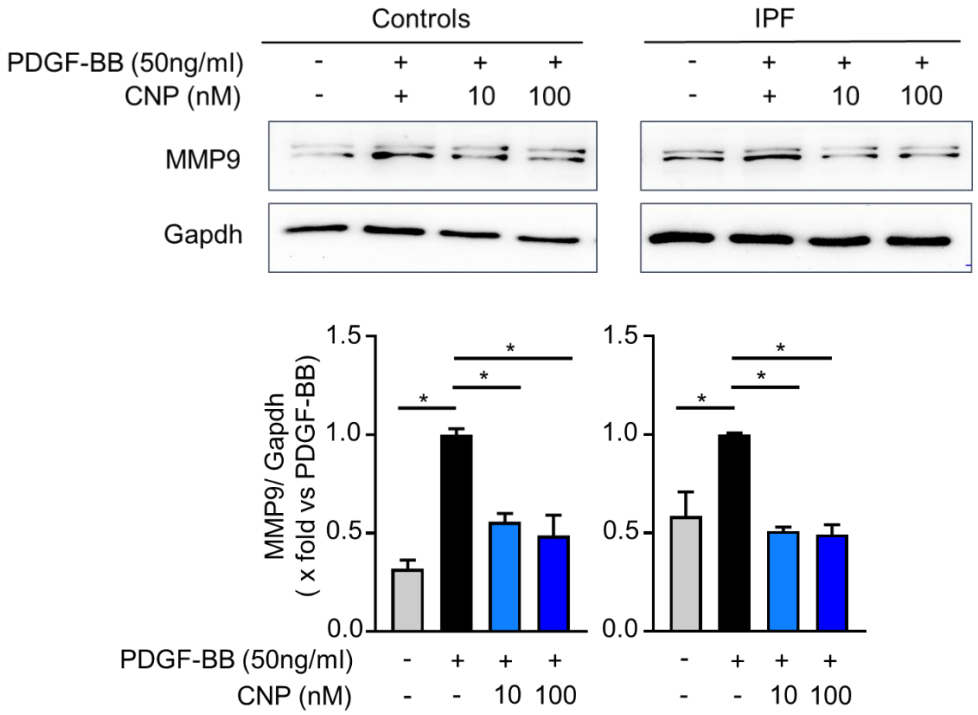

Figure 23: *Effect of CNP on PDGF-BB induced MMP9 expression*
Control and IPF fibroblasts were serum starved (24 hours), pre-treated with CNP (10nM and 100nM) for 30 minutes followed by PDGF-BB (50ng/ml) stimulation for 24 hours. Proteins were isolated and MMP9 expression was analyzed by western blotting followed by densitometric analysis. Gapdh was used as a loading control. (n= 3 per group, p<0.05)

3.2.6 IPF fibroblasts exhibit a higher migration rate compared to control fibroblasts

To check for the functional differences between the control and the IPF groups, a gap closure migration assay was performed, where the velocity of the gap closure was measured. At first, the differences between both groups at basal level, without stimulation, were examined. In the IPF group, the gap closed significantly faster relative to the controls (Figure 24,A).

Next, the impact of the peptide was assessed after stimulation with both PDGF-BB and CNP (Figure 24,B-C). On stimulation with PDGF-BB, both control and IPF fibroblasts displayed an increase in migration. Interestingly, while the control fibroblasts showed a significant increase in migration after 8 hours, the IPF fibroblasts already exhibited a similar increase in migration in 4 hours. Pretreatment with CNP (10nM for 30 minutes) reduced the migration significantly after 8 hours in control, and 4 hours in IPF, compared to the cells stimulated with PDBGF-BB only (Figure 24,C). This shows that the peptide prevented the fibroblast migration, typical of fibrosis.

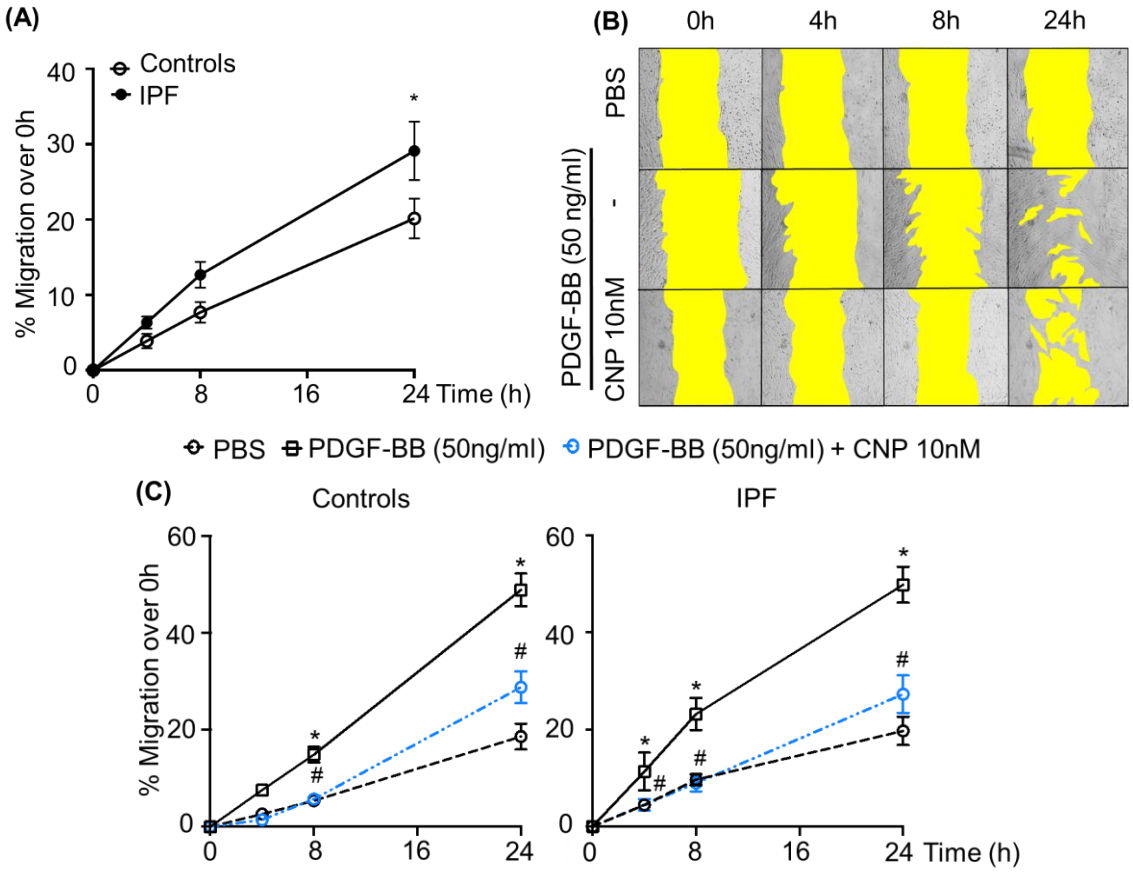

Figure 24: *Migration analysis of control and IPF fibroblasts by gap closure assay (A) Migration of IPF and control fibroblasts was compared at basal level. (B-C) Confluent control and IPF fibroblasts were serum starved (24 hours) and pre-treated with CNP (10nM) for 30 minutes, followed by PDGF-BB (50ng/ml). Migration was assessed after 0, 4, 8 and 24 hours under the microscope. The size of the scratch was measured using ImageJ and calculated as percentage of the gap size at time point 0. (n=6-9 wells from 2-3 biological replicates, *p<0.05 vs PBS, # p<0.05 vs PDGF-BB)*

3.2.7 CNP prevents PDGF-BB induced increase in proliferation in control and IPF fibroblasts

In murine lung fibroblasts, a reduction in PDGF-BB induced cell proliferation was observed after CNP pretreatment (Figure 15). As IPF fibroblasts were previously shown to proliferate at a higher rate compared to control cells *in vitro* (Al-Tamari et al., 2018), we investigated effect of CNP on PDGF-BB induced proliferation of control and IPF fibroblasts.

In both groups, stimulation with PDGF-BB led to a significant increase of BrdU incorporation, indicative of increased proliferation. A tendency towards higher proliferation after stimulation was detected in IPF fibroblasts, but this was not significant due to variability within the IPF samples (Figure 25, A). Pretreatment with CNP, at 10nM

and 100nM, prevented the PDGF-BB induced effect significantly and reduced proliferation in both groups (Figure 25, B). This shows that CNP can lower proliferation, not only in the control group, but also in IPF fibroblasts, hinting towards a therapeutic potential.

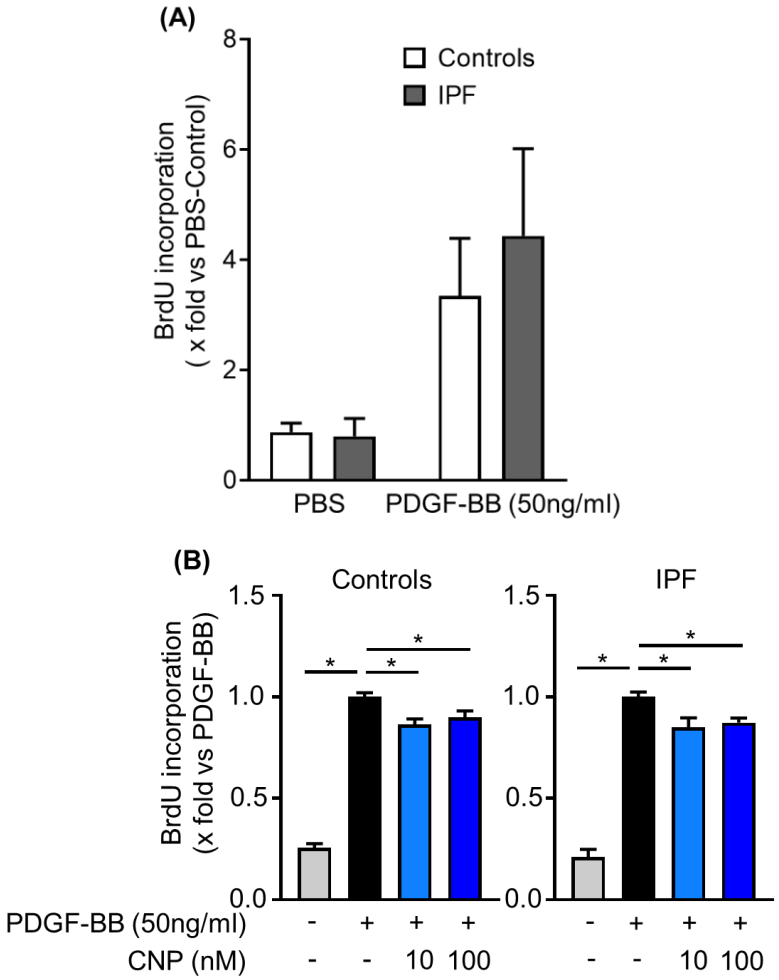

Figure 25: *BrdU incorporation assay to investigate effect of CNP on PDGF-BB induced proliferation*
*Control and IPF fibroblasts were pre-treated with CNP (10nM and 100nM) for 30 minutes, followed by PDGF-BB (50ng/ml) stimulation for 24 hours. Proliferation was analyzed by BrdU incorporation assay. (n=6 replicates from 2 biological replicates per group, *p<0.05)*

3.2.8 FoxO3 as the mediator of CNP effects on control and IPF fibroblasts

Having confirmed the antifibrotic impact of CNP in both healthy and diseased human lung fibroblasts, we focused on deciphering the underlying mechanisms. Since FoxO3 phosphorylation was reduced by CNP in murine fibroblasts, we investigated whether the effects of CNP on FoxO3 are preserved in human fibroblasts (Figure 26). Hence, control

and IPF fibroblasts were pretreated with 10nM and 100nM CNP (30 minutes) followed by PDGF-BB stimulation (30 minutes). FoxO3 phosphorylation at Threonine 32 was checked by western blotting. PDGF-BB led to a significant increase in FoxO3 phosphorylation. Pretreatment with CNP led to a significant reduction of FoxO3 phosphorylation in the control group, hinting towards an increase in active FoxO3 after CNP stimulation. Interestingly, this effect was less pronounced in the IPF group.

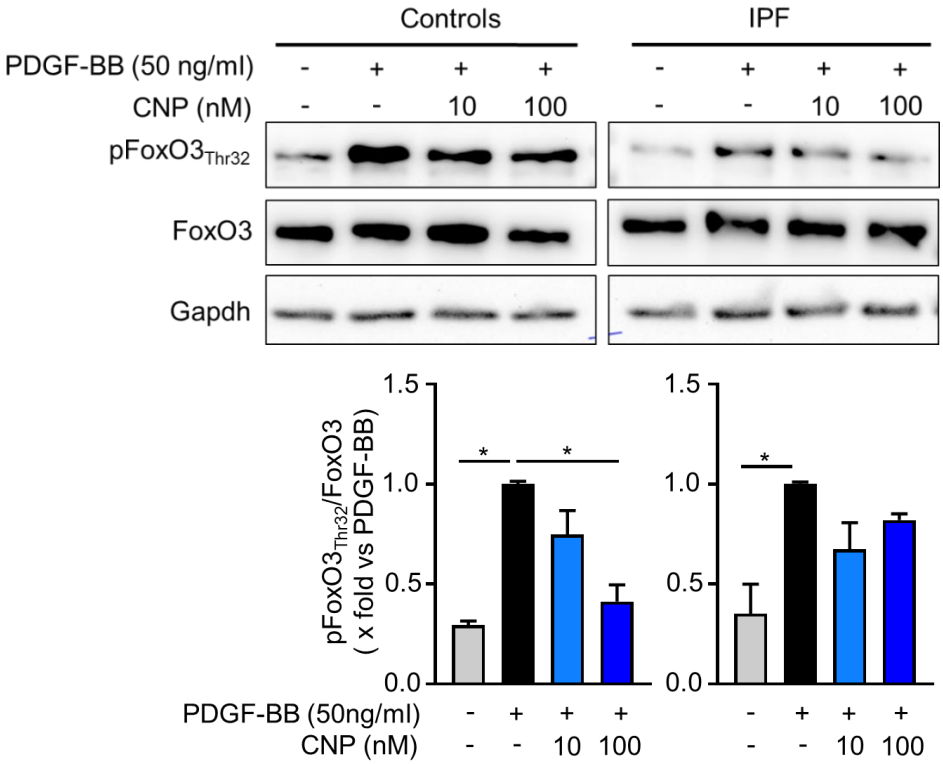

Figure 26: *Effect of CNP on PDGF-BB induced FoxO3 phosphorylation*
*Control and IPF fibroblasts were pre-treated with CNP (10nM and 100nM) for 30 minutes, followed by PDGF-BB (50ng/ml) for further 30 minutes. Proteins were isolated and FoxO3 phosphorylation (Thr32) and total FoxO3 were analyzed by western blotting followed by densitometric analysis. Gapdh was used as a loading control. (n=3 per group. *p<0.05)*

3.2.9 CNP does not prevent PDGF-BB induced phosphorylation of AKT

As described in part 1.5.2, phosphorylation of AKT is part of a PDGF-BB activated pathway which can finally lead to the phosphorylation and inactivation of FoxO3. To investigate if CNP inhibits the PDGF-BB induced phosphorylation of AKT, a western blot for AKT phosphorylation was performed. Similar to murine lung fibroblasts (Figure 17), PDGF-BB led to a significant increase in AKT phosphorylation at Serine 473, while CNP pretreatment did not have any effect in both the control and IPF fibroblasts (Figure 27).

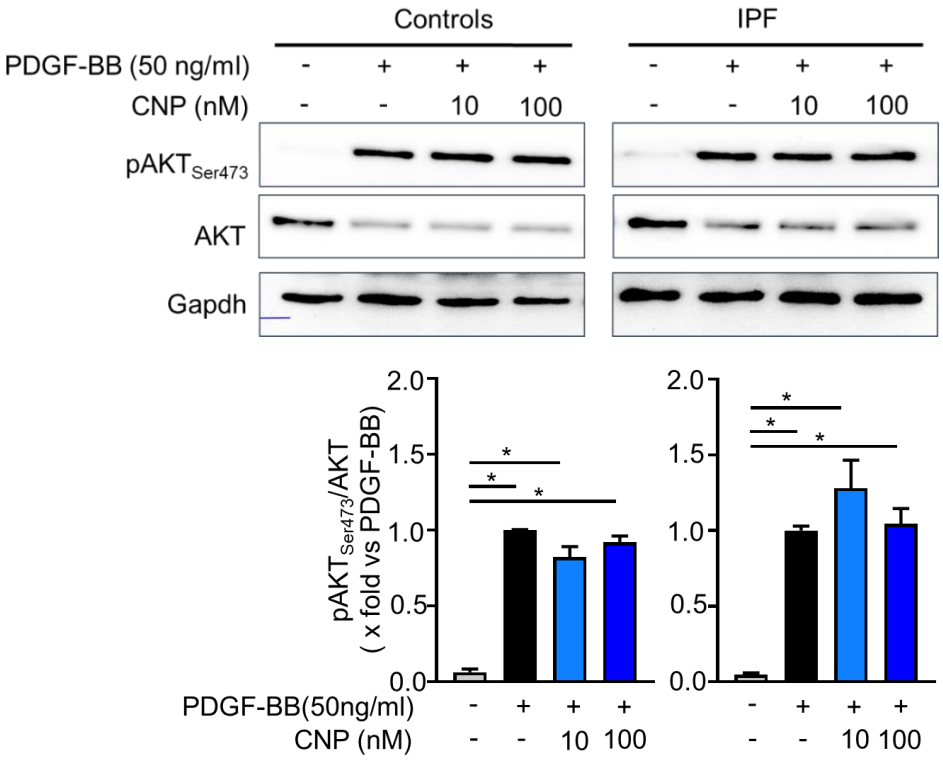

Figure 27: *Effect of CNP on PDGF-BB mediated AKT phosphorylation (serine 473) Control and IPF fibroblasts were stimulated with 10nM and 100nM CNP for 30min, followed by 50ng/ml PDGF-BB for another 30min. Proteins were isolated and phosphorylation of AKT (Ser473) and total AKT were detected by western blotting followed by densitometric analysis. Gapdh was used as a loading control. (n=3 per group, *p<0.05)*

3.2.10 CNP does not prevent PDGF-BB induced phosphorylation of ERK1/2

Another signaling pathway leading to phosphorylation of FoxO3 through PDGF-BB activation is the RAS/RAF/MEK cascade, where the kinase ERK phosphorylates FoxO3 (Lubinus et al., 1994; Roy et al., 2010). To examine if CNP can influence this kinase, ERK1/2 phosphorylation was tested by western blotting (Figure 28). In agreement with results from murine fibroblasts (Figure 18), PDGF-BB stimulation led to a substantial increase in ERK1/2 phosphorylation in both groups. No reduction of phosphorylation was evident after pretreatment with CNP at 10nM or 100nM.

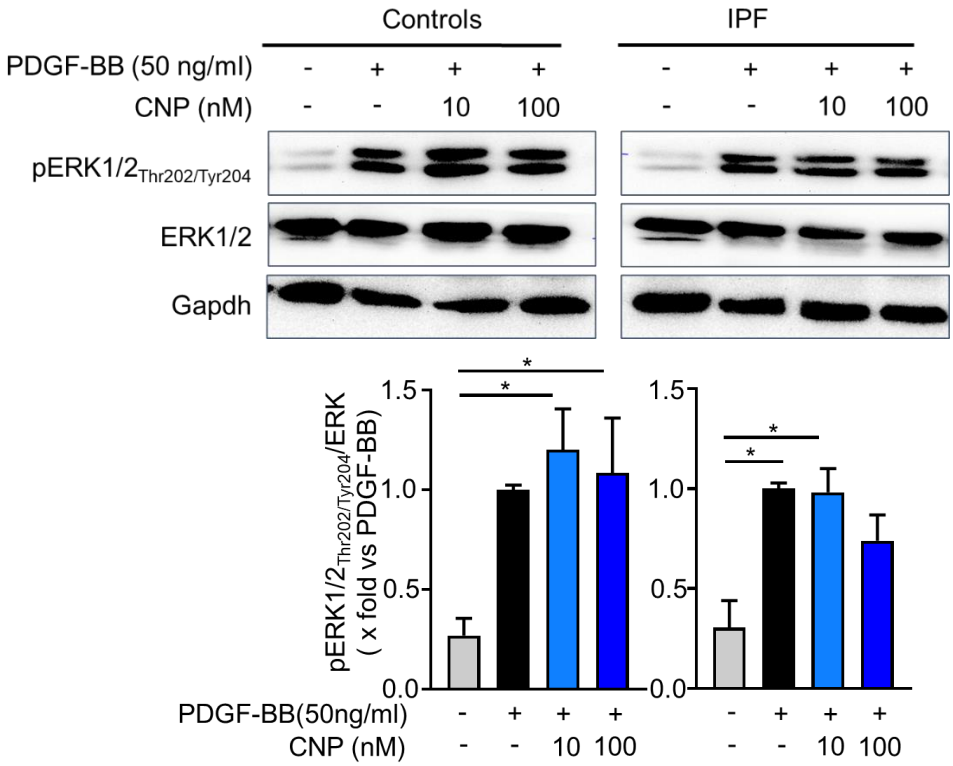

Figure 28: *Effect of CNP on PDGF-BB induced ERK phosphorylation (threonine 202/ tyrosine 204)*
*Control and IPF fibroblasts were stimulated with CNP 10nM and 100nM for 30 minutes, followed by PDGF-BB (50ng/ml) for another 30 minutes. Proteins were isolated and phosphorylation of ERK1/2 (Thr202/ Tyr204) and total ERK were detected by western blotting followed by densitometric analysis. Gapdh was used as a loading control. (n=3 per group, *p<0.05)*

4 Discussion

The pathological alteration of resident fibroblasts to myo-fibroblasts under influence of fibrogenic factors, such as PDGF-BB, has been shown to play an important role in IPF pathogenesis (Yi et al., 1996). Endogenous counter-regulating factors are barely known. Several studies have described a protective role of exogenously administered CNP in pathological tissue remodeling, for example in cardiac and hepatic fibrosis (Bae, Hino, Hosoda, Miyazato, et al., 2018; Horio et al., 2003). CNP and its cGMP producing GC-B receptor are expressed in the lung, but it is unknown whether CNP can attenuate lung fibrosis (Hirsch et al., 2003; Nakanishi et al., 1999).

By employing murine lung fibroblasts and human lung fibroblasts (from 'healthy' controls and IPF patients), this study revealed:

- an important role of CNP in regulating PDGF-BB induced collagen expression, proliferation and migration
- these inhibitory effects of CNP are mediated via the GC-B receptor
- CNP might mediate these effects via regulation of antifibrotic transcription factor, FoxO3

These results provided the foundation for further *in vivo* investigations into the therapeutic potential for targeting the signaling pathway.

4.1 CNP mediates its effects on collagen and MMP9 expression via the GC-B receptor

Studies show that CNP can target two different receptors: The GC-B receptor with guanylyl cyclase activity, and the cGMP-independent NPR-C receptor (Bennett et al., 1991). Previously, the NPR-C receptor was accepted as a clearance receptor, leading to internalization and lysosomal mediated degradation of NPs. (Almeida et al., 1989; Cohen et al., 1996). All signaling effects of CNP were thought to be mediated via the GC-B receptor. It took some time until the ability to mediate CNP signaling was also observed for the NPR-C receptor. However, in contrary to the GC-B receptor, NPR-C does not possess guanylyl cyclase activity. Instead, this receptor activates the inhibitory guanine nucleotide regulatory protein Gi, which then inhibits adenylyl cyclase activity and triggers phospholipase 2 (Anand-Srivastava et al., 1990; Anand-Srivastava et al., 1987; Hirata et al., 1989). It is still unknown how, and under which conditions, the receptor switches between its clearance and signaling functions.

To investigate the receptor responsible for mediating the preventive effect of CNP on PDGF-BB-induced collagen and MMP9 expression, a knock out (KO) of the GC-B receptor was induced in murine fibroblasts. For this purpose, lung fibroblasts isolated from mice with Col1a2Cre^{ERT2}; GC-B$^{flox/flox}$ genotype were treated with 4-OH Tamox for 72 hours to induce a KO of the receptor and compared to 4-OH Tamox treated control wildtype fibroblasts. The KO was confirmed at the genetic and protein level by DNA PCR and western blotting, respectively (Figure 6, Figure 7). The cGMP response to CNP in the KO cells was absent as compared to controls, validating a functional KO.

In agreement with previous findings from our lab, the control fibroblasts treated with 4-OH Tamox demonstrated a significant increase in the expression of collagen 1 and 3, and MMP9, after PDGF-BB treatment. Pretreatment of the cells with CNP (10nM and 100nM) prevented this effect (Figure 11, Figure 12, Figure 14). Interestingly, in KO fibroblasts, though PDGF-BB still augmented the expression of the above mentioned fibrotic markers, CNP did not display any preventive effect (Figure 11, Figure 12, Figure 14). Hence, we conclude that CNP attenuates PDGF-BB induced changes in expression of fibrotic genes through activation of the GC-B receptor.

Few earlier studies have indicated a role of CNP in regulating fibroblast phenotype. CNP was shown to inhibit DNA and collagen synthesis in cultured adult rat cardiac fibroblasts (Horio et al., 2003). CNP was further shown to ameliorate collagen increase in a bleomycin induced pulmonary fibrosis mouse model (Kimura et al., 2016). Our findings agree with these previous studies, and further, show that these effects of CNP are mediated via GC-B receptor.

Interestingly, the effect of CNP on VASP phosphorylation and expression of MMP9 and collagen was similar in concentrations of 10nM and 100nM. One plausible reason could be the saturation of the GC-B receptor at 10nM concentration, hence an increase in the CNP concentration does not show an additive effect.

4.2 CNP modulates PDGF-BB induced proliferation and migration of murine lung fibroblasts via GC-B receptor

In IPF, the lung fibroblasts exhibit significantly increased proliferation and migratory capacity. This has been attributed to the elevated levels of growth factors such as PDGF-BB and TGF-ß (Al-Tamari et al., 2018; Tisler et al., 2020). Indeed, we observed an increased migration and proliferation in control and KO fibroblasts after treatment with

PDGF-BB. Importantly, in the control group, CNP was able to reduce these functional changes. However, in the KO fibroblasts the peptide did not show any effect on the migration and proliferation induced by PDGF-BB (Figure 13, Figure 15). This confirms that the anti-proliferative and anti-migratory effects of CNP is mediated by the GC-B receptor. Intriguingly, KO fibroblasts displayed a significantly higher proliferation compared to control cells at basal conditions, hinting towards an inherent role of GC-B in regulating proliferation. This effect needs to be further investigated in future.

In bleomycin induced fibrosis mouse model, CNP infusion decreased the number of Ki-67-positive cells in lung fibrotic lesions, suggesting antiproliferative effects of CNP in PF (Murakami et al., 2004). Further, by employing a transwell migration assay using rat cardiac fibroblasts, Li *et al.* showed that CNP inhibits the migration of these cells (Li et al., 2015). Our results agree very well with these previous findings and further show that GC-B receptor mediates the effects.

4.3 CNP/GC-B signaling regulates antifibrotic transcription factor FoxO3

Recently it was shown that FoxO3 in its active, unphosphorylated form is downregulated in IPF. A knockdown of FoxO3 in healthy fibroblasts promotes fibroblast-myofibroblast conversion with increase of migration, proliferation, and collagen production. In bleomycin-induced pulmonary fibrosis, knockdown of the peptide aggravates fibrotic changes (Al-Tamari et al., 2018). FoxO3 activity is regulated by post translational modifications of the protein, mainly phosphorylation. This phosphorylation is regulated by various kinases such as AKT and ERK that are also known to be regulated by NPs via cGMP mediated signaling in different cell types (Brunet et al., 1999; Jerczynska & Pawlowska, 2009; Roy et al., 2010). Hence, we aimed to investigate whether CNP can mediate its antifibrotic effects via regulation of FoxO3. In previous studies carried out in our lab, the typical profibrotic phosphorylation of FoxO3 at Threonine 32 was detected after treatment of control lung fibroblasts with PDGF-BB. This phosphorylation was prevented after pretreatment with CNP.

As a part of the presented thesis work, the effect of GC-B KO was analyzed on the CNP mediated regulation of FoxO3 phosphorylation. Similar to our previous results, PDGF-BB induced FoxO3 phosphorylation was prevented by CNP in control murine lung fibroblasts. This effect was completely removed in GC-B KO fibroblasts (Figure 16).

To investigate the mechanism underlying CNP dependent regulation of the FoxO3 phosphorylation, AKT and ERK1/2 phosphorylation were studied. Both kinases are known to induce phosphorylation of FoxO3 and are activated by growth factors like IGF-1 (Brunet et al., 1999; Nho et al., 2011; Roy et al., 2010). This described increase in phosphorylation was observed in control and KO group after treatment with PDGF-BB. Previous studies have also shown that in endothelial cells CNP inhibits the activation of PI3K/AKT and MEK/ERK pathways by the cytokine TNFα, concomitantly reducing the expression of the fibrinolysis inhibitor PAI-1 (plasminogen activator inhibitor type 1) (Jerczynska & Pawlowska, 2009). However, depending on the cell type, opposite effect of CNP on activation of AKT and ERK1/2 are observed mediated via the NPR-C pathway (Bubb et al., 2019). In the current study, CNP did not exhibit any significant effect on PDGF-BB induced phosphorylation of AKT and ERK1/2 in the control or GC-B KO group. Based on our results, we conclude that CNP is not dephosphorylating FoxO3 via these two pathways (Figure 17, Figure 18). Hence, other signaling pathways leading to inactivation of FoxO3 need to be further explored and their regulation by CNP studied. For example, serum- and glucocorticoid-inducible kinases (SGKs), which also can be activated by growth factors and lead to cellular functions in concert with AKT, could be part of continuing studies (Brunet et al., 2001). Further, considering the high number of negative regulatory Ser/Thr phosphoacceptor sites of FoxO3, the involvement of protein Ser/Thr phosphatases in the control of transcriptional activity was investigated by Singh *et al.* in 2010. In their study, they detected a strong interaction between FoxO3 and the Protein Phosphatase 2A (PP2A). After inhibition of AKT, PP2A-mediated dephosphorylation of Thr32/Ser253 is necessary for dissociation of the scaffold protein 14-3-3, nuclear translocation, and activation of FoxO3 (Singh et al., 2010). Therefore, future studies should explore the Foxo3 reactivating, dephosphorylating phosphatases.

4.4 CNP mediated cGMP response in control and IPF fibroblasts and expression of CNP receptors (GC-B and NPR-C)

After a preventive, antifibrotic effect of CNP on PDGF-BB induced fibrosis was proven in murine lung fibroblasts, similar studies were carried out in human lung fibroblasts to verify the clinical relevance. For these experiments healthy control and diseased idiopathic pulmonary fibrosis (IPF) fibroblasts were used to compare the reaction of the physiological and pathophysiological cells to the stimulation.

In both control and IPF fibroblasts, treatment with CNP leads to a similar increase in the cGMP response, confirming that CNP can take effect under healthy and diseased conditions (Figure 19A). However, a comparison of the absolute cGMP amount at basal level demonstrated a lower formation rate in the IPF cells (Figure 19B). Also, with increasing CNP concentration the absolute cGMP level tends to be lower in the IPF cells (Figure 19C). Interestingly, the expression of the GC-B receptor is increased in the IPF fibroblasts (Figure 20). This means that the diseased cells display higher membrane receptor expression, but the receptor is producing less cGMP on binding CNP. Previous studies showed that temporal desensitization of the receptor can be a reason for the reduced cGMP formation. This conformation change happens in a time-dependent manner after exposure to the NP, leading to dephosphorylation, and therefore, inactivation of the GC-B receptor (Potter, 1998). It is also published that growth factors can inhibit the GC-B receptor by dephosphorylation (Robinson et al., 2017). In IPF fibroblasts these factors are more represented, leading to less activated receptors. In contrast, the NPR-C receptor expression was similar in both groups.

4.5 CNP prevents PDGF-BB induced collagen 1, MMP9 expression, proliferation and migration in control and IPF fibroblasts

As mentioned above, Al-Tamari *et al.* previously described an increased collagen expression and proliferation in human IPF fibroblasts *in vitro* when compared to a healthy control group (Al-Tamari et al., 2018). Also, the collagen fiber organization of control and diseased fibroblasts were compared and an increased cell migration was already detected (Tisler et al., 2020). All these results could be confirmed in this thesis to an extent. IPF fibroblasts exhibited significantly higher migration rate in comparison to control group (Figure 24). Furthermore, a tendency towards increased proliferation was observed in IPF fibroblasts (Figure 25).

Next, the protective effects of CNP (uncovered in murine lung fibroblasts) on PDGF-BB driven collagen expression, proliferation, and migration were investigated in human cells. The PDGF-BB induced increase in collagen 1 and MMP9 expression was reduced after CNP pretreatment in control and IPF fibroblasts (Figure 22, Figure 23). Moreover, the PDGF-BB mediated enhanced migration and proliferation was attenuated by CNP stimulation in both groups (Figure 24, Figure 25). Importantly, these results show that effects of CNP are preserved in healthy human control as well as IPF fibroblasts. CNP can play a preventive role not only in healthy patients, but also in IPF where it could help

to ameliorate the disease. Similar to the murine cells, CNP concentrations of 10nM and 100nM displayed a similar effect, that can again be due to the saturation of GC-B receptor already at the lower CNP concentration. Indeed, as observed from the RIA, cGMP response to 10nM and 100nM CNP were quite similar in both control and IPF fibroblasts.

4.6 CNP prevents PDGF-BB-induced phosphorylation of FoxO3 in control fibroblasts, while the effect was attenuated in IPF fibroblasts

In previous studies, a decreased FoxO3 expression was detected in IPF fibroblasts compared to a control group, whereas the inactive, phosphorylated FoxO3 form was upregulated (Al-Tamari et al., 2018). This underpins the idea that regulation of the transcription factor plays an important role in this disease. To study whether CNP can influence FoxO3 as in murine fibroblasts, the phosphorylation of FoxO3, AKT and ERK1/2 were investigated by western blotting. All three, FoxO3, AKT, and ERK1/2, exhibited increased phosphorylation in response to PDGF-BB stimulation, in both control and IPF fibroblasts. Similar to murine cells, CNP prevented FoxO3 phosphorylation significantly in control cells, while this was less pronounced in IPF cells (Figure 26). Furthermore, AKT and ERK1/2 phosphorylation were not affected by CNP (Figure 27, Figure 28). In conclusion, PDGF-BB mediated FoxO3 phosphorylation is prevented by CNP in human fibroblasts. Consistent with murine fibroblasts, this effect is via GC-B receptor. Further studies need to be carried out in order to determine the mechanism underlying this regulation.

4.7 Conclusion and Outlook

Taken together, the results of this thesis show that CNP moderates the PDGF-BB-induced activation and differentiation of human and murine lung fibroblasts to myofibroblasts. The peptide prevents an increase of collagen and MMP9 expression and reduces the migratory and proliferative capacity of the cells. This effect is mediated by GC-B/cGMP signaling and by FoxO3 regulation/stabilization. Importantly, the observation that the antifibrotic effect is preserved in IPF fibroblasts confirms the therapeutically relevance of these findings.

To follow up the pathophysiological and therapeutic importance of these results, we are generating mice with fibroblast-restricted GC-B deletion for studies in the model of

bleomycin-induced pulmonary fibrosis. Additionally, the desensitization of the GC-B receptor detected in the IPF cells will be further explored. Therefore, a cyclase assay is planned to investigate the guanylyl cyclase activity of the GC-B receptor and the phosphorylation status of the GC-B receptor in control and IPF fibroblasts will be checked.

5 Summary

Idiopathic Pulmonary Fibrosis (IPF) is a progressive parenchymal lung disease with limited therapeutic treatments. Pathologically altered lung fibroblasts, called myofibroblasts, exhibit increased proliferation, migration, and collagen production, and drive IPF development and progression. Fibrogenic factors such as Platelet derived growth factor-BB (PDGF-BB) contribute to these pathological alterations. Endogenous counter-regulating factors are barely known. Published studies have described a protective role of exogenously administered C-type Natriuretic Peptide (CNP) in pathological tissue remodeling, for example in heart and liver fibrosis. CNP and its cyclic GMP producing guanylyl cyclase B (GC-B) receptor are expressed in the lungs, but it is unknown whether CNP can attenuate lung fibrosis by this pathway. To address this question, we performed studies in primary cultured lung fibroblasts.

To examine the effects of the CNP/GC-B pathway on PDGF-BB-induced collagen production, proliferation, and migration *in vitro*, lung fibroblasts were cultured from wild-type control and GC-B knockout mice. Human lung fibroblasts from patients with IPF and healthy controls were obtained from the UGMLC Biobank. In RIA experiments, CNP, at 10nM and 100nM, markedly and similarly increased cGMP levels in both the murine and human lung fibroblasts, demonstrating GC-B/cGMP signaling. CNP reduced PDGF-BB-induced proliferation and migration of lung fibroblasts in BrdU incorporation and gap closure assays, respectively. CNP strongly decreased PDGF-BB-induced collagen 1/3 expression as measured by immunocytochemistry and immunoblotting. Importantly, the protective actions of CNP were preserved in IPF fibroblasts. It is known that the profibrotic actions of PDGF-BB are partly mediated by phosphorylation and nuclear export of Forkhead Box O3 (FoxO3), a transcription factor downregulated in IPF. CNP prevented PDGF-BB elicited FoxO3 phosphorylation and nuclear exclusion in both murine and human control and IPF fibroblasts. CNP signaling and functions were abolished in GC-B-deficient lung fibroblasts.

Taken together, the results show that CNP moderates the PDGF-BB-induced activation and differentiation of human and murine lung fibroblasts to myofibroblasts. This effect is mediated CNP-dependent by GC-B/cGMP signaling and FoxO3 regulation. To follow up the patho-physiological relevance of these results, we are generating mice with fibroblast-restricted GC-B deletion for studies in the model of bleomycin-induced pulmonary fibrosis.

6 Zusammenfassung

Idiopathische pulmonale Fibrose (IPF) ist eine progressiv fortschreitende, parenchymale Lungenerkrankung mit beschränkten therapeutischen Behandlungsmöglichkeiten. Pathologisch veränderte Lungenfibroblasten, sogenannte Myofibroblasten, zeigen eine verstärkte Proliferation, Migration und Kollagenproduktion, die zu einem permanenten Fortschreiten der Erkrankung führen. Während fibrogene Faktoren wie Platelet derived growth factor-BB (PDGF-BB) zu dieser pathologischen Veränderung beitragen, sind endogene Faktoren, die diesem Wandel entgegenwirken, kaum bekannt. Allerdings konnten Studien bereits eine protektive Wirkung von exogen verabreichten C-typ natriuretischen Peptid (CNP) auf krankhaft verändertes Gewebe beschreiben, wie beispielsweise bei Herz- und Leberfibrose. Es ist bekannt, dass CNP und sein cGMP produzierender Rezeptor Guanylyl-Cyclase-B Rezeptor (GC-B) in der Lunge exprimiert werden. Allerdings konnte noch nicht nachgewiesen werden, ob CNP durch diesen Signalweg den Fortschritt einer Lungenfibrose verzögern kann. Um dies herauszufinden, wurden Experimente mit kultivierten, primären Lungenfibroblasten durchgeführt.

Um die Effekte des CNP/ GC-B Signalwegs auf die PDGF-BB induzierte Kollagenproduktion, Proliferation und Migration *in vitro* zu überprüfen, wurden Lungenfibroblasten von Kontroll- und GC-B-Knock-Out Mäusen kultiviert. Weiterhin erhielten wir von der UGMLC Biobank menschliche Fibroblasten von IPF-erkrankten Patienten, sowie gesunde Kontrollfibroblasten. Zur Bestätigung der Funktionalität des GC-B/cGMP Weges, wurde in murinen und humanen Fibroblasten mithilfe eines RIAs ein durch CNP (10nM und 100nM) deutlich erhöhtes cGMP-Level gemessen. CNP reduzierte die durch PDGF-BB induzierte Beschleunigung von Proliferation und Migration der Lungenfibroblasten, was mit Hilfe von BrdU incorporation und Gap closure assay nachgewiesen wurde. Ebenfalls zeigten Immunocytochemistrie und -blotting, dass CNP den PDGF-BB induzierten Anstieg an Kollagenexpression verhindert. Somit wurde festgestellt, dass der schützende Effekt von CNP auch in IPF Fibroblasten erhalten bleibt. Weiterhin ist bekannt, dass die PDGF-BB-induzierten, profibrotischen Veränderungen durch Phosphorylierung und Export des Transkriptionsfaktors Forkhead Box O3 (FoxO3) aus dem Zellkern vermittelt werden, welcher in IPF Fibroblasten vermindert exprimiert ist. CNP verhindert diese PDGF-BB aktivierte Phosphorylierung und Translokation in murinen und humanen Kontroll- und IPF-Fibroblasten. In Lungenfibroblasten mit Deletion des GC-B- Rezeptors war das CNP-Signal und auch dessen Effekt ausgelöscht.

Zusammengefasst zeigen die Ergebnisse, dass CNP die PDGF-BB induzierte Aktivierung und Differenzierung von menschlichen und murinen Lungenfibroblasten zu Myofibroblasten beeinflusst. Dieser Effekt wird CNP-abhängig durch den GC-B/cGMP Signalweg und durch die Regulierung von FoxO3 vermittelt. Um abschließend die pathophysiologische Relevanz dieser Erkenntnisse zu zeigen, werden zukünftig Mäuse mit einer fibroblasten-spezifischen Deletion des GC-B Rezeptors für Studien in Bleomycin-induzierter Lungenfibrose genutzt.

7 References

Al-Tamari, H. M., Dabral, S., Schmall, A., Sarvari, P., Ruppert, C., Paik, J., DePinho, R. A., Grimminger, F., Eickelberg, O., Guenther, A., Seeger, W., Savai, R., & Pullamsetti, S. S. (2018). FoxO3 an important player in fibrogenesis and therapeutic target for idiopathic pulmonary fibrosis. *EMBO Mol Med*, *10*(2), 276-293. https://doi.org/10.15252/emmm.201606261

Almeida, F. A., Suzuki, M., Scarborough, R. M., Lewicki, J. A., & Maack, T. (1989). Clearance function of type C receptors of atrial natriuretic factor in rats. *Am J Physiol*, *256*(2 Pt 2), R469-475. https://doi.org/10.1152/ajpregu.1989.256.2.R469

Ambrosini, V., Cancellieri, A., Chilosi, M., Zompatori, M., Trisolini, R., Saragoni, L., & Poletti, V. (2003). Acute exacerbation of idiopathic pulmonary fibrosis: report of a series. *Eur Respir J*, *22*(5), 821-826. https://doi.org/10.1183/09031936.03.00022703

Anand-Srivastava, M. B., Sairam, M. R., & Cantin, M. (1990). Ring-deleted analogs of atrial natriuretic factor inhibit adenylate cyclase/cAMP system. Possible coupling of clearance atrial natriuretic factor receptors to adenylate cyclase/cAMP signal transduction system. *J Biol Chem*, *265*(15), 8566-8572. https://www.ncbi.nlm.nih.gov/pubmed/2160462

Anand-Srivastava, M. B., Srivastava, A. K., & Cantin, M. (1987). Pertussis toxin attenuates atrial natriuretic factor-mediated inhibition of adenylate cyclase. Involvement of inhibitory guanine nucleotide regulatory protein. *J Biol Chem*, *262*(11), 4931-4934. https://www.ncbi.nlm.nih.gov/pubmed/3031034

Anderson, M. J., Viars, C. S., Czekay, S., Cavenee, W. K., & Arden, K. C. (1998). Cloning and characterization of three human forkhead genes that comprise an FKHR-like gene subfamily. *Genomics*, *47*(2), 187-199. https://doi.org/10.1006/geno.1997.5122

Antoniades, H. N., Scher, C. D., & Stiles, C. D. (1979). Purification of human platelet-derived growth factor. *Proc Natl Acad Sci U S A*, *76*(4), 1809-1813. https://doi.org/10.1073/pnas.76.4.1809

Aoki, M., Jiang, H., & Vogt, P. K. (2004). Proteasomal degradation of the FoxO1 transcriptional regulator in cells transformed by the P3k and Akt oncoproteins. *Proc Natl Acad Sci U S A*, *101*(37), 13613-13617. https://doi.org/10.1073/pnas.0405454101

Bae, C. R., Hino, J., Hosoda, H., Miyazato, M., & Kangawa, K. (2018). C-type natriuretic peptide (CNP) in endothelial cells attenuates hepatic fibrosis and inflammation in non-alcoholic steatohepatitis. *Life Sci*, *209*, 349-356. https://doi.org/10.1016/j.lfs.2018.08.031

Bae, C. R., Hino, J., Hosoda, H., Son, C., Makino, H., Tokudome, T., Tomita, T., Hosoda, K., Miyazato, M., & Kangawa, K. (2018). Adipocyte-specific expression of C-type natriuretic peptide suppresses lipid metabolism and adipocyte hypertrophy in adipose tissues in mice fed high-fat diet. *Sci Rep*, *8*(1), 2093. https://doi.org/10.1038/s41598-018-20469-z

Baumgartner, K. B., Samet, J. M., Stidley, C. A., Colby, T. V., & Waldron, J. A. (1997). Cigarette smoking: a risk factor for idiopathic pulmonary fibrosis. *Am J Respir Crit Care Med*, *155*(1), 242-248. https://doi.org/10.1164/ajrccm.155.1.9001319

Bennett, B. D., Bennett, G. L., Vitangcol, R. V., Jewett, J. R., Burnier, J., Henzel, W., & Lowe, D. G. (1991). Extracellular domain-IgG fusion proteins for three human natriuretic peptide receptors. Hormone pharmacology and application to solid phase screening of synthetic peptide antisera. *J Biol Chem*, *266*(34), 23060-23067. https://www.ncbi.nlm.nih.gov/pubmed/1660465

Bergsten, E., Uutela, M., Li, X., Pietras, K., Ostman, A., Heldin, C. H., Alitalo, K., & Eriksson, U. (2001). PDGF-D is a specific, protease-activated ligand for the PDGF beta-receptor. *Nat Cell Biol*, *3*(5), 512-516. https://doi.org/10.1038/35074588

Betsuyaku, T., Fukuda, Y., Parks, W. C., Shipley, J. M., & Senior, R. M. (2000). Gelatinase B is required for alveolar bronchiolization after intratracheal bleomycin. *Am J Pathol*, *157*(2), 525-535. https://doi.org/10.1016/S0002-9440(10)64563-4

Bonnans, C., Chou, J., & Werb, Z. (2014). Remodelling the extracellular matrix in development and disease. *Nat Rev Mol Cell Biol*, *15*(12), 786-801. https://doi.org/10.1038/nrm3904

Bonner, J. C. (2004). Regulation of PDGF and its receptors in fibrotic diseases. *Cytokine Growth Factor Rev*, *15*(4), 255-273. https://doi.org/10.1016/j.cytogfr.2004.03.006

Brunet, A., Bonni, A., Zigmond, M. J., Lin, M. Z., Juo, P., Hu, L. S., Anderson, M. J., Arden, K. C., Blenis, J., & Greenberg, M. E. (1999). Akt promotes cell survival by phosphorylating and inhibiting a Forkhead transcription factor. *Cell*, *96*(6), 857-868. https://doi.org/10.1016/s0092-8674(00)80595-4

Brunet, A., Park, J., Tran, H., Hu, L. S., Hemmings, B. A., & Greenberg, M. E. (2001). Protein kinase SGK mediates survival signals by phosphorylating the forkhead transcription factor FKHRL1 (FOXO3a). *Mol Cell Biol*, *21*(3), 952-965. https://doi.org/10.1128/MCB.21.3.952-965.2001

Bubb, K. J., Aubdool, A. A., Moyes, A. J., Lewis, S., Drayton, J. P., Tang, O., Mehta, V., Zachary, I. C., Abraham, D. J., Tsui, J., & Hobbs, A. J. (2019). Endothelial C-Type Natriuretic Peptide Is a Critical Regulator of Angiogenesis and Vascular Remodeling. *Circulation*, *139*(13), 1612-1628. https://doi.org/10.1161/CIRCULATIONAHA.118.036344

Carter, M. E., & Brunet, A. (2007). FOXO transcription factors. *Curr Biol*, *17*(4), R113-114. https://doi.org/10.1016/j.cub.2007.01.008

Cataliotti, A., Giordano, M., De Pascale, E., Giordano, G., Castellino, P., Jougasaki, M., Costello, L. C., Boerrigter, G., Tsuruda, T., Belluardo, P., Lee, S. C., Huntley, B., Sandberg, S., Malatino, L. S., & Burnett, J. C., Jr. (2002). CNP production in the kidney and effects of protein intake restriction in nephrotic syndrome. *Am J Physiol Renal Physiol*, *283*(3), F464-472. https://doi.org/10.1152/ajprenal.00372.2001

Chang, M. S., Lowe, D. G., Lewis, M., Hellmiss, R., Chen, E., & Goeddel, D. V. (1989). Differential activation by atrial and brain natriuretic peptides of two different receptor guanylate cyclases. *Nature*, *341*(6237), 68-72. https://doi.org/10.1038/341068a0

Chinkers, M., Garbers, D. L., Chang, M. S., Lowe, D. G., Chin, H. M., Goeddel, D. V., & Schulz, S. (1989). A membrane form of guanylate cyclase is an atrial natriuretic peptide receptor. *Nature*, *338*(6210), 78-83. https://doi.org/10.1038/338078a0

Chusho, H., Tamura, N., Ogawa, Y., Yasoda, A., Suda, M., Miyazawa, T., Nakamura, K., Nakao, K., Kurihara, T., Komatsu, Y., Itoh, H., Tanaka, K., Saito, Y., Katsuki, M., & Nakao, K. (2001). Dwarfism and early death in mice lacking C-type natriuretic peptide. *Proc Natl Acad Sci U S A*, *98*(7), 4016-4021. https://doi.org/10.1073/pnas.071389098

Claesson-Welsh, L., Eriksson, A., Westermark, B., & Heldin, C. H. (1989). cDNA cloning and expression of the human A-type platelet-derived growth factor (PDGF) receptor establishes structural similarity to the B-type PDGF receptor. *Proc Natl Acad Sci U S A*, *86*(13), 4917-4921. https://doi.org/10.1073/pnas.86.13.4917

Cohen, D., Koh, G. Y., Nikonova, L. N., Porter, J. G., & Maack, T. (1996). Molecular determinants of the clearance function of type C receptors of natriuretic peptides. *J Biol Chem*, *271*(16), 9863-9869. https://doi.org/10.1074/jbc.271.16.9863

de Bold, A. J., Borenstein, H. B., Veress, A. T., & Sonnenberg, H. (1981). A rapid and potent natriuretic response to intravenous injection of atrial myocardial extract in rats. *Life Sci*, *28*(1), 89-94. https://doi.org/10.1016/0024-3205(81)90370-2

Desmouliere, A., Geinoz, A., Gabbiani, F., & Gabbiani, G. (1993). Transforming growth factor-beta 1 induces alpha-smooth muscle actin expression in granulation tissue myofibroblasts and in quiescent and growing cultured fibroblasts. *J Cell Biol*, *122*(1), 103-111. https://doi.org/10.1083/jcb.122.1.103

Donovan, J., Shiwen, X., Norman, J., & Abraham, D. (2013). Platelet-derived growth factor alpha and beta receptors have overlapping functional activities towards fibroblasts. *Fibrogenesis Tissue Repair*, *6*(1), 10. https://doi.org/10.1186/1755-1536-6-10

Douglas, W. W., Ryu, J. H., & Schroeder, D. R. (2000). Idiopathic pulmonary fibrosis: Impact of oxygen and colchicine, prednisone, or no therapy on survival. *Am J Respir Crit Care Med*, *161*(4 Pt 1), 1172-1178. https://doi.org/10.1164/ajrccm.161.4.9907002

Fabisiak, J. P., Evans, J. N., & Kelley, J. (1989). Increased expression of PDGF-B (c-sis) mRNA in rat lung precedes DNA synthesis and tissue repair during chronic hyperoxia. *Am J Respir Cell Mol Biol*, *1*(3), 181-189. https://doi.org/10.1165/ajrcmb/1.3.181

Flynn, T. G., de Bold, M. L., & de Bold, A. J. (1983). The amino acid sequence of an atrial peptide with potent diuretic and natriuretic properties. *Biochem Biophys Res Commun*, *117*(3), 859-865. https://doi.org/10.1016/0006-291x(83)91675-3

Ghosh Choudhury, G., Lenin, M., Calhaun, C., Zhang, J. H., & Abboud, H. E. (2003). PDGF inactivates forkhead family transcription factor by activation of Akt in glomerular mesangial cells. *Cell Signal*, *15*(2), 161-170. https://doi.org/10.1016/s0898-6568(02)00057-8

Gingery, A., Yang, T. H., Passe, S. M., An, K. N., Zhao, C., & Amadio, P. C. (2014). TGF-beta signaling regulates fibrotic expression and activity in carpal tunnel syndrome. *J Orthop Res*, *32*(11), 1444-1450. https://doi.org/10.1002/jor.22694

Hardman, J. G., & Sutherland, E. W. (1969). Guanyl cyclase, an enzyme catalyzing the formation of guanosine 3',5'-monophosphate from guanosine trihosphate. *J Biol Chem*, *244*(23), 6363-6370. https://www.ncbi.nlm.nih.gov/pubmed/4982201

Heldin, C. H., & Westermark, B. (1999). Mechanism of action and in vivo role of platelet-derived growth factor. *Physiol Rev*, *79*(4), 1283-1316. https://doi.org/10.1152/physrev.1999.79.4.1283

Hermanns-Le, T., Pierard, G. E., Jennes, S., & Pierard-Franchimont, C. (2015). Protomyofibroblast Pathway in Early Thermal Burn Healing. *Skin Pharmacol Physiol*, *28*(5), 250-254. https://doi.org/10.1159/000430102

Hinz, B., Mastrangelo, D., Iselin, C. E., Chaponnier, C., & Gabbiani, G. (2001). Mechanical tension controls granulation tissue contractile activity and myofibroblast differentiation. *Am J Pathol*, *159*(3), 1009-1020. https://doi.org/10.1016/S0002-9440(10)61776-2

Hirata, M., Chang, C. H., & Murad, F. (1989). Stimulatory effects of atrial natriuretic factor on phosphoinositide hydrolysis in cultured bovine aortic smooth muscle cells. *Biochim Biophys Acta*, *1010*(3), 346-351. https://doi.org/10.1016/0167-4889(89)90060-8

Hirsch, J. R., Skutta, N., & Schlatter, E. (2003). Signaling and distribution of NPR-Bi, the human splice form of the natriuretic peptide receptor type B. *Am J Physiol Renal Physiol*, *285*(2), F370-374. https://doi.org/10.1152/ajprenal.00049.2003

Hodgson, U., Laitinen, T., & Tukiainen, P. (2002). Nationwide prevalence of sporadic and familial idiopathic pulmonary fibrosis: evidence of founder effect among multiplex families in Finland. *Thorax*, *57*(4), 338-342. https://doi.org/10.1136/thorax.57.4.338

Horio, T., Tokudome, T., Maki, T., Yoshihara, F., Suga, S., Nishikimi, T., Kojima, M., Kawano, Y., & Kangawa, K. (2003). Gene expression, secretion, and autocrine action of C-type natriuretic peptide in cultured adult rat cardiac fibroblasts. *Endocrinology*, *144*(6), 2279-2284. https://doi.org/10.1210/en.2003-0128

Hunt, P. J., Richards, A. M., Espiner, E. A., Nicholls, M. G., & Yandle, T. G. (1994). Bioactivity and metabolism of C-type natriuretic peptide in normal man. *J Clin Endocrinol Metab*, *78*(6), 1428-1435. https://doi.org/10.1210/jcem.78.6.8200946

Ichiki, T., Dzhoyashvili, N., & Burnett, J. C., Jr. (2019). Natriuretic peptide based therapeutics for heart failure: Cenderitide: A novel first-in-class designer natriuretic peptide. *Int J Cardiol*, *281*, 166-171. https://doi.org/10.1016/j.ijcard.2018.06.002

Igaki, T., Itoh, H., Suga, S., Hama, N., Ogawa, Y., Komatsu, Y., Mukoyama, M., Sugawara, A., Yoshimasa, T., Tanaka, I., & Nakao, K. (1996). C-type natriuretic peptide in chronic renal failure and its action in humans. *Kidney Int Suppl*, *55*, S144-147. https://www.ncbi.nlm.nih.gov/pubmed/8743538

Itoh, T., Nagaya, N., Murakami, S., Fujii, T., Iwase, T., Ishibashi-Ueda, H., Yutani, C., Yamagishi, M., Kimura, H., & Kangawa, K. (2004). C-type natriuretic peptide ameliorates monocrotaline-induced pulmonary hypertension in rats. *Am J Respir Crit Care Med*, *170*(11), 1204-1211. https://doi.org/10.1164/rccm.200404-455OC

Iwai, K., Mori, T., Yamada, N., Yamaguchi, M., & Hosoda, Y. (1994). Idiopathic pulmonary fibrosis. Epidemiologic approaches to occupational exposure. *Am J Respir Crit Care Med*, *150*(3), 670-675. https://doi.org/10.1164/ajrccm.150.3.8087336

Iyer, S., Ambrogini, E., Bartell, S. M., Han, L., Roberson, P. K., de Cabo, R., Jilka, R. L., Weinstein, R. S., O'Brien, C. A., Manolagas, S. C., & Almeida, M. (2013). FOXOs attenuate bone formation by suppressing Wnt signaling. *J Clin Invest*, *123*(8), 3409-3419. https://doi.org/10.1172/JCI68049

Jackson, B. C., Carpenter, C., Nebert, D. W., & Vasiliou, V. (2010). Update of human and mouse forkhead box (FOX) gene families. *Hum Genomics*, *4*(5), 345-352. https://doi.org/10.1186/1479-7364-4-5-345

Jacobs, F. M., van der Heide, L. P., Wijchers, P. J., Burbach, J. P., Hoekman, M. F., & Smidt, M. P. (2003). FoxO6, a novel member of the FoxO class of transcription factors with distinct shuttling dynamics. *J Biol Chem*, *278*(38), 35959-35967. https://doi.org/10.1074/jbc.M302804200

Jerczynska, H., & Pawlowska, Z. (2009). Intracellular signaling pathways involved in inhibition of PAI-1 expression by CNP in endothelial cells. *Regul Pept*, *155*(1-3), 150-155. https://doi.org/10.1016/j.regpep.2009.02.004

Jo, H. E., Glaspole, I., Grainge, C., Goh, N., Hopkins, P. M., Moodley, Y., Reynolds, P. N., Chapman, S., Walters, E. H., Zappala, C., Allan, H., Keir, G. J., Hayen, A., Cooper, W. A., Mahar, A. M., Ellis, S., Macansh, S., & Corte, T. J. (2017). Baseline characteristics of idiopathic pulmonary fibrosis: analysis from the Australian Idiopathic Pulmonary Fibrosis Registry. *Eur Respir J*, *49*(2), 1601592. https://doi.org/10.1183/13993003.01592-2016

Kaestner, K. H., Knochel, W., & Martinez, D. E. (2000). Unified nomenclature for the winged helix/forkhead transcription factors. *Genes Dev*, *14*(2), 142-146. https://www.ncbi.nlm.nih.gov/pubmed/10702024

Kendall, R. T., & Feghali-Bostwick, C. A. (2014). Fibroblasts in fibrosis: novel roles and mediators. *Front Pharmacol*, *5*, 123. https://doi.org/10.3389/fphar.2014.00123

Kenny, A. J., Bourne, A., & Ingram, J. (1993). Hydrolysis of human and pig brain natriuretic peptides, urodilatin, C-type natriuretic peptide and some C-receptor ligands by endopeptidase-24.11. *Biochem J*, *291 (Pt 1)*, 83-88. https://doi.org/10.1042/bj2910083

Kim, J. Y., Choeng, H. C., Ahn, C., & Cho, S. H. (2009). Early and late changes of MMP-2 and MMP-9 in bleomycin-induced pulmonary fibrosis. *Yonsei Med J*, *50*(1), 68-77. https://doi.org/10.3349/ymj.2009.50.1.68

Kimura, T., Nojiri, T., Hino, J., Hosoda, H., Miura, K., Shintani, Y., Inoue, M., Zenitani, M., Takabatake, H., Miyazato, M., Okumura, M., & Kangawa, K. (2016). C-type natriuretic peptide ameliorates pulmonary fibrosis by acting on lung fibroblasts in mice. *Respir Res*, *17*, 19. https://doi.org/10.1186/s12931-016-0335-6

Kisch, B. (1956). Electron microscopy of the atrium of the heart. I. Guinea pig. *Exp Med Surg*, *14*(2-3), 99-112. https://www.ncbi.nlm.nih.gov/pubmed/13365605

Kohler, N., & Lipton, A. (1974). Platelets as a source of fibroblast growth-promoting activity. *Exp Cell Res*, *87*(2), 297-301. https://doi.org/10.1016/0014-4827(74)90484-4

Kuhn, C., 3rd, Boldt, J., King, T. E., Jr., Crouch, E., Vartio, T., & McDonald, J. A. (1989). An immunohistochemical study of architectural remodeling and connective tissue synthesis in pulmonary fibrosis. *Am Rev Respir Dis*, *140*(6), 1693-1703. https://doi.org/10.1164/ajrccm/140.6.1693

Kuhn, M. (2003). Structure, regulation, and function of mammalian membrane guanylyl cyclase receptors, with a focus on guanylyl cyclase-A. *Circ Res*, *93*(8), 700-709. https://doi.org/10.1161/01.RES.0000094745.28948.4D

Kuhn, M. (2012). Endothelial actions of atrial and B-type natriuretic peptides. *Br J Pharmacol*, *166*(2), 522-531. https://doi.org/10.1111/j.1476-5381.2012.01827.x

Kuhn, M. (2016). Molecular Physiology of Membrane Guanylyl Cyclase Receptors. *Physiol Rev*, *96*(2), 751-804. https://doi.org/10.1152/physrev.00022.2015

Lam, E. W., Brosens, J. J., Gomes, A. R., & Koo, C. Y. (2013). Forkhead box proteins: tuning forks for transcriptional harmony. *Nat Rev Cancer*, *13*(7), 482-495. https://doi.org/10.1038/nrc3539

LaRochelle, W. J., Jeffers, M., McDonald, W. F., Chillakuru, R. A., Giese, N. A., Lokker, N. A., Sullivan, C., Boldog, F. L., Yang, M., Vernet, C., Burgess, C. E., Fernandes, E., Deegler, L. L., Rittman, B., Shimkets, J., Shimkets, R. A., Rothberg, J. M., & Lichenstein, H. S. (2001). PDGF-D, a new protease-activated growth factor. *Nat Cell Biol*, *3*(5), 517-521. https://doi.org/10.1038/35074593

Lee, E. G., Lee, T. H., Hong, Y., Ryoo, J., Heo, J. W., Gil, B. M., Kang, H. S., Kwon, S. S., & Kim, Y. H. (2021). Effects of low-dose pirfenidone on survival and lung function decline in patients with idiopathic pulmonary fibrosis (IPF): Results from a real-world study. *PLoS One*, *16*(12), e0261684. https://doi.org/10.1371/journal.pone.0261684

Lee, J. S. (2014). The Role of Gastroesophageal Reflux and Microaspiration in Idiopathic Pulmonary Fibrosis. *Clin Pulm Med*, *21*(2), 81-85. https://doi.org/10.1097/cpm.0000000000000031

Legrand, C., Gilles, C., Zahm, J. M., Polette, M., Buisson, A. C., Kaplan, H., Birembaut, P., & Tournier, J. M. (1999). Airway epithelial cell migration dynamics. MMP-9 role in cell-extracellular matrix remodeling. *J Cell Biol*, *146*(2), 517-529. https://doi.org/10.1083/jcb.146.2.517

Li, X., Ponten, A., Aase, K., Karlsson, L., Abramsson, A., Uutela, M., Backstrom, G., Hellstrom, M., Bostrom, H., Li, H., Soriano, P., Betsholtz, C., Heldin, C. H., Alitalo, K., Ostman, A., & Eriksson, U. (2000). PDGF-C is a new protease-activated ligand for the PDGF alpha-receptor. *Nat Cell Biol*, *2*(5), 302-309. https://doi.org/10.1038/35010579

Li, Y., Jiang, D., Liang, J., Meltzer, E. B., Gray, A., Miura, R., Wogensen, L., Yamaguchi, Y., & Noble, P. W. (2011). Severe lung fibrosis requires an invasive fibroblast phenotype regulated by hyaluronan and CD44. *J Exp Med*, *208*(7), 1459-1471. https://doi.org/10.1084/jem.20102510

Li, Z. Q., Liu, Y. L., Li, G., Li, B., Liu, Y., Li, X. F., & Liu, A. J. (2015). Inhibitory effects of C-type natriuretic peptide on the differentiation of cardiac fibroblasts, and secretion of monocyte chemoattractant protein-1 and plasminogen activator inhibitor-1. *Mol Med Rep*, *11*(1), 159-165. https://doi.org/10.3892/mmr.2014.2763

Lin, L., Miller, C. T., Contreras, J. I., Prescott, M. S., Dagenais, S. L., Wu, R., Yee, J., Orringer, M. B., Misek, D. E., Hanash, S. M., Glover, T. W., & Beer, D. G. (2002). The hepatocyte nuclear factor 3 alpha gene, HNF3alpha (FOXA1), on chromosome band 14q13 is amplified and overexpressed in esophageal and lung adenocarcinomas. *Cancer Res*, *62*(18), 5273-5279. https://www.ncbi.nlm.nih.gov/pubmed/12234996

Lowe, D. G., Camerato, T. R., & Goeddel, D. V. (1990). cDNA sequence of the human atrial natriuretic peptide clearance receptor. *Nucleic Acids Res*, *18*(11), 3412. https://doi.org/10.1093/nar/18.11.3412

Lowe, D. G., Klisak, I., Sparkes, R. S., Mohandas, T., & Goeddel, D. V. (1990). Chromosomal distribution of three members of the human natriuretic peptide receptor/guanylyl cyclase gene family. *Genomics*, *8*(2), 304-312. https://doi.org/10.1016/0888-7543(90)90286-4

Lubinus, M., Meier, K. E., Smith, E. A., Gause, K. C., LeRoy, E. C., & Trojanowska, M. (1994). Independent effects of platelet-derived growth factor isoforms on mitogen-activated protein kinase activation and mitogenesis in human dermal fibroblasts. *J Biol Chem*, *269*(13), 9822-9825. https://www.ncbi.nlm.nih.gov/pubmed/7511594

Lüllmann-Rauch. (2003). *Taschenlehrbuch Histologie*.

Lynch, D. A., Godwin, J. D., Safrin, S., Starko, K. M., Hormel, P., Brown, K. K., Raghu, G., King, T. E., Jr., Bradford, W. Z., Schwartz, D. A., Richard Webb, W., & Idiopathic Pulmonary Fibrosis Study, G. (2005). High-resolution computed tomography in idiopathic pulmonary fibrosis: diagnosis and prognosis. *Am J Respir Crit Care Med*, *172*(4), 488-493. https://doi.org/10.1164/rccm.200412-1756OC

Markart, P., Seeger, W., & Gunther, A. (2006). Differential therapy of pulmonary fibrosis. *Internist (Berl)*, *47 Suppl 1*, S26-32. https://doi.org/10.1007/s00108-006-1641-8 (Differenzielle Therapie bei Lungenfibrosen.)

Martinet, Y., Rom, W. N., Grotendorst, G. R., Martin, G. R., & Crystal, R. G. (1987). Exaggerated spontaneous release of platelet-derived growth factor by alveolar macrophages from patients with idiopathic pulmonary fibrosis. *N Engl J Med*, *317*(4), 202-209. https://doi.org/10.1056/NEJM198707233170404

Massberg, S., Sausbier, M., Klatt, P., Bauer, M., Pfeifer, A., Siess, W., Fassler, R., Ruth, P., Krombach, F., & Hofmann, F. (1999). Increased adhesion and aggregation of platelets lacking cyclic guanosine 3',5'-monophosphate kinase I. *J Exp Med*, *189*(8), 1255-1264. https://doi.org/10.1084/jem.189.8.1255

McMurray, J., & Struthers, A. D. (1988). Effects of angiotensin II and atrial natriuretic peptide alone and in combination on urinary water and electrolyte excretion in man. *Clin Sci (Lond)*, *74*(4), 419-425. https://doi.org/10.1042/cs0740419

Medema, R. H., Kops, G. J., Bos, J. L., & Burgering, B. M. (2000). AFX-like Forkhead transcription factors mediate cell-cycle regulation by Ras and PKB through p27kip1. *Nature*, *404*(6779), 782-787. https://doi.org/10.1038/35008115

Mirczuk, S. M., Lessey, A. J., Catterick, A. R., Perrett, R. M., Scudder, C. J., Read, J. E., Lipscomb, V. J., Niessen, S. J., Childs, A. J., McArdle, C. A., McGonnell, I.

M., & Fowkes, R. C. (2019). Regulation and Function of C-Type Natriuretic Peptide (CNP) in Gonadotrope-Derived Cell Lines. *Cells*, *8*(9), 1086. https://doi.org/10.3390/cells8091086

Moyes, A. J., Chu, S. M., Aubdool, A. A., Dukinfield, M. S., Margulies, K. B., Bedi, K. C., Hodivala-Dilke, K., Baliga, R. S., & Hobbs, A. J. (2020). C-type natriuretic peptide co-ordinates cardiac structure and function. *Eur Heart J*, *41*(9), 1006-1020. https://doi.org/10.1093/eurheartj/ehz093

Mukoyama, M., Nakao, K., Hosoda, K., Suga, S., Saito, Y., Ogawa, Y., Shirakami, G., Jougasaki, M., Obata, K., Yasue, H., & et al. (1991). Brain natriuretic peptide as a novel cardiac hormone in humans. Evidence for an exquisite dual natriuretic peptide system, atrial natriuretic peptide and brain natriuretic peptide. *J Clin Invest*, *87*(4), 1402-1412. https://doi.org/10.1172/JCI115146

Murakami, S., Nagaya, N., Itoh, T., Fujii, T., Iwase, T., Hamada, K., Kimura, H., & Kangawa, K. (2004). C-type natriuretic peptide attenuates bleomycin-induced pulmonary fibrosis in mice. *Am J Physiol Lung Cell Mol Physiol*, *287*(6), L1172-1177. https://doi.org/10.1152/ajplung.00087.2004

Nakanishi, K., Tajima, F., Itoh, H., Nakata, Y., Hama, N., Nakagawa, O., Nakao, K., Kawai, T., Torikata, C., Suga, T., Takishima, K., Aurues, T., & Ikeda, T. (1999). Expression of C-type natriuretic peptide during development of rat lung. *Am J Physiol*, *277*(5), L996-L1002. https://doi.org/10.1152/ajplung.1999.277.5.L996

Nho, R. S., Hergert, P., Kahm, J., Jessurun, J., & Henke, C. (2011). Pathological alteration of FoxO3a activity promotes idiopathic pulmonary fibrosis fibroblast proliferation on type i collagen matrix. *Am J Pathol*, *179*(5), 2420-2430. https://doi.org/10.1016/j.ajpath.2011.07.020

Nho, R. S., Im, J., Ho, Y. Y., & Hergert, P. (2014). MicroRNA-96 inhibits FoxO3a function in IPF fibroblasts on type I collagen matrix. *Am J Physiol Lung Cell Mol Physiol*, *307*(8), L632-642. https://doi.org/10.1152/ajplung.00127.2014

Nishikimi, T., Minamino, N., Ikeda, M., Takeda, Y., Tadokoro, K., Shibasaki, I., Fukuda, H., Horiuchi, Y., Oikawa, S., Ieiri, T., Matsubara, M., & Ishimitsu, T. (2010). Diversity of molecular forms of plasma brain natriuretic peptide in heart failure--different proBNP-108 to BNP-32 ratios in atrial and ventricular overload. *Heart*, *96*(6), 432-439. https://doi.org/10.1136/hrt.2009.178392

Ogawa, H., Qiu, Y., Ogata, C. M., & Misono, K. S. (2004). Crystal structure of hormone-bound atrial natriuretic peptide receptor extracellular domain: rotation mechanism for transmembrane signal transduction. *J Biol Chem*, *279*(27), 28625-28631. https://doi.org/10.1074/jbc.M313222200

Pfeifer, A., Aszodi, A., Seidler, U., Ruth, P., Hofmann, F., & Fassler, R. (1996). Intestinal secretory defects and dwarfism in mice lacking cGMP-dependent protein kinase II. *Science*, *274*(5295), 2082-2086. https://doi.org/10.1126/science.274.5295.2082

Porter, J. G., Scarborough, R. M., Wang, Y., Schenk, D., McEnroe, G. A., Kang, L. L., & Lewicki, J. A. (1989). Recombinant expression of a secreted form of the atrial natriuretic peptide clearance receptor. *J Biol Chem*, *264*(24), 14179-14184. https://www.ncbi.nlm.nih.gov/pubmed/2547785

Potter, L. R. (1998). Phosphorylation-dependent regulation of the guanylyl cyclase-linked natriuretic peptide receptor B: dephosphorylation is a mechanism of desensitization. *Biochemistry*, *37*(8), 2422-2429. https://doi.org/10.1021/bi972303k

Prickett, T. C., & Espiner, A. E. (2020). Circulating products of C-type natriuretic peptide and links with organ function in health and disease. *Peptides*, *132*, 170363. https://doi.org/10.1016/j.peptides.2020.170363

Qu, C., Liu, X., Ye, T., Wang, L., Liu, S., Zhou, X., Wu, G., Lin, J., Shi, S., & Yang, B. (2019). miR216a exacerbates TGFbetainduced myofibroblast

transdifferentiation via PTEN/AKT signaling. *Mol Med Rep*, *19*(6), 5345-5352. https://doi.org/10.3892/mmr.2019.10200

Raghu, G., Collard, H. R., Egan, J. J., Martinez, F. J., Behr, J., Brown, K. K., Colby, T. V., Cordier, J. F., Flaherty, K. R., Lasky, J. A., Lynch, D. A., Ryu, J. H., Swigris, J. J., Wells, A. U., Ancochea, J., Bouros, D., Carvalho, C., Costabel, U., Ebina, M., Hansell, D. M., Johkoh, T., Kim, D. S., King, T. E., Jr., Kondoh, Y., Myers, J., Muller, N. L., Nicholson, A. G., Richeldi, L., Selman, M., Dudden, R. F., Griss, B. S., Protzko, S. L., Schunemann, H. J., & Fibrosis, A. E. J. A. C. o. I. P. (2011). An official ATS/ERS/JRS/ALAT statement: idiopathic pulmonary fibrosis: evidence-based guidelines for diagnosis and management. *Am J Respir Crit Care Med*, *183*(6), 788-824. https://doi.org/10.1164/rccm.2009-040GL

Raghu, G., Remy-Jardin, M., Myers, J. L., Richeldi, L., Ryerson, C. J., Lederer, D. J., Behr, J., Cottin, V., Danoff, S. K., Morell, F., Flaherty, K. R., Wells, A., Martinez, F. J., Azuma, A., Bice, T. J., Bouros, D., Brown, K. K., Collard, H. R., Duggal, A., Galvin, L., Inoue, Y., Jenkins, R. G., Johkoh, T., Kazerooni, E. A., Kitaichi, M., Knight, S. L., Mansour, G., Nicholson, A. G., Pipavath, S. N. J., Buendia-Roldan, I., Selman, M., Travis, W. D., Walsh, S., Wilson, K. C., American Thoracic Society, E. R. S. J. R. S., & Latin American Thoracic, S. (2018). Diagnosis of Idiopathic Pulmonary Fibrosis. An Official ATS/ERS/JRS/ALAT Clinical Practice Guideline. *Am J Respir Crit Care Med*, *198*(5), e44-e68. https://doi.org/10.1164/rccm.201807-1255ST

Raghu, G., Rochwerg, B., Zhang, Y., Garcia, C. A., Azuma, A., Behr, J., Brozek, J. L., Collard, H. R., Cunningham, W., Homma, S., Johkoh, T., Martinez, F. J., Myers, J., Protzko, S. L., Richeldi, L., Rind, D., Selman, M., Theodore, A., Wells, A. U., Hoogsteden, H., Schunemann, H. J., American Thoracic, S., European Respiratory, s., Japanese Respiratory, S., & Latin American Thoracic, A. (2015). An Official ATS/ERS/JRS/ALAT Clinical Practice Guideline: Treatment of Idiopathic Pulmonary Fibrosis. An Update of the 2011 Clinical Practice Guideline. *Am J Respir Crit Care Med*, *192*(2), e3-19. https://doi.org/10.1164/rccm.201506-1063ST

Raghu, G., Weycker, D., Edelsberg, J., Bradford, W. Z., & Oster, G. (2006). Incidence and prevalence of idiopathic pulmonary fibrosis. *Am J Respir Crit Care Med*, *174*(7), 810-816. https://doi.org/10.1164/rccm.200602-163OC

Rasband, M. N., Tayler, J., Kaga, Y., Yang, Y., Lappe-Siefke, C., Nave, K. A., & Bansal, R. (2005). CNP is required for maintenance of axon-glia interactions at nodes of Ranvier in the CNS. *Glia*, *50*(1), 86-90. https://doi.org/10.1002/glia.20165

Robinson, J. W., Egbert, J. R., Davydova, J., Schmidt, H., Jaffe, L. A., & Potter, L. R. (2017). Dephosphorylation is the mechanism of fibroblast growth factor inhibition of guanylyl cyclase-B. *Cell Signal*, *40*, 222-229. https://doi.org/10.1016/j.cellsig.2017.09.021

Roskoski, R., Jr. (2018). The role of small molecule platelet-derived growth factor receptor (PDGFR) inhibitors in the treatment of neoplastic disorders. *Pharmacol Res*, *129*, 65-83. https://doi.org/10.1016/j.phrs.2018.01.021

Ross, R., Glomset, J., Kariya, B., & Harker, L. (1974). A platelet-dependent serum factor that stimulates the proliferation of arterial smooth muscle cells in vitro. *Proc Natl Acad Sci U S A*, *71*(4), 1207-1210. https://doi.org/10.1073/pnas.71.4.1207

Roy, S. K., Srivastava, R. K., & Shankar, S. (2010). Inhibition of PI3K/AKT and MAPK/ERK pathways causes activation of FOXO transcription factor, leading to cell cycle arrest and apoptosis in pancreatic cancer. *J Mol Signal*, *5*, 10. https://doi.org/10.1186/1750-2187-5-10

Russell, A. M., Adamali, H., Molyneaux, P. L., Lukey, P. T., Marshall, R. P., Renzoni, E. A., Wells, A. U., & Maher, T. M. (2016). Daily Home Spirometry: An Effective Tool for Detecting Progression in Idiopathic Pulmonary Fibrosis. *Am J Respir Crit Care Med*, *194*(8), 989-997. https://doi.org/10.1164/rccm.201511-2152OC

Sausbier, M., Schubert, R., Voigt, V., Hirneiss, C., Pfeifer, A., Korth, M., Kleppisch, T., Ruth, P., & Hofmann, F. (2000). Mechanisms of NO/cGMP-dependent vasorelaxation. *Circ Res*, *87*(9), 825-830. https://doi.org/10.1161/01.res.87.9.825

Savarirayan, R., Irving, M., Bacino, C. A., Bostwick, B., Charrow, J., Cormier-Daire, V., Le Quan Sang, K. H., Dickson, P., Harmatz, P., Phillips, J., Owen, N., Cherukuri, A., Jayaram, K., Jeha, G. S., Larimore, K., Chan, M. L., Huntsman Labed, A., Day, J., & Hoover-Fong, J. (2019). C-Type Natriuretic Peptide Analogue Therapy in Children with Achondroplasia. *N Engl J Med*, *381*(1), 25-35. https://doi.org/10.1056/NEJMoa1813446

Schmidt, M., Fernandez de Mattos, S., van der Horst, A., Klompmaker, R., Kops, G. J., Lam, E. W., Burgering, B. M., & Medema, R. H. (2002). Cell cycle inhibition by FoxO forkhead transcription factors involves downregulation of cyclin D. *Mol Cell Biol*, *22*(22), 7842-7852. https://doi.org/10.1128/MCB.22.22.7842-7852.2002

Scodelaro Bilbao, P., & Boland, R. (2013). Extracellular ATP regulates FoxO family of transcription factors and cell cycle progression through PI3K/Akt in MCF-7 cells. *Biochim Biophys Acta*, *1830*(10), 4456-4469. https://doi.org/10.1016/j.bbagen.2013.05.034

Selman, M., Carrillo, G., Estrada, A., Mejia, M., Becerril, C., Cisneros, J., Gaxiola, M., Perez-Padilla, R., Navarro, C., Richards, T., Dauber, J., King, T. E., Jr., Pardo, A., & Kaminski, N. (2007). Accelerated variant of idiopathic pulmonary fibrosis: clinical behavior and gene expression pattern. *PLoS One*, *2*(5), e482. https://doi.org/10.1371/journal.pone.0000482

Selman, M., & Pardo, A. (2002). Idiopathic pulmonary fibrosis: an epithelial/fibroblastic cross-talk disorder. *Respir Res*, *3*, 3. https://doi.org/10.1186/rr175

Sime, P. J., Xing, Z., Graham, F. L., Csaky, K. G., & Gauldie, J. (1997). Adenovector-mediated gene transfer of active transforming growth factor-beta1 induces prolonged severe fibrosis in rat lung. *J Clin Invest*, *100*(4), 768-776. https://doi.org/10.1172/JCI119590

Singh, A., Ye, M., Bucur, O., Zhu, S., Tanya Santos, M., Rabinovitz, I., Wei, W., Gao, D., Hahn, W. C., & Khosravi-Far, R. (2010). Protein phosphatase 2A reactivates FOXO3a through a dynamic interplay with 14-3-3 and AKT. *Mol Biol Cell*, *21*(6), 1140-1152. https://doi.org/10.1091/mbc.E09-09-0795

Smith, P. K., Krohn, R. I., Hermanson, G. T., Mallia, A. K., Gartner, F. H., Provenzano, M. D., Fujimoto, E. K., Goeke, N. M., Olson, B. J., & Klenk, D. C. (1985). Measurement of protein using bicinchoninic acid. *Anal Biochem*, *150*(1), 76-85. https://doi.org/10.1016/0003-2697(85)90442-7

Smolenski, A., Bachmann, C., Reinhard, K., Honig-Liedl, P., Jarchau, T., Hoschuetzky, H., & Walter, U. (1998). Analysis and regulation of vasodilator-stimulated phosphoprotein serine 239 phosphorylation in vitro and in intact cells using a phosphospecific monoclonal antibody. *J Biol Chem*, *273*(32), 20029-20035. https://doi.org/10.1074/jbc.273.32.20029

Soeki, T., Kishimoto, I., Okumura, H., Tokudome, T., Horio, T., Mori, K., & Kangawa, K. (2005). C-type natriuretic peptide, a novel antifibrotic and antihypertrophic agent, prevents cardiac remodeling after myocardial infarction. *J Am Coll Cardiol*, *45*(4), 608-616. https://doi.org/10.1016/j.jacc.2004.10.067

Spruit, M. A., Singh, S. J., Garvey, C., ZuWallack, R., Nici, L., Rochester, C., Hill, K., Holland, A. E., Lareau, S. C., Man, W. D., Pitta, F., Sewell, L., Raskin, J.,

Bourbeau, J., Crouch, R., Franssen, F. M., Casaburi, R., Vercoulen, J. H., Vogiatzis, I., Gosselink, R., Clini, E. M., Effing, T. W., Maltais, F., van der Palen, J., Troosters, T., Janssen, D. J., Collins, E., Garcia-Aymerich, J., Brooks, D., Fahy, B. F., Puhan, M. A., Hoogendoorn, M., Garrod, R., Schols, A. M., Carlin, B., Benzo, R., Meek, P., Morgan, M., Rutten-van Molken, M. P., Ries, A. L., Make, B., Goldstein, R. S., Dowson, C. A., Brozek, J. L., Donner, C. F., Wouters, E. F., & Rehabilitation, A. E. T. F. o. P. (2013). An official American Thoracic Society/European Respiratory Society statement: key concepts and advances in pulmonary rehabilitation. *Am J Respir Crit Care Med*, *188*(8), e13-64. https://doi.org/10.1164/rccm.201309-1634ST

Sudoh, T., Kangawa, K., Minamino, N., & Matsuo, H. (1988). A new natriuretic peptide in porcine brain. *Nature*, *332*(6159), 78-81. https://doi.org/10.1038/332078a0

Sudoh, T., Minamino, N., Kangawa, K., & Matsuo, H. (1990). C-type natriuretic peptide (CNP): a new member of natriuretic peptide family identified in porcine brain. *Biochem Biophys Res Commun*, *168*(2), 863-870. https://doi.org/10.1016/0006-291x(90)92401-k

Takaishi, H., Konishi, H., Matsuzaki, H., Ono, Y., Shirai, Y., Saito, N., Kitamura, T., Ogawa, W., Kasuga, M., Kikkawa, U., & Nishizuka, Y. (1999). Regulation of nuclear translocation of forkhead transcription factor AFX by protein kinase B. *Proc Natl Acad Sci U S A*, *96*(21), 11836-11841. https://doi.org/10.1073/pnas.96.21.11836

Tamura, N., Doolittle, L. K., Hammer, R. E., Shelton, J. M., Richardson, J. A., & Garbers, D. L. (2004). Critical roles of the guanylyl cyclase B receptor in endochondral ossification and development of female reproductive organs. *Proc Natl Acad Sci U S A*, *101*(49), 17300-17305. https://doi.org/10.1073/pnas.0407894101

Tawaragi, Y., Fuchimura, K., Tanaka, S., Minamino, N., Kangawa, K., & Matsuo, H. (1991). Gene and precursor structures of human C-type natriuretic peptide. *Biochem Biophys Res Commun*, *175*(2), 645-651. https://doi.org/10.1016/0006-291x(91)91614-i

Thannickal, V. J., Toews, G. B., White, E. S., Lynch, J. P., 3rd, & Martinez, F. J. (2004). Mechanisms of pulmonary fibrosis. *Annu Rev Med*, *55*, 395-417. https://doi.org/10.1146/annurev.med.55.091902.103810

Ting, A. Y., & Zelinski, M. B. (2017). Characterization of FOXO1, 3 and 4 transcription factors in ovaries of fetal, prepubertal and adult rhesus macaques. *Biol Reprod*, *96*(5), 1052-1059. https://doi.org/10.1093/biolre/iox034

Tisler, M., Alkmin, S., Chang, H. Y., Leet, J., Bernau, K., Sandbo, N., & Campagnola, P. J. (2020). Analysis of fibroblast migration dynamics in idiopathic pulmonary fibrosis using image-based scaffolds of the lung extracellular matrix. *Am J Physiol Lung Cell Mol Physiol*, *318*(2), L276-L286. https://doi.org/10.1152/ajplung.00087.2019

Tomasek, J. J., Gabbiani, G., Hinz, B., Chaponnier, C., & Brown, R. A. (2002). Myofibroblasts and mechano-regulation of connective tissue remodelling. *Nat Rev Mol Cell Biol*, *3*(5), 349-363. https://doi.org/10.1038/nrm809

Vivar, R., Humeres, C., Anfossi, R., Bolivar, S., Catalan, M., Hill, J., Lavandero, S., & Diaz-Araya, G. (2020). Role of FoxO3a as a negative regulator of the cardiac myofibroblast conversion induced by TGF-beta1. *Biochim Biophys Acta Mol Cell Res*, *1867*(7), 118695. https://doi.org/10.1016/j.bbamcr.2020.118695

Vollmar, A. M., & Schulz, R. (1995). Expression and differential regulation of natriuretic peptides in mouse macrophages. *J Clin Invest*, *95*(6), 2442-2450. https://doi.org/10.1172/JCI117944

Walsh, J., Absher, M., & Kelley, J. (1993). Variable expression of platelet-derived growth factor family proteins in acute lung injury. *Am J Respir Cell Mol Biol*, *9*(6), 637-644. https://doi.org/10.1165/ajrcmb/9.6.637

Weigel, D., & Jackle, H. (1990). The fork head domain: a novel DNA binding motif of eukaryotic transcription factors? *Cell*, *63*(3), 455-456. https://doi.org/10.1016/0092-8674(90)90439-l

Weigel, D., Jurgens, G., Kuttner, F., Seifert, E., & Jackle, H. (1989). The homeotic gene fork head encodes a nuclear protein and is expressed in the terminal regions of the Drosophila embryo. *Cell*, *57*(4), 645-658. https://doi.org/10.1016/0092-8674(89)90133-5

Westermark, B., & Wasteson, A. (1976). A platelet factor stimulating human normal glial cells. *Exp Cell Res*, *98*(1), 170-174. https://doi.org/10.1016/0014-4827(76)90476-6

Wilson, E. M., & Chinkers, M. (1995). Identification of sequences mediating guanylyl cyclase dimerization. *Biochemistry*, *34*(14), 4696-4701. https://doi.org/10.1021/bi00014a025

Worke, L. J., Barthold, J. E., Seelbinder, B., Novak, T., Main, R. P., Harbin, S. L., & Neu, C. P. (2017). Densification of Type I Collagen Matrices as a Model for Cardiac Fibrosis. *Adv Healthc Mater*, *6*(22), 1002. https://doi.org/10.1002/adhm.201700114

Wu, C., Wu, F., Pan, J., Morser, J., & Wu, Q. (2003). Furin-mediated processing of Pro-C-type natriuretic peptide. *J Biol Chem*, *278*(28), 25847-25852. https://doi.org/10.1074/jbc.M301223200

Xie, Q., Chen, J., & Yuan, Z. (2012). Post-translational regulation of FOXO. *Acta Biochim Biophys Sin (Shanghai)*, *44*(11), 897-901. https://doi.org/10.1093/abbs/gms067

Yan, W., Wu, F., Morser, J., & Wu, Q. (2000). Corin, a transmembrane cardiac serine protease, acts as a pro-atrial natriuretic peptide-converting enzyme. *Proc Natl Acad Sci U S A*, *97*(15), 8525-8529. https://doi.org/10.1073/pnas.150149097

Yi, E. S., Lee, H., Yin, S., Piguet, P., Sarosi, I., Kaufmann, S., Tarpley, J., Wang, N. S., & Ulich, T. R. (1996). Platelet-derived growth factor causes pulmonary cell proliferation and collagen deposition in vivo. *Am J Pathol*, *149*(2), 539-548. https://www.ncbi.nlm.nih.gov/pubmed/8701993

Zhang, Z., Xiao, Z., & Diamond, S. L. (1999). Shear stress induction of C-type natriuretic peptide (CNP) in endothelial cells is independent of NO autocrine signaling. *Ann Biomed Eng*, *27*(4), 419-426. https://doi.org/10.1114/1.203

Appendix

I List of Abbreviations

AKT	Ak strain transforming/ Proteinkinase B
ALAT	Latin American Thoracic Association
ANP	Atrial natriuretic peptide
ATS	American Thoracic Society
BCA	Bicinchonine acid-Assay
bFGF	Basic fibroblast growth factor
BNP	Brain natriuretic peptide
BrdU	Bromodeoxuridine
BSA	Bovine serum albumin
cAMP	Cyclic adenosine monophosphate
CF-CYT	Cell fractioning buffer-cytoplasma
CF-MEM	Cell fractioning buffer-membrane
CF-NE	Cell fractioning buffer-nucleus
cGK	cGMP-dependent protein kinase
cGMP	Cyclic guanosine monophosphate
CNP	C-type natriuretic peptide
DMEM	Dulbecco's Modified Eagle Medium
DMSO	Dimethylsulfoxide
DNA	Deoxyribonucleic acid
EGF	Epidermal growth factor
ERK	Extracellular-signal related kinase
ERS	European Respiratory society
FCS	Fetal calf serum
FGF	Fibroblast growth factor
Fox	Forkhead box transcription factor
GC-A	Guanylyl-cyclase receptor A
GC-B	Guanylyl-cyclase receptor B
GTP	Guanosine triphosphate
HRCT	High-resolution computed tomography
IBMX	3-Isobutyl-1-Methylxanthin
ICAM	Intercellular adhesion molecule
IFNɣ	Interferon ɣ
IGF 1	Insulin-like growth factor 1
IPF	Idiopathic pulmonary fibrosis
JRS	Japanese Respiratory Society
KO	knock out
MEK	Mitogen activated protein-kinase
microRNA	Micro-ribonucleic acid
mRNA	Messenger-ribonucleic acid

MMP	Matrix-metalloproteinase
NO	Nitrogen monoxide
NPR-A	Natriuretic peptide receptor A
NPR-B	Natriuretic peptide receptor B
NPR-C	Natriuretic peptide receptor C
PAI-1	Plasminogen activator inhibitor type 1
PBS	Phosphate-buffered saline
PCR	Polymerase chain reaction
PDE	Phosphodiesterase
PDGF	Platelet derived growth factor
PDK1	Phosphoinositide-dependent kinase-1
PF	Pulmonary fibrosis
PFA	Paraformaldehyde
PI3K	Phosphoinositid-3-kinase
PKG	Proteinkinase G
RAAS	Renin-angiotensin-aldosterone-system
RAF	Rapidly accelerated Fibrosarcoma
RAS	Rat sarcoma virus
RIA	Radioimmuno-assay
RIPA buffer	Radioimmunoprecipitation assay buffer
RT	Room temperature
SGK	Serum- and glucocorticoid-inducible kinase
α-SMA	Alpha-smooth muscle actin
SDS	Sodium-Dodecyl-Sulfate
SDS-Page	Sodium-Dodecyl-sulfate-polyacrylamide-gelelctrophorese
Tamox	Tamoxifen
TBS-T	Tris-buffered saline with Tween20
TGF β	Transforming growth factor β
UIP	Usual interstitial pneumonia
VASP	Vasodilator-stimulated phosphoprotein

II List of Figures

III List of Tables

IV Buffer, Gels and Antibodies

Table 11: Digestion buffer

Name:	Concentration:
Ethylene diamine tetra acetate (EDTA)	5mM
PCR-H_2O	50ml
Sodium Chloride (NaCl)	200mM
Sodium-Dodecylsulfate (SDS)	0,2% (w/v)
Tris	100mM

Table 12: Laemmli-Buffer (3x)

Name	Concentration
Bromphenolblue, pH 6.7	0.01% (w/v)
Glycerol	15% (v/v)
SDS	6% (w/v)
Tris-HCl (pH 6.8)	200mM
ß-Mercaptoethanol	10% (v/v)

Table 13: PBS

Name:	Concentration:
Disodium phosphate ($Na_2HPO_{4)}$	10mM
NaCl	137mM
Potassium Chloride (KCl)	2.7mM
Potassium dihydrogen phosphate (KH_2PO_4)	1.8mM

Table 14: Resolving gel

Name	Concentration 8%	Concentration 10%
Ammoniumpersulfat (APS, 10 %)	150µl	150µl
ddH_2O	7.0ml	5.9ml
N.N.N´,N´-tetramethylethylendiamine	9µl	6µl
Rotiphorese®Gel 30	4.0ml	5.0ml
SDS (10%)	150µl	150µl
Tris-HCl (1.5M, pH 8.8)	3.8ml	3.8ml

Table 15: Running Buffer

Name:	Concentration:
Glycine	200mM
SDS	0.1% (w/v)
Trizma®base	25mM

Table 16: Stacking gel

Name	Concentration
APS (10 %),	100µl
ddH_2O	6.8ml
N.N.N´,N´-tetramethylethylendiamine	10µl
Rotiphorese®Gel 30	1.7ml
SDS (10%)	100µl
Tris-HCl (1,0 M, pH 6.8)	1.24ml

Table 17: Stripping Buffer

Name:	Concentration:
ddH_2O	44.35ml
SDS	12ml
Trizma®base	3.75ml
ß-Mercaptoethanol	480µl

Table 18: TAE buffer (50x)

Name:	Concentration:
EDTA	50mM
Natriumacetate	0.25M
Trizma®base	2M

Table 19: TBS-T

Name:	Concentration:
NaCl	94.6mM
Trizma®base	19.8mM
Tween®20	0.1% (v/v)

Table 20: Transfer buffer

Name:	Concentration:
Glycine	192mM
Methanol	20% (v/v)
Trizma®base	25mM

Table 21: TE Buffer

Name:	Concentration:
EDTA	20µM
Trizma®base	10mM

Table 22: Antibodies

Name:	Company:
AKT	Cell signaling (9272)
Alexa Fluor® 488 donkey anti-rabbit	Life technologies (A21206)
Collagen 1 (WB for human fibroblasts)	Proteintech (14695-1-AP)
Collagen 1 (WB for murine fibroblasts)	Meridian (T40777R)
Collagen 3 (Immunofluorescence)	Abcam (ab7778)
ERK	Cell signaling (9102S)
FoxO3	Cell signaling (2497)
GAPDH	Cell signaling (2118S)
GC-B	From Prof. Hannes Schmidt
MMP9	Proteintech (10375-2-AP)
Na^+-K^+-ATPase	Abcam (ab26020)
NPR-C	Origene (TA501080)
$pAKT_{Ser473}$	Cell signaling (9271S)
$pERK_{Thr202/Tyr204}$	Cell signaling (9102)
$pFoxO3_{Thr32}$	Cell signaling (9464)
$pVASP_{Ser239}$	Cell signaling (3114)
Sec. AB guinea pig	Dianova (106-545-003)
Sec. AB mouse	Dianova (115-035-062)

Sec. AB rabbit	Dianova (111-035-144)
VASP	Cell signaling (3112)

V Acknowledgment

At this point I want to say thank you to all the people without whom I would not have been able to complete this research and accomplish the thesis:

My deepest gratitude goes to Professor Dr. med. Michaela Kuhn for her scientific guidelines, kind support and encouragement throughout the project time. I want to thank you for giving me the opportunity to do my thesis in your laboratory and supporting me in all steps. With constructive discussions and advice, you gave me the base for my scientific development. Also, for the possibility to attend at an international congress in Frankfurt and present a poster, I want to thank.

Many thanks go to Dr. Swati Dabral, who introduced me with infinitely patience to the world of cell culture and passed on her great enthusiasm for scientific work. Thank you for always having a sympathetic ear, answering all the questions and solving the big and small problems in the daily lab life. I am really thankful for all the time you took, to perform experiments and discuss results with me. I will never forget all the hours we spent together in the cell culture lab.

My special thanks go to Minhee Noh, Rebecca Bosch and Dr. Swati Dabral for their great help and support. You made me enjoy the time in the lab a lot and especially the lunch breaks together have always been highlights of the day. I could rely on your aid in every situation and it was a pleasure to work with you.

I would also like to thank Lisa Krebes for her daily, contagious good mood and of course for performing the RIA experiments for me.

Also, I want to thank Dr. Franziska Werner, Tamara Potapenko, Katharina Völker and the staff of the animal facilities for their helpful and friendly nature and for answering many questions. You facilitated the work in the lab a lot and contributed to a nice ambience.

I would also like to thank the members of AG Schuh and Friebe for the friendly cooperation and Simone Baumann and Winfried Keller for the favors they did for me.

My special thanks go to my family for their continual support. You enabled me to study my dream profession and your belief in me gave me the confidence to do my thesis. In many phone calls and meetings you dissolved arising insecurities.

Last, but not least, I want to say thank you to Lukas. Over all the time you were supporting me, listening patiently to all difficulties and giving me helpful advice. Even when some problems occurred from time to time, your encouragement and trust in me kept me going on.

VII Publications and Congress Participation

Friedrich et al. “C-type natriuretic peptide prevents the activation of lung fibroblasts to myofibroblasts” **100th Annual Meeting of the German Physiology Society, Frankfurt, Germany,** Sep 30.- Oct. 2. 2021

A-L. Friedrich, R. Weyer, E. Lessmann, L. Krebes[1] , H. Schmidt[2] , C. Ruppert, A. Günther, M. Kuhn, S. Dabral. C-type natriuretic peptide—Guanylyl cyclase B signalling counter-regulates the activation of human lung fbroblasts to myofbroblasts. Journal of Translational Medicine volume 21, Article number: 35 (2022), **Cyclic GMP conference 2022: Augsburg, Germany**

R. Weyer, A.-L. Friedrich, E. Lessmann, A. Khadim, L. Krebes, C. Ruppert, A. Günther, E. El Agha, M. Kuhn, S. Dabral. Unravelling the role of C-type natriuretic peptide - Guanylyl cyclase Bsignalling in the pathogenesis of Idiopathic Pulmonary Fibrosis.
This study was funded by the Else-Kröner-Fresenius Stiftung (2020 EKEA.131, to Swati Dabral),
Acta Physiologica Volume 236: Abstracts of the Europhysiology 2022, 16-18 September 2022, Copenhagen, Denmark